VITAMIN E FORMS - BIOAVAILABILITY AND PROTECTIVE EFFECTS ON COLITIS AND COLON CANCER

by

Kilia Y. Liu

A Dissertation

Submitted to the Faculty of Purdue University

In Partial Fulfillment of the Requirements for the degree of

Doctor of Philosophy

Department of Nutrition Science

West Lafayette, Indiana

May 2019

THE PURDUE UNIVERSITY GRADUATE SCHOOL
STATEMENT OF COMMITTEE APPROVAL

Dr. Qing Jiang, Chair
Department of Nutrition Science
Dr. John R. Burgess
Department of Nutrition Science
Dr. Kimberly K. Buhman
Department of Nutrition Science
Dr. Yava L. Jones-Hall
Department of Comparative Pathobiology

Approved by:

Dr. Michele Forman
Head of the Graduate Program

To my beloved parents and Yang Zhao for their unconditional love and support.

ACKNOWLEDGMENTS

First, I would like to express my sincere gratitude to my advisor Dr. Qing Jiang for her continuous support and guidance throughout my Ph.D. study and research. I would not have gone this far without her help, especially her patience, motivation, and immense knowledge. She has always believed in and encouraged me during the tough time of my study, even when I lost faith in myself. Her passion and her persistence for research inspire me and make me realized what is needed to be a successful scientist. Her earnestness and rigorous during scientific investigation have greatly influenced my attitude toward research. I could not imagine having a better mentor for my Ph.D. study other than Dr. Jiang.

Besides my advisor, I would like to acknowledge the my committee members: Dr. John R. Burgess, Dr. Kimberly Buhman, and Dr. Yava Jones-Hall, for their insightful comments and contribution on my work, and most importantly, their precious time.

I also want to thank the past and current members of the Jiang lab, Yumi Jang, Nayoung Park, Tianlin Xu, Chao Yang, Suji Im, and Yiying Zhao for their help, support, and companionship over the years. I will never forget all the stimulating discussions we have on research and working together during sacrifices. Their presence makes all the difficult works fun. Additionally, I would like to thank Dr. Cindy Nakatsu, Ariangela Davis Kozik, and YooJung Heo for their kind help with my research and sharing their resources, especially Dr. Nakatsu for her precious time and invaluable feedback.

Last but not the least, I would like to express my appreciation to my family, my parents and Yang Zhao for their genuine support and care during this long journey. Without their unconditional love and support, I would not able to stay this strong and get this far.

TABLE OF CONTENTS

LIST OF TABLES

LIST OF FIGURES

ABSTRACT

Author: Liu, Kilia, Y. PhD
Institution: Purdue University
Degree Received: May 2019
Title: Vitamin E Forms – Bioavailability and Protective Effects on Colitis and Colon Cancer
Committee Chair: Qing Jiang

Vitamin E is a natural lipophilic antioxidant contains eight structurally related forms, i.e., α-, β-, γ-, δ-tocopherols (αT, βT, γT, and δT) and corresponding tocotrienols. Recent research indicates that vitamin E forms are differentially metabolized to various carboxychromanols. Some these vitamin E metabolites have been shown to exhibit strong anti-inflammatory and anticancer effects, yet little is known about their bioavailability. Without this knowledge, it is impossible to assess the role of vitamin E metabolism in biological functions of vitamin E forms and their protective effects on chronic diseases. While αT and γT appear to improved gut health, the underlying mechanisms are not well understood. Furthermore, specific forms of vitamin E such as γT have been reported to have cancer-preventing effects, but their anticancer efficacy is relatively modest. For these reasons, this dissertation focused on the characterization of the pharmacokinetic formation of vitamin E metabolites after supplementation, and the investigation of the underlying mechanisms of the protective effect of vitamin E forms, αT and γT, on gut health, as well as anticancer efficacy of the combination of aspirin and γT on carcinogen-induced colon tumorigenesis.

The first project focuses on characterizing the pharmacokinetic formation of vitamin E metabolites after single dose supplementation of γ-tocopherol-rich mixed tocopherol (γTmT) and δ-tocotrienol (δTE). With our recently developed LC/MS/MS assay

for quantifying vitamin E metabolites, we can simultaneously quantify the level of short-chain, long-chain, and sulfated carboxychromanols in plasma, urine, and fecal samples of supplemented animals. In this study, we investigated the pharmacokinetics including excretion of vitamin E forms and the formation of their metabolites after a single dose intragastric administration of tocopherols and tocotrienols in rats. We also measured vitamin E metabolites in the serum obtained from healthy humans after γT supplementation. In the plasma of rat, the pharmacokinetic profiles of γT and δTE are described as the following: γT, C_{max} = 25.6 ± 9.1 μM, T_{max} = 4 h; δTE, C_{max} = 16.0 ± 2.3 μM, T_{max} = 2 h. Sulfated CEHCs and sulfated 11'-COOHs were the predominant metabolites in the plasma of rat with C_{max} of 0.4-0.5 μM (T_{max} ~ 5-7 h) or ~0.3 μM (T_{max} at 4.7 h), respectively. In 24-h urine, 2.7% of γT and 0.7% of δTE were excreted as conjugated CEHCs, the major identified urinary metabolites. In the feces, 17-45% of supplemented vitamers were excreted as un-metabolized forms and 4.9-9.2% as metabolites. The majority of metabolites excreted in feces were unconjugated carboxychromanols, among which 13'-COOHs constituted ~50% of total metabolites. Interestingly, 13'-COOHs derived from δTE were 2-fold higher than 13'-COOH from γT. Unlike rats, γ-CEHC is the predominant metabolites found in human plasma, although 11'-COOHs and 13'-COOHs (sulfated and unconjugated) were elevated by >20 folds responding to γT supplement. In this study, we found that tocopherols and tocotrienols, when taken as supplements, are mainly excreted as un-metabolized forms and long-chain carboxychromanols in feces. High fecal availability of 13'-COOHs may contribute to modulating effects on gut health.

The second project of my dissertation investigated the effect of vitamin E forms, αT and γT, on intestinal barrier function in a cellular model and a mouse colitis model.

Inflammatory bowel diseases (IBD) are chronic idiopathic inflammatory conditions characterized by disruption of intestinal barrier integrity. Previous studies by others and us had demonstrated that vitamin E forms, αT and γT, can protect against chemical-induced colitis in animal models. However, the role of these vitamin E forms on intestinal barrier function has not been studied. Herein, we investigated the potential protective effects of vitamin E forms, αT and γT, on intestinal barrier function in a Caco-2 colon epithelial cell model and a dextran sodium sulfate (DSS)-induced colitis mouse model. In Caco-2 cells, pretreatment with 25μM αT and γT attenuated Caco-2 monolayer barrier dysfunction induced by 10 ng/mL TNF-α/IFN-γ, suggesting that these vitamin E forms protect intestinal barrier integrity in this cellular model. In male BALB/c mice, the supplementation of αT (0.05%) or γTmT (0.05%) when given 3 weeks before DSS treatment or at the same time as DSS treatment alleviated DSS-induced fecal bleeding and diarrhea symptoms in mice, and attenuated colon inflammation and colitis-associated damages. Additionally, αT and γTmT supplementation attenuated DSS-induced intestinal barrier dysfunction, as indicated by improving the level of occludin, a tight junction protein, in the colon and reducing lipopolysaccharide-binding protein (LBP) in the plasma. Furthermore, gut microbiota analysis demonstrated that αT and γTmT supplementation could modulate intestinal microbiome composition in mice with DSS treatment. DSS treatment reduced the relative abundance of Lachnospiraceae compared to healthy mice, and supplementation of αT and γT partially reversed this effect. Interestingly, the family Lachnospiraceae has been reported to decrease in IBD patients. Our study demonstrated the protective effects of vitamin E forms on intestinal barrier integrity in a cell-based model

and a colitis model in mice. Furthermore, we demonstrated that these vitamin E forms caused favorable changes in the intestinal microbial population under colitis condition.

The third project of my dissertation evaluated the anticancer efficacy of the combination of aspirin and γT using an azoxymethane (AOM)-induced and colitis-promoted colon tumorigenesis mouse model. Extensive inflammation in the colon promotes the development of colorectal cancer (CRC). Eicosanoid production by pro-inflammatory enzymes, cyclooxygenases (COX-1 and COX-2) and 5-lipoxygenase (5-LOX) play a critical role in the initiation, progression, and invasion of CRC. Thus, nonsteroidal anti-inflammatory drugs (NSAIDs), such as aspirin, have been recommended for chemoprevention of CRC. However, long-term use of aspirin can cause many side effects, and the anticancer activity of aspirin is very modest. Previously, we have demonstrated that the combination of γT with aspirin prolonged the anti-inflammatory activity of aspirin and alleviated aspirin-associated adverse effects in a carrageenan-induced inflammation model in rats. Additionally, we found that the combination of γT and aspirin has stronger anticancer activity than aspirin or γT alone against HCT-116 human colorectal carcinoma cells. Therefore, we examined the anticancer effect of the combination of 0.025% aspirin and 0.05% γT against AOM-induced and DSS-promoted tumorigenesis in mice. In this study, we have found that the combination of aspirin and γT, but not aspirin or γT alone, suppressed colon tumorigenesis in mice, as indicated by 40% and 50% reduction in the multiplicity of total polyps ($P < 0.05$) and large adenomatous polyps (>2mm^2, $P < 0.05$), respectively. More strikingly, the combination of aspirin and γT reduced the overall tumor area by 60% ($P < 0.05$). Noteworthy, the supplementation of γT also alleviated aspirin-induced stomach lesion and appeared to modulate intestinal

microbial composition. Our study demonstrated that the combination of aspirin and γT has stronger anticancer activity than aspirin or γT alone while alleviates aspirin-associated adverse effect, suggesting that the combination of γT and aspirin is a more effective and safer chemopreventive agent for CRC than aspirin alone.

CHAPTER 1. LITERATURE REVIEW

1.1 Vitamin E

1.1.1 Different vitamin E forms and food sources

Vitamin E is a generic name for eight structurally related fat-soluble antioxidants, including α-, β-, γ-, δ-tocopherols (αT, βT, γT, δT) and α-, β-, γ-, δ-tocotrienols (αTE, βTE, γTE, δTE). The different isoforms of vitamin E are distinguished by the methylation on the 5- or 7-position of the chromanol ring and the saturation on the 16-carbon phytyl-like side chain [1] (**Figure 1.1**). Tocopherols are vitamin E with saturated side chain, and tocotrienols contain three double bonds. Vitamin E was first discovered by Evans and Bishop in 1922 as an essential nutrient for reproductive health in rats [2]. Naturally occurring vitamin E forms are found in plant existing in RRR configuration at 2', 4', 8'-position for tocopherols and R-configuration at 2-position for tocotrienols [3]. Although synthetic forms of vitamin E, such as RRR- and SRR-α-tocopheryl acetate, are commercially available for supplementation, RRR-stereoisomer is the preferred form by the liver for very-low-density lipoprotein (VLDL) assembly [4].

Natural forms of vitamin E are synthesized in plants, with a small amount in fruits and vegetables [5], but most commonly in plant seeds [6,7]. Almonds, hazelnuts, pine nuts, sunflower seeds, and peanuts are good sources of αT, whereas γT is rich in pecans, pistachios, walnuts, flaxseeds, sesame seeds and pumpkin seeds [7]. Palm oils, barley, and oats are excellent sources of tocotrienols especially, γTE [8,9], and δTE can be extracted from annatto seeds [10]. However, the level of tocotrienols is much lower than tocopherols in the diet. The majority of vitamin E in the U.S. diet comes from corn and soybean oil, which are highly consumed by the U.S. population [11]. Because of that the predominant form of

vitamin E consumed in a typical U.S. diet is γT, which accounts for ~60-70% [1,12]. Additionally, different preparation methods can alter vitamin E contents in foods [6]. Although the level of γT is relatively high in the U.S. diet, αT is still the predominant form of vitamin E in the body, and αT deficiency can lead to degenerative disorder, ataxia [13]. The differences in tissue retention between αT and other vitamin E forms are likely due to the distinct binding affinity of liver proteins for αT, which are critical for the transport and metabolism of vitamin E.

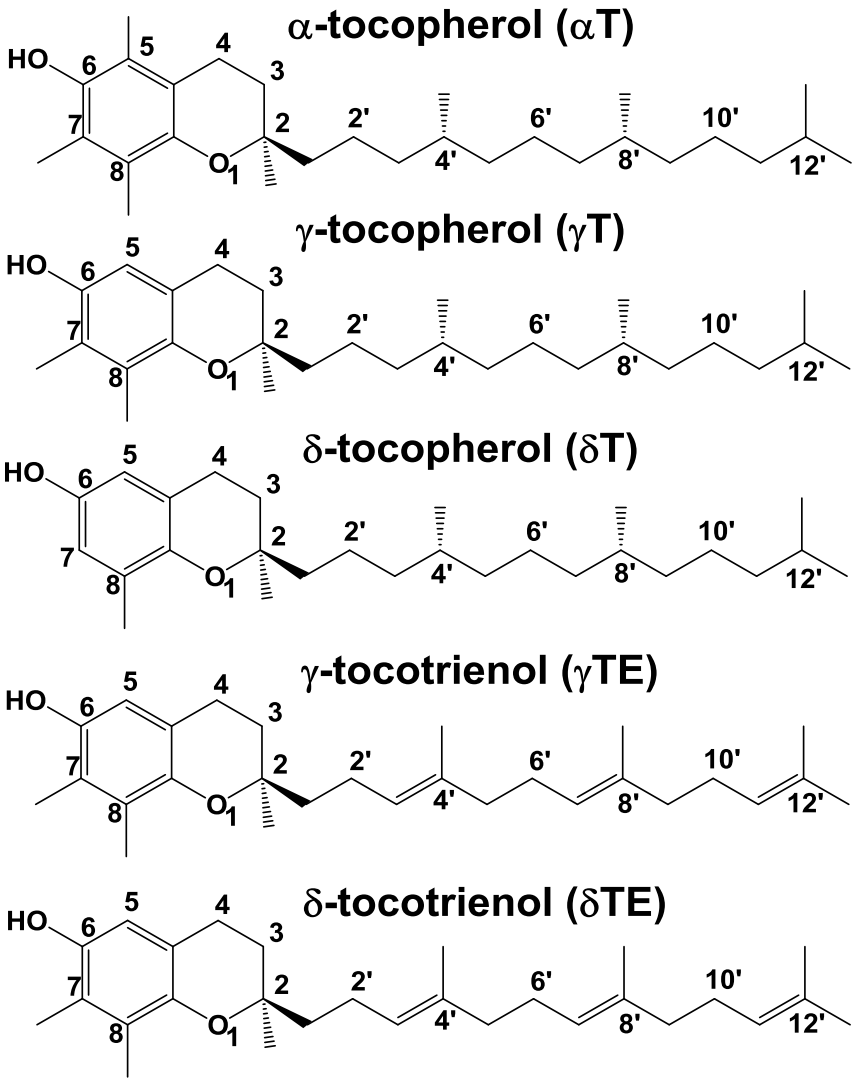

Figure 1.1 Structures of natural vitamin E forms.

1.1.2 Absorption, metabolism, and excretion

Dietary tocopherols and tocotrienols are absorbed along with dietary fats in the intestine and transported in chylomicron particles with other lipid molecules to parenchymal cells of the liver [14]. The absorption of vitamin E is mediated by cholesterol membrane transporters including the scavenger receptor class B type 1 (SR-BI) [15], CD36 molecules [16], Niemann-Pick C1-like transporter 1 (NPC1L1) [17], and ATP-binding cassettes A1 and G1 (ABCA1 and ABCG1) [18]. Accumulating SR-B1 is presented in the basolateral membrane of ileal enterocytes and facilitates the absorption of micellar vitamin E in the distal small intestine [19]. Upon vitamin E uptake across the brush border membrane, micellar vitamin E is packaged into chylomicrons and secreted to various peripheral tissues via the lymphatic system [20]. Although specific receptors for the uptake of vitamin E has not been identified, all lipoprotein receptors should have the ability to pick up vitamin E, and thus can be taken up by various tissues since vitamin E is bound to chylomicron [21]. The accumulation of non-αT forms of vitamin E, such as γT in human skin and adipose tissue [22], or tocotrienols in rat skin [23], may due to chylomicron-associated vitamin E uptake by various tissues.

Among the different isoforms of vitamin E, αT is the predominant form in plasma and tissues due to the high binding affinity to hepatic α-tocopherol transfer protein (αTTP) that transfers αT extrahepatically and prevents it from being extensively metabolized in the liver [1]. Contrarily, other vitamin E forms has low binding affinity to αTTP, and thus are extensively metabolized in the liver by cytochrome P450 via ω-hydroxylation and oxidation to generate 13'-hydroxychromanol (13'-OH) and 13'-carboxychromanol (13'-COOH), which can be further metabolized via β-oxidation to various shorter-chain

carboxychromanols including the terminal metabolite, 3'-COOH or 2-(β-carboxyethyl)-6-hydroxychroman (CEHC) [24] (**Figure 1.2**). Conjugation of these carboxychromanols occurs along with β-oxidation by adding a sulfate or glucuronide group to the hydroxyl group on the chromanol ring [25,26]. With decreased hydrophobicity via catabolism and conjugation, the terminal metabolite CEHCs and the conjugated metabolites can be excreted in the urine, whereas the unconjugated long-chain carboxychromanols and the un-metabolized vitamers are primarily excreted in feces after supplementation of γT and δT [27-33].

It has well established that hepatic αTTP selectively facilitates the distribution of αT from the liver to other tissues. αTTP belongs to the CARL-TRIO family, which is a lipid-binding protein for the regulation of the intracellular trafficking of hydrophobic molecules [1]. In liver, αTTP preferentially binds to αT than other vitamin E forms with 100% binding affinity. The binding affinity of αTTP for βT, γT, and δT is 50%, 10-30%, and 1%, respectively [1,34]. The low binding affinity to non-αT forms of vitamin E suggesting that all three methyl group on the chromanol ring is important for the binding to αTTP. However, αT-acetate and α-tocopheryl quinone, with no free hydrogen group on the chromanol ring, are also poor substrates for αTTP [34], further suggesting that αTTP can also distinguish naturally occurring RRR-αT vs. synthetic stereoisomers, which favors the retention of naturally occurring RRR-αT over synthetic αT [34,35].

αTTP is required for transferring tocopherols from the lysosome to the plasma membrane before vitamin E secretion from the liver [36]. In addition to αTTP, the secretion of vitamin E requires ABCA1 as mice deficient in ABCA1 had lower plasma levels of tocopherols and cholesterol than those in wild-type mice [18]. Since αTTP is preferentially bound to αT, it protects αT from being catabolized in the liver whereas other forms of

vitamin E are substantially broken down by CYP4F2. Therefore, αT is predominantly accumulated in the body. Genetic mutations of αTTP in humans is associated with a deficient level of αT in the plasma, resulting in a neurological disorder called ataxia [13]. Despite the low αT level in the plasma of patients with αTTP mutation, urinary excretion of α-CEHC continued to increase in these patients [37]. Thus, αTTP is critical in protecting αT from degradation by hepatic enzymes.

The terminal metabolite CEHC was first identified in the urine of rats supplemented with δT in 1984 [27]. Since then, numerous studies have reported that similar metabolites derived from αT and γT were detected in human plasma and urine [28,38,39]. However, the mechanism involving vitamin E metabolism was not resolved until 2002. Sontag and Parker [24] and Birringer et al. [40] showed that HEpG2 cells, human liver cancer cells, can metabolize γT, δT, and γTE to various length of metabolites including long-chain 13'-OH, 13'-COOH, 11'-COOH, and 9'-COOH, and shorter-chain 7'-COOH, 5'-COOH and terminal metabolite 3'-COOH. The identification of these intermediate metabolites in cell culture media suggests stepwise β-oxidation occurs after ω-hydroxylation and oxidation of the thirteen carbon to remove two- or three-carbon moieties at each cycle until yielding the 3'-COOH.

Catabolism of vitamin E initiates by cytochrome P450 (CYP450) mediated ω-hydroxylation and oxidation of the phytyl side chain. CYP450 enzymes are common phases I enzymes to catalyze a variety of hydrophobic substances for drug deactivation, steroid metabolism, xenobiotic detoxification, fatty acid metabolism, generation of active metabolites and converting pre-carcinogen to an active carcinogen [41]. CYP450 4F2 (CYP4F2) is the critical enzyme for vitamin E metabolism. In mice, deletion of *Cyp4f14,*

a murine orthologue of human CYP4F2, impaired vitamin E metabolism [31]. CYP4F2 initiates vitamin E catabolism by inserting one oxygen atom into lipophilic substrates [42]. This CYP450-dependent monooxygenase requires the transfer of reducing equivalents from NADPH via a Flavin-containing reductase in the microsome [42]. Additionally, CYP4F2 has higher activities toward vitamin E form with unsubstituted 5-carbon position in the chromanol ring [30], and thus more reactive to non-αT forms of vitamin E. Upon CYP4F2-initiated ω-hydroxylation and oxidation, subsequent β-oxidation occurs in parallel to conjugation such as sulfation and glucuronidation of the phenolic on the chromanol ring in the mitochondria generate various carboxychromaols and terminal metabolites 3'-COOH [1] (Figure 1.2).

Conjugation such as sulfation and glucuronidation is essential in vitamin E metabolism. In addition to unconjugated carboxychromanols, sulfated long-chain carboxychromanols including sulfated 13'-COOH, 11'-COOH, and 9'-COOH were identified in the cell culture media of human A549 cells after cultured with γT, δT, and γTE [25] and in plasma and liver of rats after γT supplementation [25,26,43]. The identification of conjugated long-chain carboxychromanols indicates that conjugation co-occurs with β-oxidation. More interestingly, conjugated carboxychromanols are the predominant forms of metabolites found in the plasma of rats supplemented with γT and γTE [26]. Findings from these *in vitro* and *in vivo* studies support the notion that vitamin E forms are metabolized by CYP4F2 via ω-hydroxylation followed by β-oxidation and concurrently conjugation.

Different steps of vitamin E metabolism take place in different subcellular compartments of hepatocytes. By isolating microsomes, mitochondria, and peroxisomes from the liver of rats with αT injection, Mustacich et al. [44] found that unmetabolized αT

and 13'-OH is predominant in microsomes followed by peroxisome, and end metabolite α-CEHC was found exclusively in mitochondria. These findings suggest that ω-hydroxylation and oxidation occur in microsome and peroxisome compartment of hepatocytes, whereas β-oxidation and conjugation take place in the mitochondria.

A large amount of tocopherols, tocotrienols, and their metabolites were found in feces of rats supplemented with γT, δT, γTE, and δTE [33,45], suggesting that fecal excretion is the major route of vitamin E elimination. On the other hand, terminal metabolite CEHCs and conjugated CEHCs are primarily excreted in the urine [27,28,46,47]. Bardowell et al. [30] reported higher fecal excretion of metabolites than those in the urine when mice were fed with tocopherols. Unmetabolized vitamin E forms can also be eliminated in bile, although higher preference to excrete γT over αT [48]. Interestingly, Traber et al. [49] reported that some phase III transporters, such as the ABC transporters, may be involved in the elimination of vitamin E and vitamin E metabolites, and the expression of these transporters are regulated by vitamin E intake. The elimination of excess αT and non-αT forms of vitamin E is to prevent excess accumulation of vitamin E in the body.

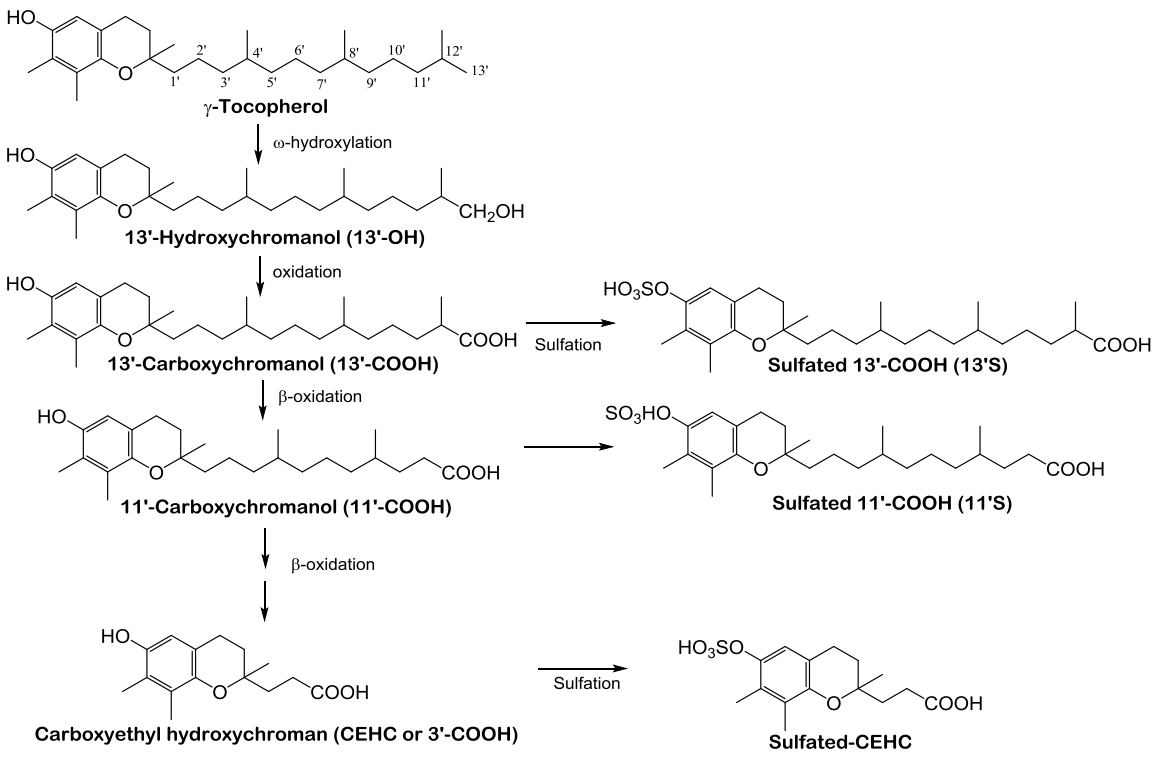

Figure 1.2 Molecular mechanism of vitamin E metabolism and the formation of metabolites.

1.1.3 Biological activities of vitamin E forms

Although non-αT forms of vitamin E have lower tissue bioavailability, these vitamers have different and superior biological functions in disease prevention and therapy compared to αT [1,50,51]. Long-chain metabolites 13'-COOHs derived from vitamin E forms showed stronger bioactivities compared to their corresponding vitamers [1]. These 13'-COOHs have been shown to exhibit dual inhibitory activities against pro-inflammatory enzymes, cyclooxygenases [52,53] and 5-lipoxygenase [54], that contribute to cancer development and progression. Additionally, recent research reveals that 13'-COOHs could induce apoptosis and autophagy in human cancer cells through the modulation of sphingolipids, which leads to suppression of colon tumor development in mice [55].

1.1.3.1 Antioxidant activities of vitamin E forms and carboxychromanols

All vitamin E forms possess similar phenolic moiety, and thus all of them are potent antioxidants that can scavenge lipid peroxyl radical by donating hydrogen atom from the phenolic group [1,11]. Antioxidants are essential for protecting against oxidative damages in tissues, which can prevent many diseases. Vitamin E is well known for its antioxidant activity against lipid peroxidation. Although all vitamin E forms possess similar capability to scavenge lipid peroxyl radical, natural vitamin E forms with an unsubstituted 5-carbon position, i.e., γT, can trap electrophils like reactive nitrogen species [56], whereas αT, vitamin E with methylated 5-carbon position, lack of this ability [56]. Therefore, γT appears to have more superior activity than αT in detoxifying reactive nitrogen species by forming 5-nitro-γT [1,11,56-58]. Reactive nitrogen species are often enhanced during inflammation, which exacerbates tissue damages. In rats with zymosan induced-peritonitis, the level of 5-nitro-γT increased, suggesting nitration of γT under inflammatory condition traps reactive nitrogen species [59]. Besides tocopherols, tocotrienols with three double bonds on the phytyl-chain appear to better at scavenging peroxyl radicals in phospholipid bilayer than αT [60,61]. Due to more even distribution in the phospholipid bilayer, tocotrienols can more effectively interact with lipid peroxyl radicals in the membrane environment than tocopherols [60,61]. As a result, tocotrienols may be more efficient in scavenging lipid peroxyl radical in cellular or the whole-body environment. In addition to tocopherols and tocotrienols, long-chain metabolites, 13'-OH and 13'-COOH, from δT or δTE have been reported to have potent antioxidant activities against lipid peroxidation in vitro [62]. All vitamin E forms including long-chain metabolites are potent antioxidants.

1.1.3.2 Anti-inflammatory properties of vitamin E forms and metabolites

Chronic inflammation in the body can lead to the development of various chronic diseases including asthma, inflammatory bowel diseases, and cancer [63-70]. Inflammation is an immune response to injuries or infection, which is beneficial to the host to impair injury and evacuate virus and pathogens under normal condition [63]. However, aberrant immune response to commensal bacteria in the gut [71] or non-pathogenic stimuli in the airway [63] can cause chronic inflammatory response leading to the pathogenesis of the disease. During an inflammatory response, the production of reactive oxygen/nitrogen species increases along with elevated production of pro-inflammatory mediators including lipid mediates, and pro-inflammatory cytokines, such as TNFα, IFN-γ, IL-1β, and IL-6 [72-74]. These reactive chemical species and pro-inflammatory mediators exacerbate inflammation and cause further damages to the host. Vitamin E forms and their metabolites not only contain antioxidant activities to scavenge reactive species as mentioned earlier but can also inhibit the production of pro-inflammatory mediators [52,54] (Figure 1.3), which can protect against inflammatory damages.

Prostaglandins and leukotrienes are lipid mediators synthesized from polyunsaturated fatty acid, arachidonic acid, which are critical in generating inflammatory response [74,75]. Prostaglandin E_2 (PGE_2) is one of the most abundant prostaglandins produced in the body via the oxidation of arachidonic acid catalyzed by cyclooxygenase-1/2 (COX-1/2) that exhibits multiple biological functions, including regulation of immune responses, blood pressure, and gastrointestinal integrity [75]. Dysregulated synthesis of PGE_2 can lead to signs of inflammation, such as redness, swelling, fever, and pain [76]. Another lipid mediator, leukotriene B_4 (LTB_4), can be biosynthesized from arachidonic acid via 5-lipoxygenase (5-LOX)-catalyzed reaction in neutrophil [74]. LTB_4 is a potent

chemoattractant that stimulates the adhesion of leukocytes to endothelial cells [76]. Patients with inflammatory bowel diseases (IBD) had shown to have a higher mucosal concentration of LTB_4 than healthy individuals [77], which is associated with epithelial damage and leukocyte infiltration into the intestinal [78]. Eicosanoids produced from COXs and 5-LOX-catalyzed reactions are known to promote various types of cancers [79]. Due to the critical roles of eicosanoids in inflammation, drugs targeting COXs and 5-LOX are often used to treat chronic inflammatory diseases [79-81].

Cytokines are essential molecules involving in the regulation of inflammatory response and pathogenesis of inflammation-associated diseases. Patients with IBD and colorectal cancer (CRC) reported having elevated levels of pro-inflammatory cytokines including TNFα, IL-1β, IL-6, and IL8 [66]. Infliximab, an anti-TNFα antibody, has been used to treat Crohn's disease clinically [82]. The expression of cytokines and chemokines are mediated by transcription factors such as nuclear factor (NF)-κB and JAK-STAT6/3 as a result of receptor-mediated signaling activation in immune cells in response to inflammatory conditions. Many studies had revealed the mechanisms underlying the anti-inflammatory properties of specific vitamin E forms (γT, δT, γTE, and δTE) and their long-chain 13'-COOH metabolites via the inhibition of COX-2 and 5-LOX and suppression of various signaling pathways including NF-κB, JAK-STAT6, and JAK-STAT3.

In terms of COX-2 inhibition, vitamin E forms differentially inhibit COX-2-mediated PGE_2 synthesis in immune cells and epithelial cells [52,83]. In 2000, Jiang et al. [83] were the first identified that γT potently reduce PGE_2 production in LPS-stimulated RAW264.7 murine macrophages and IL1β-treated A549 human epithelial cells with IC_{50} of 7.5 μM and 4 μM, respectively. Later in 2008, Jiang et al. [52] discovered that γTE and δT

showed even better inhibition activity than γT against COX-2-mediated PGE_2 production in IL-1β-induced A549 cells without affecting COX-2 expression. The relative potency for COX-2 inhibition by these vitamin E forms is ranked as γTE ≈ δT > γT >> αT. Interestingly, these vitamin E forms fail to inhibit the activity of purified COX-2, suggesting these vitamin E forms are weak COX-2 inhibitors [52]. More importantly, the cellular inhibition of vitamin E forms was significantly diminished when co-incubated with sesamin in which blocked the metabolism of vitamin E in A549 cells, suggesting that vitamin E metabolites are the major player for the inhibition of COX-2 [52]. This notion is supported by the fact that conditioned media enriched with long-chain carboxychromanols without sulfated counterparts potently inhibited COX-2 activity in intact-cell assay and purified COX-1/2 enzyme assay [52]. The length of the side chains of these metabolites also exhibits different strength in COX-2 inhibition with 13'-COOH ≈ ibuprofen > 9'-COOH >> 5'-COOH > acetaminophen > 3'-COOH [52,83]. Enzyme kinetic data demonstrated that 13'-COOH is a competitively inhibiting the cyclooxygenase activity, not peroxidase activity of COX-1 and COX-2 with Ki of 3.9 and 10.7 μM, respectively [52]. These data along with computer simulation support that 13'-COOH binds to the substrate binding site of COX by forming hydrogen-bonds with Tyr 355 and Arg120 with the carboxyl group of 13'-COOH [52]. Furthermore, the chromanol ring of 13'-COOH appears to provide further interaction with Phe209, Phe381, and His226 via hydrophobic interaction and hydrogen bond formation [52].

Besides inhibition against COX-1 and COX-2, vitamin E forms differentially inhibit LTB_4 and LTC_4 productions from ionophore (A23187)-stimulated neutrophil-like differentiated HL-60 cells and human neutrophils isolated from peripheral blood, with IC_{50} of 5-20 μM for γT, δT, and γTE, but much higher IC_{50} for αT [54]. However, none of these

vitamin E forms inhibits human recombinant 5-LOX at physiological dose [54]. Nevertheless, δT-derived 13'-COOH potently inhibits human recombinant 5-LOX activity with IC_{50} of 0.5-1 μM [54]. Interestingly, these vitamin E forms, γT and δT, despite showing no effect on human recombinant 5-LOX activity, strongly suppressed ionophore-stimulated ERK-phosphorylation and activation of 5-LOX by inhibiting the translocation of 5-LOX from cytosol to the nucleus [54]. Additionally, vitamin E forms can reverse membrane perturbation by induced by ionophore, as a result, suppress calcium influx and prevent the activation of downstream signaling [54]. Noteworthy, vitamin E forms suppress calcium influx and LTB_4 formation triggered by stimuli such ionophores, sphingosine 1-phosphate, and lysophosphatidic, but not by fMLP or thapsigargin, whereas 13'-COOH can decrease LTB_4 formation regardless of different stimuli [54]. These observations are consistent with 13-COOH's strong inhibition for 5-LOX.

The inhibitory effects of vitamin E forms on pro-inflammatory cytokines and chemokines are via the modulation of key transcription factors including CCAAT-enhancer binding protein β (C/EBPβ), NF-κB, and STAT6/3 [84-89]. Vitamin E forms show inhibition against LPS-induced IL-6 production in macrophage with δTE and γTE being the strongest in this activity [84,86,87,90]. However, this inhibitory effect of vitamin E forms is not due to the upregulation of anti-inflammatory cytokines [86,87], but instead is by the downregulation the gene expression of COX-2 [86] and suppression of C/EBPβ and NF-κB [84]. With the inhibition of C/EBPβ, γTE also decreases granulocyte-colony stimulating factor (G-CSF), a target gene of C/EBPβ, induced by LPS [84]. In addition to the suppression of C/EBPβ, γTE exhibits strong inhibitory activities against activation of NF-κB stimulated by LPS [84]. Previously, γTE has been shown to inhibit NF-κB activation in various cancer

cells and TNFα-stimulated KBM-5 cells, myelogenous leukemia cell [89]. Consistently, γTE inhibits TNFα-triggered activation of NF-κB by up-regulation of an anti-inflammatory molecule, A20, induction of cellular stress and modulation of sphingolipid metabolism [90]. δTE, an analog of γTE, exerts these same actions as γTE, but δTE exhibits more robust activities against NF-κB activation than γTE by increasing the level of CYLD, a negative regulator of NF-κB, which is not up-regulated by γTE [85].

Besides acting immune cells, vitamin E forms, especially γTE dose-dependently inhibits the secretion of eotaxin-3 induced by IL-13 in A549 cells by blocking the phosphorylation and DNA-binding of STAT6 [88]. This obstruction of IL-13-stimulated STAT6 phosphorylation by γTE is due to increase expression of prostate-apoptosis-response 4 (PAR4) and enhance formation of PAR4/atypical protein kinase C (aPKC) complex, as a result, blocks STAT6 activation by aPKC [88]. This inhibition of eotaxin-3 production is critical for the pathogenesis of asthma as eotaxin-3 acts as a chemoattractant for airway eosinophils leading to the development of eosinophilia in the airway, which is a characteristic of asthma [1]. Additionally, Rajendran et al. demonstrated that γTE inhibit the activation of STAT3 via induction of protein-tyrosine phosphatase SHP-1 in human hepatocellular carcinoma cells [91]. γTE up-regulated the expression of SHP-1, which is involved in the negative regulation of JAK/STAT3 cell signaling pathway by suppression the phosphorylation, translocation, and DNA-binding of STAT3 [91].

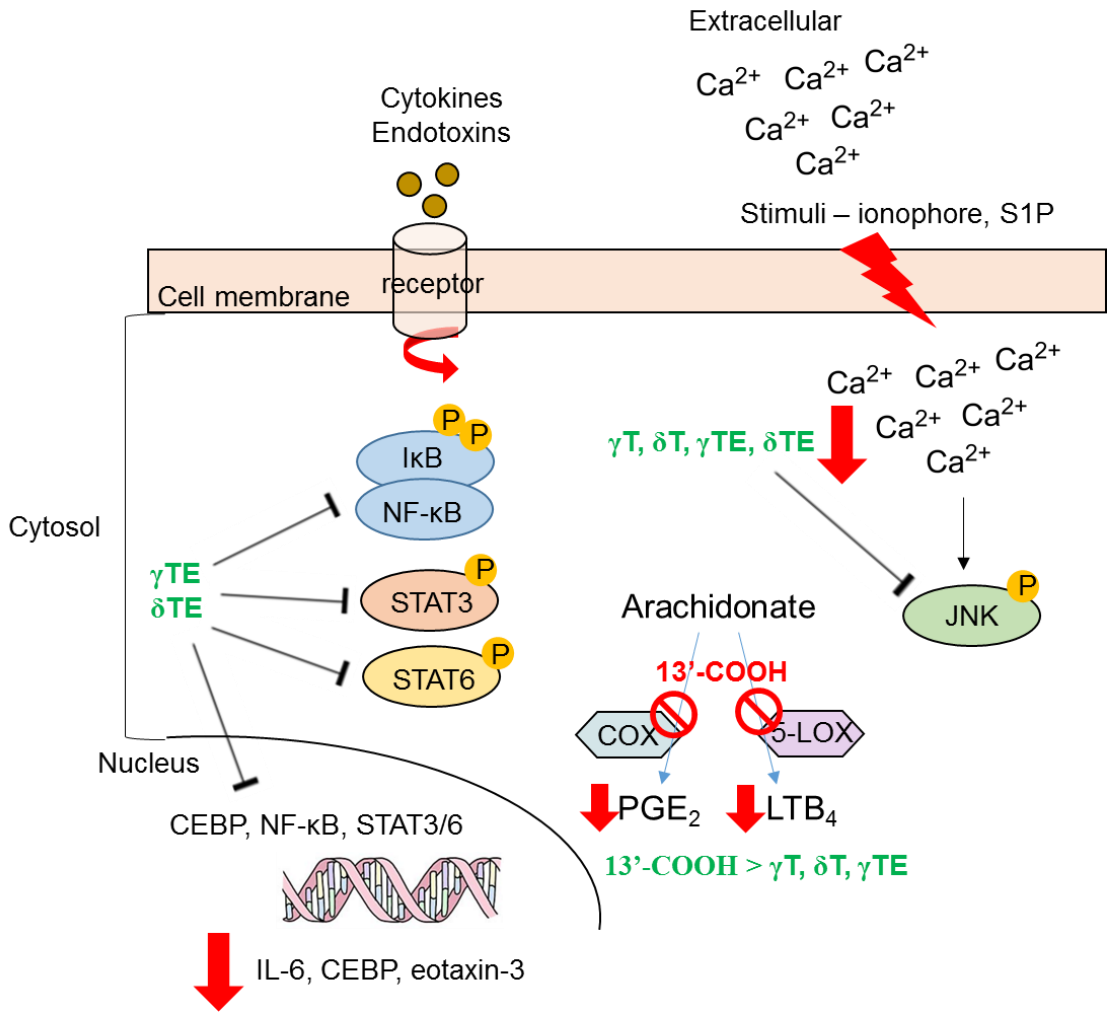

Figure 1.3 Mechanisms underlying the anti-inflammatory properties of vitamin E forms and long-chain carboxychromanols metabolites.

1.1.3.3 Chemoprevention effects of vitamin E forms against cancer

As a powerful antioxidant that can block DNA damages induced by oxidative stress, vitamin E forms are viewed as potential options for cancer prevention. Earlier vitamin E research on cancer prevention are mostly focus on αT due to the high bioavailability in the body. Even though epidemiologic studies consistently showed a negative association between αT and cancer risk, many large randomized studies on using αT for cancer prevention showed inconsistent and disappointing results [11,92,93]. One of the primary reason

is due to the lack of preclinical model and mechanistic investigations on the role of αT in cancer prevention. Recent research has shown that other vitamin E forms and their long-chain metabolites exhibited potent anti-cancer activities in preclinical cancer models and mechanistic studies, while αT often showed disappointing outcomes in these models [94].

As discussed in the previous section, non-αT forms of vitamin E are not only powerful antioxidants, but also contain anti-inflammatory properties via inhibition of COXs and 5-LOX as well as NF-κB and STAT6/3 cell signaling pathways. Inflammation in tumor microenvironment can contribute to the initiation, promotion, and progress of cancer [69,95]. Besides anti-inflammatory properties, these vitamin E forms and metabolites can directly target the fate of cancer cells by promoting apoptosis and inhibiting proliferation via various signaling pathways [50,51].

Vitamin E forms, γT, δT, γTE, and δTE, and long-chain 13'-COOHs have been shown to activate various pathways associated with anti-proliferation, promote apoptosis and autophagy in numerous cancer cell type. Treatment with these vitamin E forms and 13'-COOHs led to PARP cleavage, activation of caspase 9 and elevated LC-3 expression, all of which are markers for apoptosis and autophagy in various types of cancer cells [55,96,97]. These biological events induced by vitamin E and 13'-COOH may due to their ability to modulate sphingolipid metabolism. Sphingolipids such as dihydroceramide, dihydrosphingosine, and ceramides are involved in the regulation of cell death and survival, and continuous elevation of these sphingolipids could lead to cellular stress, thus inhibit cell proliferation, and promote apoptosis [98,99]. Vitamin E forms, specifically, γT [100] and γTE [96,97], and 13'-COOHs [55] derived from δT and δTE increase dihydrosphingosine, dihydroceramide, and ceramides in prostate, pancreas, and colon cancer cells, which are

consistent with the observation of cell death, apoptosis, and autophagy in these cells. Among these vitamin E forms and metabolites, δTE, γTE, and 13'-COOHs appears to be more potent than γT and δT, but still much better than αT [55,96,97,100]. This may due to the accumulation of tocotrienols instead of tocopherols in cells [96,101]. Interestingly, the accumulation of tocotrienols is also higher in cancer than normal tissues *in vivo* [102,103]. Although the mechanism underlying tocotrienol accumulation in cancerous tissues is unclear, the current evidence suggests that tocotrienols may have better anticancer efficacy than tocopherols in the body.

1.2 Colon inflammation

1.2.1 Prevalence and characteristics of IBD

IBD is comprised of two idiopathic, chronic, inflammatory disorders of the gastrointestinal tract, Crohn's Disease (CD) and Ulcerative Colitis (UC). An estimation of 3 million adults in the U.S. was reported being diagnosed with IBD [104], which does not include children under the age of 18 who may also have IBD [105]. The prevalence of IBD not only increased in the U.S but worldwide [106]. Patients with IBD often have delayed response to pathogens recognition and clearance in addition to impaired intestinal barrier function resulting in a bacterially drive, abnormal immune-mediated response [107]. The pathoetiology of IBD remains unclear, yet predisposing genetic factors, disrupted microbial composition, defect in the gastrointestinal epithelial barrier and the immune system tend to play essential roles in the development of IBD [108].

Postulated pathogenesis of IBD is that the development of an inappropriate adaptive immune response toward a subset of commensal enteric bacteria in a genetically susceptible host, then triggered by environmental factors leading to epithelial barrier impairment and the activation of disease [65]. Genetic variation and mutation in genes

involved in immune regulation, cellular activation, and epithelial barrier functions are often associated with the pathogenesis of IBD, such as NOD2, IL23R, DLG5, and PPAR-γ [67]. Under normal condition, intestinal epithelial cells and innate immune cells recognize microorganisms through unique identification of molecular markers to prevent the invasion of pathogens and to regulate the immune response to commensals [109]. The pathogen recognition receptors (PRRs), such as toll-like receptors (TLRs) or the NOD-like receptor (NLR) family, are presented on the cell surface of immune cells to identify pathogenic bacteria or cellular stress, and play very critical role in the innate immune system and the onset of colitis via various inflammatory pathways [110]. Genetic mutation in these pathways can induce inappropriate immune response toward commensal microorganisms through stimulation by environmental factors leading to activation of IBD (Figure 1.4).

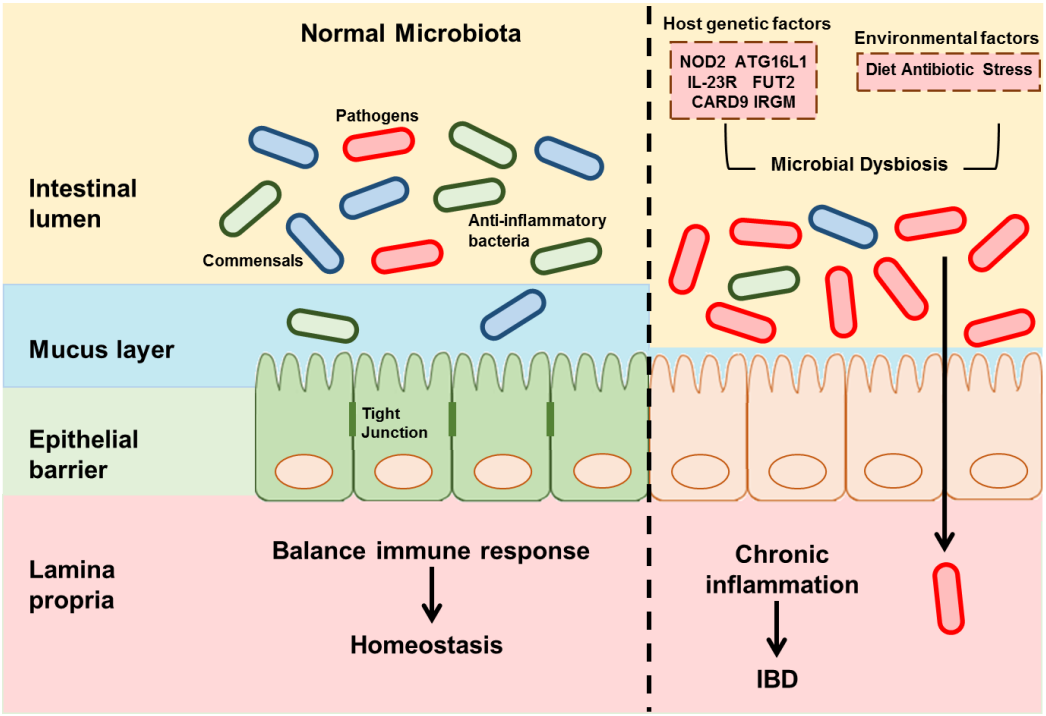

Figure 1.4 Interactions between intestinal microbiota and host immune response in inflammatory bowel disease.

1.2.1.1 Environmental factors associated with IBD

Environmental risk factors for IBD development, such as smoking, dietary styles, and personal hygiene, are shared by all populations regardless of race, ethnicity and geographical location [108,111]. A meta-analysis in 1989 showed a causal relationship between smoking and Crohn's disease [112]. Smoking was shown to exacerbate dysbiosis of gastrointestinal microbiome in patients with Crohn's disease [113] leading to aggravation of the disease. Smoking cessation was able to improve the prognosis of the disease [114].

Westernized dietary habits such as low fiber and high dietary fat also increase the risk for IBD [115]. Dietary fiber may act as a substrate for the microbes via direct interaction, or indirectly influence the composition of microbiome via immunomodulation [116]. A western diet high in saturated fat could modulate host bile acid composition resulting in alteration of gut microbial population and distribution, leading to an abnormal immune response that causes IBD [117].

Other factors such as breastfeeding and physical activity also play a critical role in the development of IBD. A short breastfeeding period and physical inactivity tend to increase the risk for IBD [118]. Breastfeeding during infancy may reduce the infant's risk of developing CD or UC later in life [119]. The bioactive components in breastmilk can protect against childhood infection, which reduces the use of antibiotics. Human milk oligosaccharides have prebiotic activities, which interact with neonatal intestinal microbiome and influence the development of the innate mucosal immunity.

The hygiene hypothesis postulates that urbanization of society becomes a significant risk factor for the development of IBD due to the lack of early childhood exposure to microbes with improved sanitation, which leads to a greater susceptibility to develop an abnormal host immune response upon microbial exposure later in life [120]. Over-

exposure of antibiotics increases the risk of new-onset IBD in children due to the disruptions of healthy microbial population and distribution in the gut [121]. Many risk factors for IBD are associated with the influence of intestinal microbiota suggesting that gut microorganisms play a crucial role in the pathogenesis of IBD.

1.2.1.2 Disturbed microbial composition

Generally, intestinal microorganisms are viewed as symbionts by establishing a mutual relationship with the host. The host provides a nutritious environment and residence for the gut microbes, and as return, the microbes produce short-chain fatty acids and essential vitamins for the host [122]. However, disease or poor dietary habits will disrupt microbial communities, reduce microbial diversity and give rise to harmful microorganisms that could negatively affect host health [122-124]. This perturbance in gut microbial population is referred to as "dysbiosis," which is a pattern often observed in patients with IBD. Increased penetration of bacteria in mucosa and decreased bacterial species richness are observed in IBD patients. These two markers are often correlated with increased disease activity. Several bacterial taxa are enriched in IBD, such as *Proteobacteria*, *Escherichia coli*, *Bacteroides*, *Desulfovibrio*, *Ruminococcus*, and *Clostridium difficile* [124,125]. Butyrate-producers in the class Clostridia are commonly depleted in IBD patients [123]. *Faecalibacterium prausnitzii*, a butyrate-producer, is reduced in the fecal samples from IBD patients. The family Lachnospiraceae also tends to decrease in IBD patients. This family has been found to contain many butyrate-producers [123,124,126]. These microbial patterns of dysbiosis may be useful indicators and effective screening markers for IBD.

Although dysbiosis or presence of pathogens on colonic mucosal has been linked to the pathogenesis of inflammatory bowel diseases, the role of microbiota in the induction and progression of IBD has not yet been fully elucidated. In order to investigate the participation of bacteria in the development of IBD, the analysis of microbiota is not sufficient, and the gnotobiotic model becomes a necessity. A study using human microbiota-associated (HMA) mice by gavage of colon biopsy from patients with active ulcerative colitis to gnotobiotic BALB/c mice showed that mucosa-associated microbes from UC patients did not induce spontaneous colitis but increased the susceptibility to DSS-induced colitis after four generations compared to the first generation HMA mice or germ-free (GF) mice without human microbiome transplant [127]. These findings suggest microbiota from UC patients may contain certain protective species, but became faded or took over by pathogens during natural colonization with co-housing. Interesting, the conventional mice had more severe colitis symptoms and colon damage than the GF mice after DSS treatment [127], suggesting that the presence of pathogens may exacerbate DSS-induced colitis. Contrarily, a group from Sweden showed that although GF and pseudo-GF mice, treated with antibiotics, had significantly lower colon and systemic inflammation after DSS treatment than conventional mice, GF mice appeared to have more rectal bleeding and epithelial barrier damage compared to the pseudo-GF and conventional mice [128]. This suggests that the presence of some beneficial microbes may have protective effect against epithelial damage induced by DSS. Similarly, to examine the effect of *Enterococcus faecalis*, a pathogen found in the GI tract of both human and animals, on IBD, the GF and conventional interleukin-10 (IL-10) knockout (KO) mouse model were used [129]. GF mice developed a more rapid and robust response toward *E. faecalis*

colonization compared to the conventional animals, suggesting that the presence of commensal bacteria may contribute the protection against pathogen colonization for IBD development [129]. The results from the first study contradict with the other two studies. This could be that different the mouse strains used in these studies, which may lead to a different response to DSS treatment. BALB/c mice are known to be a susceptible strain to DSS [130-133], and GF model of BALB/c mice may have a lower susceptibility to DSS than the conventional BALB/c, which contributes to the contradicting results in these studies. Despite the contradictory results, these studies using the GF model provide valuable information on the roles of gut microbiota on IBD development.

Besides the damages caused by pathogenic microorganisms, several strains of *Lactococcus* are identified as probiotics that may be protective against IBD [134]. *L. lactis* is a lactic acid bacterium commonly used in the industry for the production of safe, healthy, and tasteful milk fermentation products [135]. Recently, *L. lactis* has been used as a vehicle for delivery of therapeutics into the gastrointestinal tract due to the high tolerance to low pH and bile [134-137]. By using *L. lactis* as a vehicle to delivery antimicrobial peptides, *L. lactis* enhanced the effect of the antimicrobial peptide by reducing the clinical symptoms and maintaining epithelial integrity after DSS treatment in BALB/c mice [138]. In addition to the facilitating activity for therapeutic drugs, *L. lactis* alone contains anti-oxidation and anti-inflammatory effect against colitis in murine models. Oxidative stress and excess formation of reactive oxygen species (ROS) are detrimental to intestinal epithelial cells, which contribute to the pathogenesis of IBD [139]. The strain *I-1631* of *L. lactis* possesses genes encoding enzymes that can detoxify ROS, such as superoxide dismutase (SodA), which is essential in the attenuation of colitis in mice [140]. Inactivation of SodA gene

abolished the superoxide scavenging effect of *L. lactis*, suggesting that this strain of *L. lactis* may be a novel vehicle to deliver antioxidant, SodA, to the inflamed colon. Another strain of *L. lactis, NZ9000*, secretes anti-inflammatory molecule, heme oxygenase-1, which increased the production of anti-inflammatory cytokine IL-10 and reduced the expression of pro-inflammatory cytokines IL-6 in the colon of DSS treated mice [141]. Other probiotic bacteria such as *Lactobacillus* and *Bifidobacterium* have been shown to promote recovery from DSS-induced colitis in mice [142]. The clinical symptoms induced by DSS were significantly ameliorated by orally delivered probiotics cocktail containing *L. acidophilus*, *L. plantarum*, *B. lactis*, and *B. breve* [142]. The probiotic treatments also reduced the level of nitric oxide and Interferon-γ (IFN-γ) in the plasma by reducing the colonic expression of TLR4, iNOS, and nuclear factor (NF)-κB [142]. Increase probiotic bacteria in the gut or promote the growth of probiotics by dietary prebiotics may protect against IBD.

1.2.1.3 Impaired barrier function

The gastrointestinal epithelium is the body's largest protective barrier from the external environment. The epithelium allows nutrient absorption by specific transporters and channels. Water and ions can also cross the epithelium through the intercellular space between the adjacent epithelial cells. This selective permeability that allows passage for water and ions but not pro-inflammatory molecules, such as pathogens, toxins, and antigens, is controlled by the paracellular pathway [143]. The tight junction (TJ) complex is a group of apical structural proteins that regulate the paracellular pathway of selective permeability. These TJ proteins can be modified by various extracellular stimuli that can influence the epithelial permeability, and the modification of TJ proteins is closely associated with disease susceptibility [144]. Under pathophysiological conditions, pro-inflammatory

cytokines, antigens, pathogens, and other mediators contribute to epithelial barrier dysfunction.

Accumulating evidence suggests that a defect in the gastrointestinal epithelial barrier is an essential factor for the development of IBD. Many studies have demonstrated that patients with IBD are suffered from inflammation-induced leak flux diarrhea due to impaired intestinal barrier [145-147]. Gerova et al. showed increased intestinal permeability in IBD patients [146]. Schulzke et al. also found that patients with CD or UC had increased intestinal epithelial leakiness due to reduced TJ complexity with lower TJ strands and increase of the appearance of strand discontinuities [147]. TJ strands are critical for the maintenance of the TJ integrity. The interaction of TJ proteins on the apical cell membrane of the epithelial cells with the TJ proteins on the adjacent epithelial cells forms a barrier strand that protects against the permeation of harmful molecules cross the intestinal lumen [148]. Consistent with studies in human, studies in the mouse model of colitis with dextran sodium sulfate (DSS) treatment also demonstrated an impaired intestinal barrier function indicated by increase colonic permeability and loss of TJ protein, zonula occluden-1 (ZO-1) [149]. The increased passage of intestinal antigens from the lumen to the mucosal tissue and the circulation activates the mucosal and systemic inflammatory response that accelerates the progression of IBD [150]. Based on the current findings, intestinal barrier dysfunction appears to be one of the major characteristics of IBD.

TJ proteins are multiple protein complexes located at the apical ends of the lateral membranes of epithelial and endothelial cells to regulate the passage of ions, water, and molecules through the paracellular pathway. TJ acts as a fence for maintenance of cell polarity by blocking the free intercellular diffusion of proteins and lipids across the

intestinal lumen [151]. There are four transmembrane proteins, occludin, claudins, junctional adhesion molecules (JAMs), and tricellulin, located on the membrane of the intestinal epithelial cells. The extracellular domains of transmembrane proteins form a selective barrier with the TJ proteins on the neighboring epithelial cells [152]. The intracellular domains of transmembrane proteins are linked to the peri-junctional actomyosin ring via the interaction with the cytosolic scaffold proteins called ZO-1 [153]. In addition to the vital role in the maintenance of TJ structure and function, the interaction of TJ protein with the actomyosin ring allows regulation of TJ barrier integrity by the cytoskeleton. Phosphorylation of myosin light chain (MLC) by MLC kinase (MLCK) contracts and tenses junctional actomyosin ring, resulting in loosening of the TJ [154].

Many factors have a direct impact on tight junction proteins and consequently influence the intestinal epithelial barrier. In particular, pro-inflammatory cytokines and other inflammatory mediators play a critical role in the regulation of intestinal epithelial barrier in IBD patients. Elevate levels of pro-inflammatory cytokines, such as TNF-α, IL-1β, IFN-γ, IL-6, and IL-8, have been reported in CD and UC patients [66]. The elevation of pro-inflammatory cytokines causes epithelial damage and disturbs TJ structures by affecting the distribution and expression of TJ proteins [147,155].

Pro-inflammatory cytokines can cause barrier dysfunction through the modification of TJ protein assembly and expression. In a Caco-2 cell model, TNF-α increased monolayer permeability, reduced ZO-1 protein and disrupted the localization of ZO-1 by activating transcription factor NFκB [156]. The addition of NFκB inhibitors, curcumin and triptolide, mitigated TNF-α-mediated increase in permeability and prevent redistribution of ZO-1 in Caco-2 cells, suggesting that NFκB activation is associated with barrier dysfunction

induced by TNF-α. Moreover, the activation and translocation of NFκB to the nucleus can be bound to the promoter region of MLCK gene, which increases MLCK promoter activity [157]. Deletion of the NFκB binding site on MLCK promoter region prevented TNF-α-induced NFκB activation in promoter activity [157].

In addition to TNF-α, IL-1β also affect intestinal permeability through modification of TJ proteins. In the Caco-2 cellular model, IL-1β dose- and time-dependently increased epithelial permeability [158] by rapidly activated NFκB. NFκB inhibitors, pyrrolidine dithiocarbamate (PDTC) and curcumin, abolished IL-1β-induced increase in Caco-2 epithelial permeability. Furthermore, silencing NFκB p65 expression by siRNA transfection completely inhibited the IL-1β-induced increase in Caco-2 epithelial permeability. Additionally, IL-1β significantly reduced occludin mRNA and protein, which was attenuated by in the presence of PDTC. Overall, these studies suggest that pro-inflammatory cytokines stimulate intestinal epithelial leakage through inflammatory pathways.

Additionally, loss of intestinal barrier function in IBD patients is associated with increased inflammatory mediators, including reactive oxygen species (ROS) such as nitric oxide, and prostaglandins [159]. These inflammatory mediators promote inflammation by increasing the production of pro-inflammatory cytokines. TJ composition is altered in response to the cytokine activity, which allows further passage of inflammatory mediators. This repeated cycle of chronic inflammation associated with increased intestinal permeability initiates and aggravates the progression and pathogenesis of IBD (Figure 1.5).

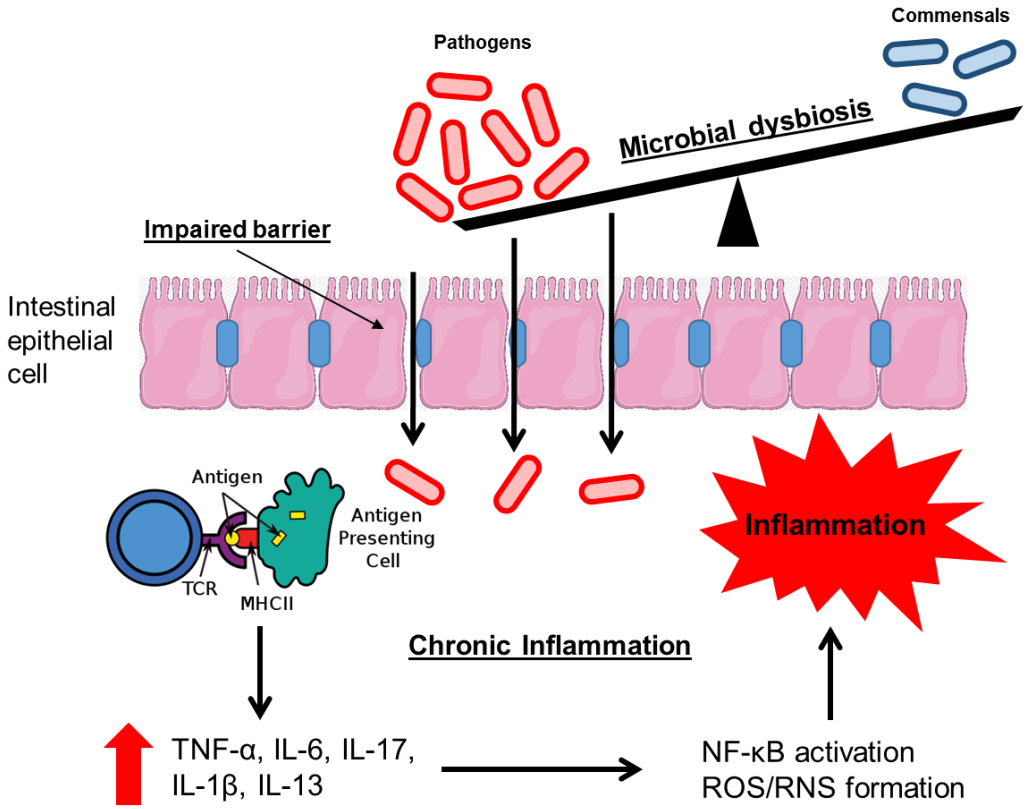

Figure 1.5 Excess inflammation, impaired barrier function, and perturbed intestinal microbial composition are common characteristics of IBD.

1.2.2 Vitamin E as a potential therapy for IBD

Inflammatory mediators including eicosanoids and pro-inflammatory cytokines are important in the pathogenesis of IBD. Patients with IBD have shown to have an elevated level of prostaglandin and LTB_4 in mucosa and serum as well as pro-inflammatory cytokines [66,77]. Vitamin E forms and 13'-COOHs as potent inhibitors of COXs and 5-LOX, in addition to their inhibitory effects on NF-κB, can be useful therapeutic options for IBD. To this end, Li et al. [160] reported that γTmT supplementation dose-dependently reduced DSS-induced colon inflammation and damage, as well as serum PGE2 in mice independent of nuclear factor (erythroid-derived-2)-like 2 (Nrf2). Additionally, Jiang et al. [32] showed

that supplementation of γT at 0.1% diet alleviated moderate colitis symptoms, attenuated colon inflammation-associated damages, and reduced plasma IL-6 level in mice treated with one cycle of DSS, but not severe colitis induced by three DSS cycles. Additionally, αT, when combined with selenium, attenuated colitis induced by acetic acid in rats [161].

1.3 Colorectal Cancer

1.3.1 Prevalence and types of colorectal cancer

Colorectal cancer is one of the leading causes of cancer death in developed countries. The expected new cases of colorectal cancer to be diagnosed in the United States will be 51,690 and 49,730 in men and women respectively [162]. The anticipated death of these newly diagnosed patients is estimated 27,640 in men and 23,380 in women [162], despite advances in detection, surgery, and chemotherapy. The trend of death from colorectal cancer is still increasing in the United States in the last few decades, suggesting that more effective tools have not yet developed at this point of time to treat this fatal disease. Therefore, more attention is required on the development of a non-toxic and simple to apply drug, that is effective for the prevention and treatment of colorectal cancer.

1.3.2 Inflammation-associated colon cancer

In the cases of colorectal cancer, only about 20% have a familial basis, such as hereditary nonpolyposis colorectal cancer and familial adenomatous polyposis [163]. The genetic model of colorectal tumorigenesis involves a multistep process that results in the aberration of chromosome and gain/loss of genetic material [164]. There are numbers of oncogenes and tumor suppressor genes play essential roles in the transformation of adenoma to carcinoma. The mutational activation of k-ras gene family is one of the mechanisms associated with malignant transformation, whereas the p53 tumor suppressor

gene is involved in the negative regulation of the cell cycle and apoptosis [163]. Adenomatous polyposis coli (APC) gene mutation also plays an essential role in tumorigenesis. APC negatively regulates β-catenin, which is considered to be the "gatekeeper" gene in the process of tumor development. However, most cases of colorectal cancer are linked to environmental causes rather than heritable genetic mutations.

Many evidence suggests a link between inflammation and tumor development. Recent research has provided evidence to support that inflammation-caused tissue damage can initiate or promote cancer development [165-168]. Risk factors for colorectal cancers include environmental and food mutagens, specific intestinal bacteria population, and chronic intestinal inflammation that leads to tumor development. Colitis-associated cancer is a subtype of colorectal cancer that is associated with inflammatory bowel disease. Colitis-associated cancer is very difficult to treat and highly mortal [169]. A meta-analysis of 8 studies showed that an average of 1.6% of patients with ulcerative colitis was diagnosed with colorectal cancer after 14 years [170]. Although the development of colitis-associated cancer is linked with inflammatory bowel disease, there are pathogenic similarities between colitis-associated cancer and other types of colorectal cancer in development [171].

The essential stages of cancer development, such as the formation of aberrant crypt foci, polyps, adenomas, and carcinomas, are similar between familial basis colorectal cancer and colitis-associated cancer. Common signaling pathways involve in the development of sporadic colorectal cancer, and colitis-associated cancer include those involved in Wnt, β-catenin, K-ras, p53, transforming growth factor (TGF)-β, and the DNA mismatch repair (MMR) proteins [165]. Additionally, even if the colorectal tumors are not associated with clinical signs of inflammatory bowel disease, these tumors still display

robust immune cell infiltration and increased expression of pro-inflammatory cytokines [172]. Furthermore, most colorectal cancer tumors or cell lines exhibit constitutive activation of transcription factors that are involved in the inflammatory pathways, such as the nuclear factor-kB (NF-kB) and signal transducer and activator of transcription 3 (STAT3) [70,173-178]. Therefore, it is possible that the inflammatory response act through similar but distinct mechanisms in the pathogenesis of colitis-associated colorectal cancer and sporadic colorectal cancers.

Activation of transcription factors, NF-κB and STAT3, acts as non-classical oncogene due to upregulation of genes involved in cell survival, proliferation, and angiogenesis [179]. These transcription factors are activated by pro-inflammatory cytokines including IL-6 and TNFα [179]. NF-κB is constitutively activated in most colorectal cancer tissues and colon cancer cell line [180]. By knocking down IκB kinase γ in colon cancer cells, which inhibits the activation of NF-κB, several chemokines that are related to angiogenesis were decreased, suggesting NF-κB activation is involved in angiogenesis of colon cancer [180]. Activation of NF-κB induces the production of cytokines including TNFα, IL-6, chemokines, growth factors, anti-apoptotic signals, and angiogenic factors that enhance the infiltration of tumor-associated immune cells into the tumor microenvironment, and promotes proliferation and angiogenesis [70]. Additionally, constitutive activation of STAT3 was also detected in dedifferentiated cancer cells and infiltrating immune cells of colorectal cancer samples through the stimulation by IL-6 [181]. Persistent activation of STAT3 induced by IL-6 is linked to the production of sphingosine-1-phosphate (S1P) in colitis-associated carcinogenesis [182].

Pro-inflammatory enzymes COXs and 5-LOX, as well as their products eicosanoids, are involved in colon tumorigenesis, angiogenesis, and even metastasis [79]. Elevated COX-2 expression was detected in most colorectal cancer tissues and is associated with the lowest survival rate among colorectal cancer patients [183]. Prostaglandins synthesized by COX-2 promotes the production of angiogenic factors by colon cancer cells and enhances angiogenesis in endothelial cells [79]. In addition to COX-2, 5-LOX is also overexpressed in some epithelial cancer cells. Leukotrienes (LTB_4 and LTD_4) and intermediate metabolite 5-hydroxyeicosatetraenoic acid (5-HETE) are involved in the survival, proliferation, and migration of cancer cells [184]. Thus, COX-2 inhibitors such as celecoxib and 5-LOX inhibitors can effectively induce apoptosis and suppress colon carcinogenesis [185-187].

1.3.2.1 Azoxymethane (AOM)-induced dextran sodium sulfate (DSS) promoted tumorigenesis model

The AOM/DSS-induced colitis-associated colorectal cancer model is a commonly used pre-clinical model to study the anti-cancer effect of various compound. DSS is a water-soluble, negatively charged sulfated polysaccharide that can induce acute colitis in rodents by inducing damage to the epithelial monolayer lining in the large intestine, which allows the permeation of pro-inflammatory intestinal content [131]. The different molecular weight of DSS can alter in the induction of colitis and colonic tumors in animals. Studies showed higher molecular weight >500 kDa did not induce colitis and lower molecular weight like 5kDa induced more severe colitis in the cecum and proximal colon [188]. DSS with molecular weight of 40-50kDa in general induced more severe colitis compared to 5kDa DSS, but colitis is more severe in the middle and distal colon [188]. Therefore, administration of DSS with molecular weight of 40-50kDa in drinking water resemble most closely to human ulcerative colitis (UC). Additionally, susceptibility to DSS-induce colitis

also varies significantly amongst inbred strains of mice. Swiss Webster, Balb/c, and C3H/HeJ are highly susceptible to DSS colitis, whereas NOD/LtJ are resistance, and C57BL/6J, 129SvPas and DBA/2J are less susceptible compared to Balb/c [189].

Features like ulcerations and edema present after DSS administration resemble histological characters in human UC [190,191]; thus DSS is a good model for human UC. However, unlike human UC, the cytokine profiles indicate a role for both Th1 and Th2 pathway in DSS-induce colitis [192]. Similar to human UC, acute DSS-induced colitis also exhibit Th-17-mediated dominant phenotype in addition to the Th1 profile. High level of TNF, IL6, IL17, IL1β, and keratinocyte-derived chemokine are observed in human UC as well as DSS-induce acute colitis[192]. Chronic colonic inflammation can also be induced by cyclical administration of DSS, which switch to predominant Th2-mediated response with increase IL-4 and IL10 [192]. Cyclical administration of DSS is often used to promote AOM-induce carcinogenesis to speed up the tumor development.

AOM is a pre-carcinogen that can be metabolized in the liver by cytochrome P450IIE1 to active carcinogen methyldiazonium ion to induce the formation of colorectal tumors in various animal models [193]. AOM augments the expression of cyclooxygenase-(COX)-2 but not COX-1 in colonic tumors, which suppresses TGFβ receptor 2 expression in colonic epithelial cells and activate intrinsic tyrosine kinase of EGFR in rodents [194]. Commonly, AOM is often used with DSS to induce colonic tumor development in a short period with the promotion of colon inflammation. In general, subcutaneous or intraperitoneal injection of 10mg/kg body weight of AOM followed by multiple cycles of DSS to animals to induce inflammation-associated tumor development. AOM/DSS-induces colonic dysplasia and adenocarcinoma showed nucleic translocation of β-catenin

and positive staining for COX-2 and inducible nitric oxide synthesis, but no immunoreactivity to p53 [195]. Molecular analysis demonstrated that both AOM and DSS induce mutation in β-catenin [194,196]. Additionally, inflammation plays an essential role in the initiation and progression of colitis-associated carcinogenesis (CAC) as described in the previous section. Although the AOM/DSS model mimics the clinical course of CAC in human, there are some differences such as lack p53 mutation in AOM/DSS model, which is an essential pathway in human CAC [197]. Additionally, the incidence of metastasis is relatively low in AOM-induced adenocarcinoma, while metastasis in colorectal cancer patients is ~50% [198].

1.3.3 The influence of gut microbiota on colorectal cancer

Colorectal cancer is the development of cancer in the large intestine where is the residence for significant proportion of microorganisms [199]. Advance metagenomics technology, such as 16s rRNA sequencing, provides a useful tool to study the association between intestinal microbiota and the development of colon cancer. Many evidence suggests that dysbiosis occurs during inflammation promotes the production of carcinogenic metabolites, which lead to neoplasia [200]. Impaired barrier function on colon tumors leads to infiltration of pathogenic and genotoxic bacteria, which activates tumor-associated immune cells and induces inflammation and genetic lesions, resulting in the initiation of colorectal carcinogenesis [200].

Fecal or mucosal samples from biopsy or resection are commonly used to investigate the relationship between microbial content and colon carcinogenesis. Alpha- and beta-diversity are common methods to illustrate the changes in gut microbiome structure during cancerous condition. Using 16S rRNA gene sequencing analysis, patients

with colorectal cancer have lower species richness in the feces, but higher richness in rectal mucosa than those of healthy subjects [201]. Higher microbial richness in rectal samples is associated with the presence of colorectal adenomas [201]. These changes may be associated with over-representation of cancer-associated bacteria, such as *Fusobacterium*, *Enterococcus faecalis*, *Streptococcus bovis*, and *Porphyromonas*, and the under-representation of beneficial bacteria, such as *Faecalibacterium*, *Parabacteroides, Akkermansia*, *Alistipes,* and *Lachnospiraceae* [200].

Epidemiologic and meta-analysis studies reveal bacterial taxa that are associated with colorectal cancer. For instance, *Streptococcus bovis*-infected patients are predisposed to premalignant adenomas and carcinomas [202]. Another species in the same genera, *Streptococcus gallolyticus* is also identified to be associated with higher colorectal cancer risk [203]. Furthermore, *Fusobacterium, Porphyromonas*, and *Peptostreptococcus* are enriched in cancerous tissue of CRC patients [204]. On the other hand, commensal bacteria such as *Faecalibacterium*, *Parabacteroides, Akkermansia*, and *Roseburia* are depleted in patients with CRC [204,205].

Mechanistic studies using animal and cellular models demonstrated the role of these bacteria, specifically *Fusobacterium nucleatum*, on colon carcinogenesis. Rubinstein et al. demonstrated that *F. nucleatum* promotes oncogenic and inflammatory responses in cancer growth by invasion and adhesion to cancer cells and tissues via activation of the FadA adhesin/E-Cadherin/β-catenin signaling cascade in cultured human colon cancer cells and colon cancer tissues in xenographic mice [206]. Noteworthy, colon tissues from patients with adenomas and adenocarcinomas have a much higher level of *fadA* gene than those from healthy individuals [206]. This elevated FadA expression in colon cancer cells is correlated

with increased expression of oncogenic and pro-inflammatory genes, suggesting that *F. nucleatum* drives colorectal carcinogenesis via its unique FadA adhesin [206]. In the $Apc^{min/+}$ mouse model of colorectal tumorigenesis, F. nucleatum increases tumor counts and selectively recruits myeloid-derived immune cells to the tumor site, leading to the progression of tumor [206]. Interesting, pro-inflammatory gene expression in tumors from $Apc^{min/+}$ mice exposed to F. nucleatum share similar signature with human fusobacteria-positive colorectal carcinomas [206]. However, F. nucleatum does not exacerbate colitis in $Il10^{-/-}$ mice and inflammation-associated colorectal carcinogenesis in T-$bet^{-/-}$$Rag2^{-/-}$ mice [206], suggesting that *F. nucleatum* generates a pro-inflammatory microenvironment via recruitment of tumor-infiltration immune cells, leading to the progression of colorectal neoplasia.

Due to the critical contribution of intestinal microbiome to colon carcinogenesis, modulation of gut microbiome becomes a target for colon cancer treatment. Several probiotics have been shown to regulate the immune systems, promotes short-chain fatty acid (SCFA) production, and suppresses the development of colon cancer. Inoculation of *Roseburia hominis*, a commensal bacterium belongs to the SCFA producer Lachnospiraceae family, in GF mice or conventional mice treated with DSS showed upregulation of genes related to antimicrobial peptide, gut barrier function, and toll-like receptors (TLR) signaling, as well as increased number of regulatory T cells in lamina propria [207]. In a 1,2-dimethylhydrazine dihydrochloride (DMH)-induced colon cancer model, probiotic cocktail enriched with *Lactobacillus acidophilu*s, *Bifidobacteria bifidum*, and *Bifidobacteria infantum* (LBB) significantly reduced tumor incidence, tumor volume, and tumor multiplicity in DMH-treated rats [208]. Consistent with *R. hominis*, LBB

upregulates genes involve in gut barrier function, mucus production, and TLR signaling, while downregulates gene related to inflammation and Wnt signaling [208]. These results suggest that probiotic treatment may be a useful therapeutic option for cancer. Prebiotics such as soluble fibers that also can promote the growth of these beneficial bacteria also exhibit anticancer properties [199]. In a TS4Cre/APC mouse model for colorectal carcinogenesis, the expression of SCFA butyrate receptor reduced along with a lower abundance of SCFA-producing bacteria in cancerous mice [209]. Supplementation of dietary fibers containing 20% insoluble fermentable fibers significantly increased SCFA-producing bacteria and SCFA production in TSA4Cre/APC mice, which were associated with an increase in SCFA butyrate receptor and reduction in tumor multiplicity [209].

1.3.4 Chemoprevention of colorectal cancer

As mentioned earlier, colorectal cancer is responsible for substantial morbidity and mortality in the United States. Despite enormous advances in the understanding the mechanisms of tumorigenesis and potent new drugs that have been treating several relatively rare forms of cancers, it is unlikely to change the mortality statistic fundamentally until reorient the emphasis in cancer research that direct more resources towards prevention of new disease instead of treatment at end-stage. The definition of chemoprevention is the use of specific compounds to prevent, inhibit, or reverse carcinogenesis [210]. There are chemotherapeutic drugs such as non-steroidal anti-inflammatory drugs (NSAIDs) available for the treatment of colorectal cancer but the outcomes are inconsistent, and most of them contain undesirable side effects [211,212]. Furthermore, aspirin as a chemopreventive agent showed a modest protective effect in some clinical trials for colorectal cancer prevention [213]. Celecoxib, a newer selective

inhibitor of cyclooxygenase-2 (COX-2), have shown inhibitory effect against colon carcinogenesis in experimental animals as well as in human subjects [214]. Patients treated with 400mg Celecoxib twice a day for six months had 28% reduction in the mean number of colorectal polyps and 30% reduction in the polyp burden, without causing additional adverse events when compared to the placebo-treated patients [215]. However, not all patients are responsive to this treatment, and the use of other NSAIDs induces many side effects such as gastrointestinal bleeding [216]. Therefore, natural compounds, such as vitamin E forms and their long-chain 13'-COOHs with anti-inflammatory properties have been considered as a potential chemopreventive agent for inflammatory bowel diseases and colorectal cancers.

1.3.4.1 Vitamin E as a chemopreventive agent for colorectal cancer

Prostaglandins and leukotrienes synthesize from COXs and 5-LOX are known to contribute to the development of cancer [217,218]. Non-αT forms of vitamin E and their long-chain metabolites are potent inhibitors of COXs and 5-LOX in mechanistic studies [56,89,54]. Consistently, supplementation of 0.3% γT-rich mixed tocopherol (γTmT) inhibited colon inflammation, eicosanoid production, including PGE_2 and LTB_4, and tumorigenesis in mice treated with AOM and DSS [219]. Similarly, Jiang et al. [32] showed that γT supplementation at 0.1% diet suppressed colon tumorigenesis promoted by moderate colitis that was induced by one cycle of DSS. However, γT supplementation is not effective toward colon tumorigenesis promoted by severe colitis with three DSS cycles [32].

Additionally, Guan et al. [94] and Newmark [220] reported that 0.2% δT γT and γTmT diet significantly reduced aberrant crypt foci (ACF) formation, a marker for precancerous lesions, in AOM-treated F344 rats. δT shows the most robust anticancer activity followed

by γT and γTmT in this model, while αT is not effective [94]. Similar anticancer activities of these vitamin E forms were observed in a colon cancer model induced by a meat-derived dietary carcinogen PhIP and promoted by DSS-induced colon inflammation in CYP1A-humanized (hCYP1A) mice [221]. Supplementation of 0.2% δT and γT but not αT showed to reduced colon tumor formation and suppressed reactive stress markers as well as activation of NF-κB and STAT3 in the PhIP/DSS-induced colon tumors and adjacent tissues [221]. Noteworthy, supplementation 0.05% of *dl*-α-tocopheryl acetate, a common form of vitamin E found in supplementations, did not affect the production of pro-inflammatory cytokines and ACF formation induced by AOM treatment in young and old C57BL/6JNIA mice [222]. Besides tocopherols, tocotrienols also appear to suppress the growth of human colon cancer in a xenographic mouse model, via down-regulating molecules involved in cancer cell proliferation and survival and inhibiting the activation of NF-κB [223,224].

CHAPTER 2. PHARMACOKINETICS OF VITAMIN E TOCOPHEROLS AND TOCOTRIENOLS, AND THEIR METABOLITES IN RATS

2.1 Abstract

Compared to αT, γT, δT, γTE, or δTE, have been demonstrated to have unique and superior bioactive functions relevant to disease prevention and therapy. Unlike αT, other vitamin E forms are highly metabolized to generate carboxychromanols (COOH). Recent studies indicate that long-chain 13'-COOH appear to have stronger anti-inflammatory and anticancer activity than un-metabolized vitamin E forms. This present study investigated the pharmacokinetics of vitamin E forms and their metabolite formation in Wistar rats. Seven-week male rats received a single gavage of δTE/γTE (8:1, 35 mg/kg BW) or γT-rich mixed tocopherol (γTmT, γT/δT/αT at ~64/24/12, 46 mg/kg BW). The vitamin E forms and metabolites in feces, urine, and plasma were quantified using HPLC-EC and LC-MS/MS, respectively. The pharmacokinetic parameters in the plasma are summarized as follows: for δTE/γTE, T_{max} at 2 h, C_{max} of 16.0 ± 3.9 μM, $T_{1/2}$ at 1.4 h; for γTmT, T_{max} at 4 h, C_{max} at 25.6 ± 9.1 μM, $T_{1/2}$ at 6.4 h. Sulfated CEHC and sulfated long-chain metabolites, 9'-, 11'-, and 13'-COOH were the predominant metabolites found in the plasma. Conjugated CEHC is the predominant metabolites found in the urine after the administration of δTE/γTE and γTmT. Fecal excretion of δTE and γT increased ~300 and 14-fold in animals after receiving δTE/γTE and γTmT, respectively. Long-chain 13'-COOH was the major metabolite found in feces of both δTE/γTE and γTmT administered animals, which accounted for ~50% of the all metabolites identified in feces. Our data indicate that δTE and γT can achieve plasma concentration comparable to those used in cell-based studies

examining anti-inflammatory and anticancer activity. High bioavailability of 13'-COOH in feces may contribute to mitigating effects for inflammatory bowel diseases and colorectal cancer.

2.2 Introduction

Vitamin E family has eight naturally occurring fat-soluble antioxidants, i.e., αT, βT, γT, and δT and αTE, βTE, γTE, and δTE [1]. All vitamin E forms contain a chromanol ring and a 16-carbon phytyl side chain, the latter of which is saturated in tocopherols and contains three double bonds in tocotrienols [1]. Among the different isoforms of vitamin E, αT is the predominant vitamin E in plasma and tissues due to the high binding affinity to hepatic α-tocopherol transfer protein (αTTP) that transports αT and prevents it from being metabolized in the liver [1,35,225]. In contrast, other vitamin E forms are substantially metabolized in the liver by cytochrome P450-4F2 via ω-hydroxylation and oxidation to generate 13'-hydroxychromanol (13'-OH) and 13'-carboxychromanol (13'-COOH), which is further metabolized via β-oxidation to various shorter-chain carboxychromanols including the terminal metabolite, 3'-COOH or 2-(β-carboxyethyl)-6-hydroxychroman (CEHC) [1,24,54]. Conjugation of carboxychromanols occurs along with β-oxidation by the addition of a sulfate or possibly glucuronide group to the hydroxyl group on the chromanol ring to generate conjugated metabolites [25,26]. The terminal metabolite CEHCs and the conjugated metabolites can be excreted in the urine, whereas unconjugated longer-chain carboxychromanols are primarily excreted in feces after supplementation of γT and δT [27-33].

While most research has been focused on the vitamin E forms, short- and long-chain metabolites have been shown to have stronger bioactivities than the vitamers [1]. For instance, γ-3'-COOH (CEHC) appears to have natriuretic activity [226]. We demonstrate that 13'-COOHs are potent dual inhibitors of pro-inflammatory enzymes, cyclooxygenases [52] and 5-lipoxygenase [54,55]. 13'-COOHs can induce apoptosis and autophagy in human cancer cells by modulating sphingolipids and suppress colon tumor development in mice [50,51]. Despite these interesting findings of vitamin E metabolites, there is limited information regarding how much these metabolites can be formed as a result of supplementation of various vitamin E forms. Without this knowledge, it is not possible to assess the role of vitamin E metabolism into the function of vitamin E forms and their protective effects on chronic diseases. Therefore, it is necessary to determine the bioavailability of various metabolites derived from vitamin E forms. We recently developed a LC/MS/MS assay for quantifying vitamin E metabolites, which allows simultaneous quantification of short-chain, long-chain and sulfated carboxychromanols [33]. In this study, we investigated the pharmacokinetics of vitamin E forms and the formation of their metabolites after single dose intragastric administration of vitamin E forms in rats. In addition, we measured the concentrations of metabolites in the serum of healthy subjects with 3 doses of γ-T supplementation.

2.3 Materials and Methods

2.3.1 Materials and Reagents

The Tocopherol mixture was gifted from BASF (Florhan Park, NJ), and contains αT (10.9%), γT (57.7%), and δT (21.7%) with total tocopherols at 91.9%. The δTE/γTE (8:1) mixture was gifted from American River Nutrition (Hadley, MA), and contains total

tocotrienols at 70%. γ-CEHC (≥98%), α-CEHC, and (±)-αT-5'-COOH (α-CMBHC) were from Cayman Chemicals (Ann Arbor, MI). δT-13'-COOH and δTE-13'-COOH, which are long-chain metabolites from δT and δTE, respectively, were synthesized according to a published procedure (18). All other chemicals were purchased from Sigma.

2.3.2 Animal Studies

All the animal studies were approved by Purdue Animal Care and Use Committee. In the pharmacokinetic study of vitamin E forms and metabolite formation in response to a single gavage of 50 mg/kg body weight of γ-tocopherol-rich mixed tocopherol (91%; γTmT; 29.5 mg/kg γT; 11 mg/kg δT; 5.5 mg/kg αT) or δ-tocotrienol (70%; δTE/γTE, 8:1, w/w; 31.1 mg/kg δTE; 3.89 mg/kg γTE), male Wistar rats (230-250 g) were purchased from Envigo (San Diego, CA). Rats were housed in Purdue Life Science Animal Facility for a week for adaptation before experiments and then randomly grouped by body weight match. Rats received chow diet (containing ~40-60 mg/kg of αT, depending on the batch) throughout the entire study. Diet and water was fed *ad libitum*. Rats were given γTmT or δTE by gavage using tocopherol-stripped corn oil (0.5 mL) as the vehicle control (n = 3 in each group). Plasma, fecal, and urinary samples were collected 24 h prior to the gavage for baseline measures. After the administration of γTmT or δTE, plasma samples were collected at 1 h, 2 h, 4 h, 6 h, and 8 h via saphenous vein. Twenty four hours after receiving γTmT or δTE, animals were euthanized, and plasma, urine, feces, liver, and colon samples were collected. The fecal and urine samples collected were between 8-24 h. Due to the limitation of the current experimental condition, we were not able to collect fecal and urine sample during the plasma collect between 0 to 8 hr. Therefore, we conducted another study just to measure the fecal and urinary excretion of vitamin E and metabolites at baseline, 0

to 8 h, 8-24 h, and 24-48 h. All samples collected from the studies were aliquoted and frozen at -80^{o}C until use.

2.3.3 Human Study

An open-label pilot study was conducted in 10 healthy volunteers aged 18-45 years as previously described [227,228]. This study was approved by the University of North Carolina Institutional Review Board. Briefly, participants consumed 2 γT-enriched gel tabs (~1,200 mg of γT) every 12 h for 3 doses. Blood samples were collected at baseline, 24 h (before dose 3), and 30 h (6 h after dose 3) to measure plasma tocopherols and their metabolites.

2.3.4 Extraction of vitamin E forms and metabolites from plasma

Vitamin E forms and metabolites from plasma sample were extracted as previously described (15). Briefly, plasma samples were extracted by a solvent mixture containing 6 volume of working methanol (0.2 mg/mL ascorbic acid) and 12 volume of hexane with butylated hydroxytoluene (BHT; 0.1 mg) via vigorous vortexing for 1 minute. Either δT-13'-COOH or δTE-13'-COOH (1 μM) was added as an internal standard (IS) depending on the vitamin E forms that were given to the animals. After centrifugation at 12,000 rpm for 2 min, the upper hexane layer was collected in a new tube. The methanol layer (90-95%) was transferred into a clean tube, and the residual pellet was extracted one more time with 4 volume of working methanol. After mixing and centrifugation, the combined methanol layers were dried under nitrogen. Both dried methanol- and hexane-extracted samples were resuspended in HPLC-grade ethanol before being analyzed by HPLC or LC/MS/MS. During the extraction procedure, samples were protected from light. Before LC/MS/MS analysis, α-CMBHC (5 μM) was added as an additional IS for injection.

2.3.5 Enzyme digestion of extracted vitamin E metabolites in the urine

One hundred microliters of urine samples were added with δT-13'-COOH or δTE-13'-COOH (1 μM) and extracted by 500 μL of working methanol (0.2 mg/mL ascorbic acid). The extraction was repeated one more time with 200 μL of working methanol. The combine methanol layer was dried under nitrogen. Enzymatic hydrolysis of conjugated metabolites was described previously with slight modification [26,43]. Briefly, Metabolites extracted from urine were dissolved in 5 μL ethanol and reconstituted in the enzyme solution containing 30 U sulfatase (Sigma S9626) and 40 U glucuronidase (Sigma, G0751) in 0.1 M sodium acetate at pH 5. Samples were incubated with the sulfatase/glucuronidase for 18-24 h at 37°C. Afterward, metabolites were extracted with 5 parts of working methanol (0.2 mg/mL ascorbic acid). Methanol layer was subsequently dried in nitrogen gas. Before LC/MS/MS analysis, samples were reconstituted in HPLC-grade ethanol, and α-CMBHC (5 μM) was added as an additional IS for injection.

2.3.6 Extraction of vitamin E forms and metabolites from feces

Approximately 200-400 mg of fecal samples was homogenized in 2 mL of methanol with ascorbate (0.2 mg/mL). Residues in feces were removed by centrifugation, and 1.4 mL of methanol layer was mixed with 200 μL of PBS and 5 mL of hexane containing BHT (0.92 mg/mL) via vigorous vortexing for 1 minute. After centrifugation, 1.4 mL of methanol layer and 4 mL of hexane layer were collected and dried under nitrogen. The dried methanol- and hexane-extracts were resuspended in 200ul of HPLC-grade ethanol and further diluted 10 times before being analyzed by HPLC or LC/MS/MS. α-CMBHC (5 μM) was added as IS before LC/MS/MS analysis.

2.3.7 Analysis of vitamin E forms by HPLC with electrochemical (EC) detection

As previously described [25,32], Tocopherols and tocotrienols were separated on a 150 x 4.6 mm, 5 μm Supelcosil LC-18-DB column (Supelco, Bellefonte, PA), and eluted with 95/5 (v/v) methanol/0.1 M lithium acetate. Vitamin E forms were monitored by coulometric detection (Model Coulochem II, ESA Inc., Chelmsford, MA) at 300 (upstream) and 500 mV (downstream electrode) using a Model 5011 analytical cell.

2.3.8 Analysis of vitamin E metabolites by LC/MS/MS

The LC/MS/MS analysis was done with an Agilent 1200 LC system coupled to an Agilent 6460 QQQ mass spectrometer equipped with a jet stream ESI source (Santa Clara, CA) as previously reported [32,33]. The chromatography utilized an Atlantis dC18 column (2.1 × 150 mm, 3 μm) from Waters Corporation (Milford, MA). Buffer A consisted of acetonitrile-ethanol-water (165:135:700, v/v/v), and buffer B was acetonitrile-ethanol-water (539:441:20, v/v/v), both of which contained 10 mM ammonium acetate with acetic acid to adjust pH to 4-4.3. The LC gradient was as follows: time 0 min, 0% B; time 1 min, 0% B; time 30 min, 99% B; time 40 min, 99% B; time 43 min, 0% B; time 48 min, 0% B. The flow rate was 0.3 mL/min with a total run time of 48 min. Multiple reaction monitoring was used to analyze each compound. Negative polarity ESI was used with the following source conditions: gas temperature, 325^{o}C; gas flow, 10 liters per min; nebulizer pressure, 30 psi; sheath gas temperature, 250^{o}C; sheath gas flow, 7 liter per min; capillary voltage, 4,000 V; nozzle voltage, 1,500 V; and an electron multiplier voltage of -300 V. All data were evaluated with Agilent MassHunter Qualitative Analysis software, version B.06.00.

2.3.9 Pharmacokinetic Analysis

Pharmacokinetic parameters were based on the plasma concentration-time data using standard non-compartmental methods [229]. Area under the curve (AUC) was calculated using the log-linear trapezoidal rule to determine the degree of exposure following the administration of vitamin E forms. Other pharmacokinetic parameters determined in this study included observed maximum plasma concentration (C_{max}), time at which C_{max} was observed (T_{max}), and elimination half-time or time at which the plasma concentration was reduced by half after reaching C_{max} ($T_{1/2}$) [230]. The bioavailability in the plasma = AUC*V/total supplement, where V= total blood (16mL for 250g of rat, https://www.nc3rs.org.uk/rat-decision-tree-blood-sampling). Percent excretion of vitamin E forms and metabolites = [(total vitamin E forms and corresponding metabolites in feces and urine of supplemented animals) – baseline]/total supplement.

2.3.10 Statistical Analysis

The normality of the data was confirmed by Shapiro-Wilk test. Log transformation was performed to normalize unequal variances between groups. Student's *t*-test was used in statistical analyses for comparison of controls with tocopherol- or tocotrienol-supplemented groups in animal studies and comparison of baseline with 24 or 30 h after γT intake in the human study. All tests were two-sided, and values of $P \leq 0.05$ were considered to be statistically significant. All results are expressed as mean ± SEM.

2.4 Results

2.4.1 Pharmacokinetics of tocopherols and tocotrienols in the plasma

After orally gavaged with of γTmT, the plasma concentration of γT gradually elevated to reach C_{max} of 25.6 ± 9.1 μM at 4 h and decreased by half of its C_{max} at 6.4 h ($T_{1/2}$) as shown in Figure 2.1A. The overall exposure of γT in plasma as calculated by AUC was 206.6 ± 24.4 μM*h. Similar to γT but at a faster rate, δT reached C_{max} of 8.6 ± 0.2 μM in the plasma at approximately 2 h with a half-life of 4.3 h (Figure 2.1B). The overall exposure of δT in the plasma after gavaged with γTmT is 48.9 ± 8.1 μM*h (Table 2.1). The plasma concentration of αT was not changed at baseline and throughout the first 24 h after γTmT gavage (ranged from 19.9 ± 1.4 to 21.3 ± 0.2 μM, $P > 0.05$).

As to the tocotrienols, the level of δTE increased rapidly in the plasma and reached C_{max} of 16 ± 2.3 μM at 2 h after receiving an oral gavage of δTE/γTE (Figure 2.1C). The plasma δTE concentration was then quickly reduced by half of C_{max} at approximately 1.4 h, and the overall exposure to δTE was 43.6 ± 7.7 μM*h. Correspondingly, the plasma concentration of γTE reached C_{max} at 2 h after the gavage and quickly reduced by 50% at approximately 1.7 h (Figure 2.1D). The overall exposure to γTE was 8.9 ± 1.6 μM*h (Table 2). With similar amounts of δTE and γT administered (29.5 mg/kg γT vs. 31.1 mg/kg δTE), the bioavailability of γT is higher than δTE in the plasma within 24 h after the supplementation.

2.4.2 Time-course formation of vitamin E metabolites in the plasma

Using our recently developed LC/MS/MS methodology [33], we are able to characterize the pharmacokinetic profiles of unconjugated and sulfated vitamin E metabolites after administration of a single dose of γTmT and δTE/γTE summarized in

Table 2.1 and 2.2, respectively. Sulfated CEHCs and sulfated 9'- and 11' were the predominant metabolites detected in the plasma of rats after gavaged with γTmT and δTE/γTE. Unlike γT that quickly reached to C_{max}, the plasma concentration of its conjugated metabolites SO_3-γ-CEHC, γT-9'S, and γT-11'S, slowly was risen and reached C_{max} at about 6-7 h after γTmT administration (Figure 2.2A-C). Afterward, the plasma concentration of these metabolites gradually dropped by half at ~4-8 h. The pattern of the overall plasma exposure of these conjugated metabolites is very similar (Figure 2.2). Compared to γT/δT, metabolites from δTE/γTE showed similar C_{max} with lowered $T_{1/2}$ (Figure 2.2D-F and Table 2.2). αT metabolites were not detected in the plasma of rats.

2.4.3 Excretion of vitamin E forms and metabolites in feces and urine

We monitored the excretion of vitamin E forms and their metabolites in feces before and after supplementation (8-24h). Compared with baseline, the supplementation of γTmT resulted in 10-, 14-, and 1.5-fold elevation of γT, δT, and αT, respectively, in the feces for both study 1 and study 2 (Table 2.3). However, the actual amount and percent excretion of γT, δT, and αT in rat feces were higher in study 2 compared to study 1. As to tocotrienols, the fecal excretion of δTE and γTE increased >300- and 6-fold after δTE/γTE supplementation compared to the baseline for study 1, but for study 2, γTE was only 2.5-fold higher compared to baseline (Table 2.3). Percent excretion of δTE and γTE in rat feces was similar for both study 1 and 2 after the subtraction of baseline.

As to vitamin E metabolites, consistent with previously published data [32,33,43], long-chain 13'-COOHs were the most abundant metabolites found in feces of rats after supplementation of γTmT and δTE/γTE (Table 2.4 and Table 2.5). For instance, δTE-13' with either 2 or 3 double bonds (DBs) on the side-chain or γT-13' and δT-13' accounted

for approximately 50% of total metabolites found in feces in response to supplementation of δTE/γTE or γTmT, respectively. Interestingly, the amount of total metabolites from γTmT was similar to those derived from δTE/γTE in the feces.

In the urine, only short-chain and conjugated short-chain metabolites were detected (Table 2.6). The percent excretion of total CEHCs (either conjugated or unconjugated) from tocopherols were 2-fold higher compared to those from tocotrienols. Interestingly, enzymatic hydrolysis study using glucuronidase and sulfatase indicated that glucuronide but not sulfated CEHCs is the predominant form of metabolites found in the urine of tocopherol-supplemented rats. However, the amount of glucuronide CEHCs and sulfated CEHCs excreted in the urine of tocotrienol-supplemented rats appeared to be similar. Overall, the total percent excretion for γT and δT ranged from 32-53%, and for γTE and δTE were 40% and 27%, respectively (Table 2.7).

2.4.4 Metabolites detected in human plasma after consumption of γT

In a recent clinical study, we evaluated the bioavailability of metabolites in the serum of participants received 3 doses of γT-enriched gel tabs. (Table 2.8**)**. Unlike metabolites in rats where sulfated CEHC and sulfated long-chain carboxychromanol are the predominant metabolites (Table 2.1), the predominant metabolite in human plasma after the consumption of γT was γ-CEHC. By 24 and 30 h, the concentration of γ-CEHC increased ~30-fold from baseline ($P< 0.001$). Sulfated 11'- and 13'-COOH and γT-13'-OH increased by >15-20 fold compared with baseline (Table 2.8). This is the first time that these sulfated long-chain metabolites are reported in human samples. As others and we have previously reported in either human or mice [26,33,45], γT supplementation resulted in an increase of γ-CEHC (Table 2.8).

2.5 Discussion

To our knowledge, this study is the first report that characterizes the pharmacokinetics of formation of short and long-chain vitamin E metabolites following a single supplementation of tocopherols or tocotrienols. Taking advantage of our recently developed LC-MS/MS method, we are able to quantify both unconjugated and sulfated metabolites. Based on the AUC and C_{max}, sulfated CEHCs, and sulfated long-chain carboxychromanols, i.e., 9'S, 11'S and 13'S, are among the major metabolites detected in the plasma in rats, which is consistent with our previous findings where these compounds appear at higher concentrations than other metabolites [26,33]. On the other hand, unconjugated vitamin E carboxychromanols or hydroxychromanol are present at much lower levels than the sulfated analogs, as indicated by lower AUC and C_{max}. According to T_{max}, unconjugated long-chain metabolites such as 13'-COOHs and 13'-OH appear to reach C_{max} more quickly than conjugated counterparts. This is expected as long-chain hydroxyl- and carboxychromanols are the initially formed metabolites as a result of ω-oxidation [1,24]. In addition, tocotrienols and their metabolites have shorter T_{max} than tocopherols and tocopherol metabolites, suggesting a more rapid turnover of tocotrienols.

Our pharmacokinetic data allow quantitative evaluation of the relative bioavailability among different vitamin E forms and metabolites. Based on the ratio of the AUC to the intake of each vitamer, the relative bioavailability of vitamin E forms in the plasma follows the order of γT (18.6%) > δT (11.2%) > γTE (5.8%) > δTE (3.5%). These data are in agreement with higher C_{max} of γT than that of δTE, despite similar amounts of intake of these two vitamin E forms. Interestingly, the ratio of total metabolites' AUC to the intake of corresponding vitamins follows the order of γTE (3%) > γT (1.3%) > δTE ≈

δT (0.6-0.7%), indicating that metabolites from γTE are more bioavailable than those from other vitamin E forms. Consistent with this observation, we previously observed higher concentrations of metabolites from γTE than those from γT, and lower γTE than γT in the plasma of rats supplemented with the same dose of these vitamin E forms [26]. Furthermore, Sontag and Parker [231] demonstrate that tocopherol-ω-hydrolase metabolizes γTE more effectively than γT or δTE, and γTE can be more rapidly metabolized in HepG2 cells expressing CYP4F2.

Our study reveals new information regarding the excretion of vitamin E forms and metabolites in rats. First, our data show that up to 90% metabolites of tocopherols and tocotrienols appear to be excreted via feces as unconjugated ω-oxidation products, while only small portions of metabolites, mostly in the conjugated form, are found in the urine. Similarly, Bardowell et al. [30] previously reported higher fecal excretion of metabolites than those in the urine when mice were fed with tocopherols. Unlike, we also detect a small quantity of fecal α-metabolites, including 9'-, 11'- and 13'-COOH. Fecal excretion of tocotrienol metabolites is higher than those derived from γT or δT, all of which are higher than αT, consistent with low metabolism of αT. This observation is consistent in both study 1 and 2. Second, our data indicate that the basal level of vitamin E form from the diet can dramatically alter fecal excretion of tocopherols but not tocotrienols. In study 2, we found that the fecal excretions of tocopherols at baseline was 2-fold higher than those in study 1. The baseline level of γTE in feces was even 3-fold higher in study 2 than in study 1. However, the percent excretion for γTE was similar in both study, whereas the percent excretion of tocopherols in feces was much higher in study 2 than study 1. Although we are aware of the fact that there were differences between the two studies, our data are more

representable for vitamin E excretion at different baseline level. Since large amounts of tocopherols, tocotrienols, and their metabolites were found in feces of rats supplemented with γTmT or δTE/γTE, we conclude that fecal excretion is the major route of vitamin E elimination when large quantities of vitamin E forms are consumed. Although Traber et al. [49] reported that some phase III transporters are involved in the elimination of vitamin E and vitamin E metabolites, many aspects regarding the involvement of transporters in vitamin E and vitamin E metabolite excretion remain to be determined. Third, while total fecal metabolites of δTE/γTE are ~20% higher than those of γTmT, the overall excretion of tocopherols from γTmT (25-45%) is higher than the excretion of tocotrienols from δTE/γTE, specifically δTE (18.6%). The measure fecal and urinary excretion up to 48 h after supplementation and found that vitamin E and metabolites were mainly excreted in the first 24 h. Based on our calculation, percent recovery of γT and its metabolites in rats after γTmT from plasma, feces, and urine is ~53-73%, but only 31% for δTE. Previous studies [23,232] reported that a considerable amount of tocotrienols were found in adipose tissue or skin of rodents after administration and the amount of tocotrienols in adipocytes can maintain up to or beyond 24 h of the administration. These data suggested that tocotrienols can be stored in the adipocyte. Future pharmacokinetic studies should measure the level of tocotrienols in fat and skin tissues.

We find that there is a clear distinction in metabolite formed between human and rats, despite noticing some similar long-chain metabolites in the plasma of rats and human. Like observations in rats, we detect sulfated CEHC, 11'S and 13'S, and various unconjugated carboxychromanols including 11'-COOH, 13'-COOH and 13'-OH in human plasma. Compared with the baseline, these metabolites increase by 20-, 20- and 40-fold,

respectively, in human plasma following supplementation of γT. However, unlike rats where conjugated CEHC and sulfated long-chain metabolites are predominant in the plasma, the major metabolite appears in human plasma is unconjugated γ-CEHC, which can reach up to 7 μM in the plasma at 6 h after supplement. Further, supplementation of γT caused an increase of α-CEHC, likely due to enhanced catabolism of αT [233]. Recently, Mahipal et al. [234] reported that δ-CEHC is the predominant metabolite found in the plasma after multiple-dose supplementation of δTE (200-1600mg) in human, although the conjugation status was not identified as sulfatase and glucuronidase was employed to remove conjugation during sample preparation. Besides, Giusepponi et al. conducted a study where healthy subjects took 1000 IU of RRR-αT daily for one week and then the level of α-metabolites in the plasma were quantified [235]. These investigators detected α-CEHC, α-13'-COOH and α-13'-OH in the plasma, but whether these metabolites are in conjugated or unconjugated forms are not clear [235]. Interestingly, amounts of metabolites from αT appear to be lower than those derived from γT, as indicated by higher concentrations of γ-CEHC and long-chain metabolites detected in our current study. This observation is consistent with the notion that γT is preferentially metabolized than αT as a result of preferential binding to α-tocopherol transfer protein and favorable catabolism of γT by CYP4F2 [1].

The bioavailability of vitamin E forms and metabolites, together with their bioactivities, determine *in vivo* beneficial effects of these compounds for disease prevention and therapy. The present study, along with published work by others and us [234,236-238], show that γT and δTE can reach concentrations of 30-40uM and 16uM, respectively, in the plasma of animals and human. At these concentrations, these vitamins

have been shown to exhibit anti-inflammatory and anticancer effects in mechanistic studies [1,51,83-85]. Consistent with being bioavailable and bioactive, these vitamin E forms exhibit anti-inflammatory actions in rats' inflammation models [239], are protective to asthma in human [228] and prevent cancer development in cancer models [32,221,240,241]. As to the metabolites, among all of the metabolites, 13'-COOHs have been demonstrated to have anti-inflammatory and anticancer activities [1,51-55,242]. Our current and previous study [32,33] show that while low in the blood, unconjugated 13'-COOHs are the predominant metabolite found in feces, which accounted for ~50% overall metabolites determined. High levels of 13'-COOHs in fecal samples may suggest that these metabolites can potentially have an impact on the GI tract. Indeed, we have previously shown that δTE-13'-COOH effectively inhibited colon cancer development in mice [55]. Further, we recently found that δTE-13'-COOH supplementation modulated gut microbiomes in a colon cancer model [85]. In the future, the pharmacokinetics of vitamin E metabolites and excretion of vitamin E and metabolites in human should be characterized.

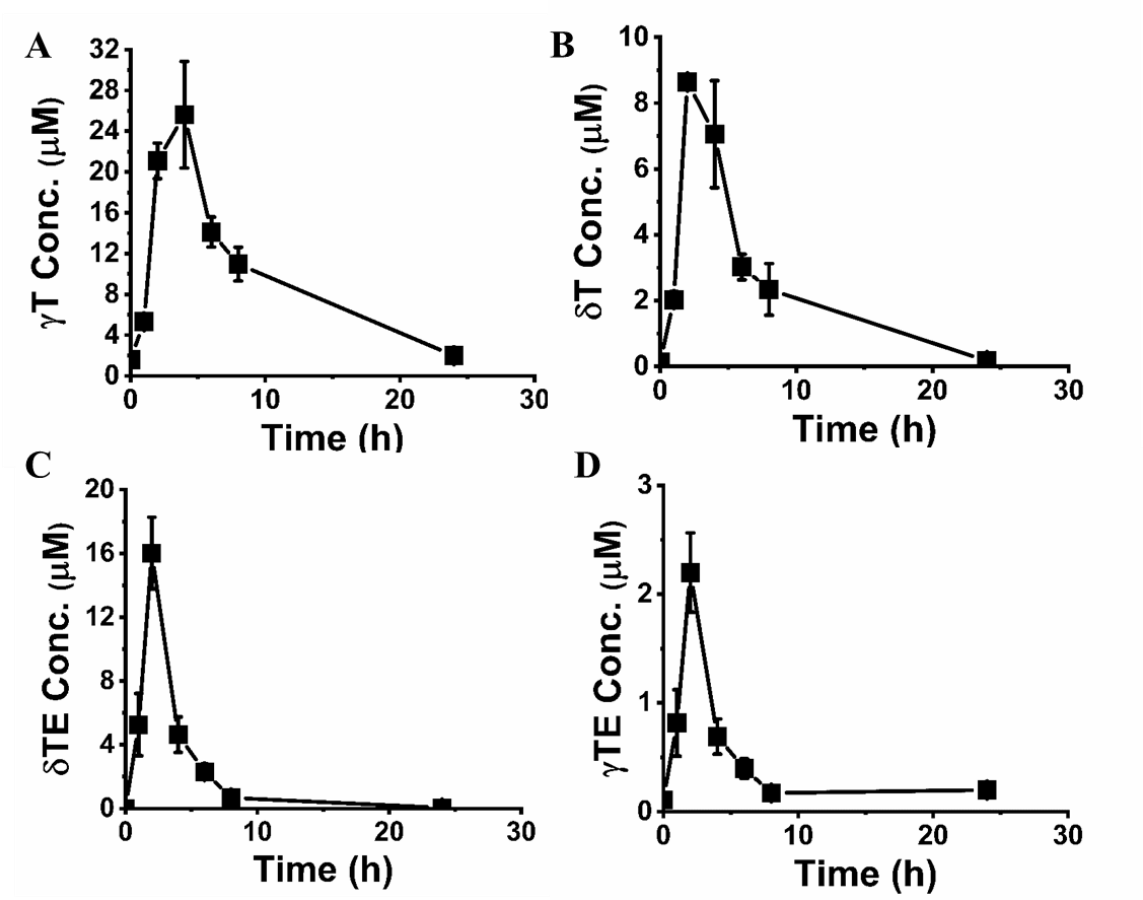

Figure 2.1 Plasma responses of vitamin E forms after supplementation.

A-B: Plasma responses of γT and δT after single dose supplementation of γTmT with a single dose of 46 mg/kg of γTmT (29.5 mg/kg γT; 11 mg/kg δT; 5.5 mg/kg αT) in rats. C-D: Plasma responses of δTE and γTE after single dose supplementation of δTE with a single dose of 35mg/kg δTE/□TE (31.1 mg/kg □TE, 3.89 mg/kg □TE) in rats. Data are expressed as mean ± SEM.

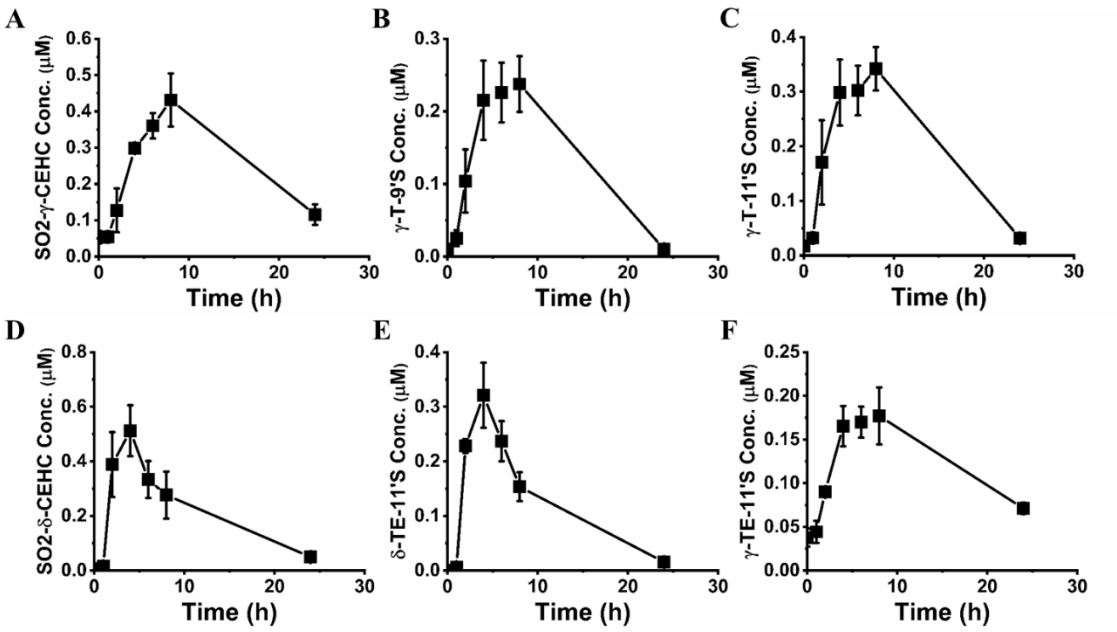

Figure 2.2 Plasma responses of major forms of vitamin E metabolites after supplementation of γTmT or δTE/γTE in rats.

A-C: Plasma responses of sulfated γ-CEHC, γT-9'S, and γT-11'S in rats after single dose supplementation of γTmT. D-F: Plasma responses of sulfated δ-CEHC, δTE-11'S, and γTE-11'S in rats after single dose supplementation of δTE. Data are expressed as mean ± SEM.

Table 2.1 Pharmacokinetic parameters of tocopherols and corresponding metabolites after supplementation of γTmT in rats.

Elimination half time ($T_{1/2}$) is presented as the time taken for the plasma concentration to fall by half after reaching the maximum concentration (C_{max}). Data are expressed as mean ± SEM.

	AUC (μM*h)	C_{max} (μM)	T_{max} (h)	$T_{1/2}$ (h)
γT	206.6 ± 24.4	25.6 ± 9.1	4 ± 0	6.4 ± 0.3
δT	48.9 ± 8.1	8.6 ± 0.2	2.7 ± 0.7	4.3 ± 0.2
γ-CEHC	2.2 ± 0.0	0.1 ± 0.0	4.7 ± 1.8	30.1 ± 11.9
SO3-γ-CEHC	5.5 ± 0.8	0.4 ± 0.1	7.3 ± 0.7	8.2 ± 1.1
SO3-δ-CEHC	2.0 ± 0.3	0.2 ± 0.0	6 ± 1.2	6.9 ± 1.0
γT-9'S	2.2 ± 0.4	0.2 ± 0.0	6 ± 1.2	3.6 ± 0.3
δT-9'S	0.2 ± 0.0	0.04 ± 0.0	7.3 ± 0.7	1.4 ± 0.0
γT-11'S	3.5 ± 0.5	0.3 ± 0.0	6 ± 2	4.6 ± 0.3
δT-11'S	0.2 ± 0.0	0.04 ± 0.0	4.7 ± 0.7	4.0 ± 2.6
γT-13'	0.03 ± 0.02	0.01 ± 0.0	4.7 ± 0.7	1.9 ± 0.2
δT-13’	0.1 ± 0.04	0.02 ± 0.0	4 ± 0	3.3 ± 0.5
γT-13'-OH	0.04 ± 0.02	0.02 ± 0.0	4 ± 0	1.7 ± 0.0
δT-13'-OH	0.04 ± 0.01	0.01 ± 0.0	4 ± 0	1.9 ± 0.3
γT-13'S	1.0 ± 0.2	0.3 ± 0.1	4 ± 0	6.1 ± 2.1
δT-13'S	0.25 ± 0.0	0.1 ± 0.01	4.7 ± 0.7	3.3 ± 1.1

Table 2.2 Pharmacokinetic parameters for tocotrienols and corresponding metabolites after supplementation of δTE/γTE in rats.

Elimination half time ($T_{1/2}$) is presented as the time taken for the plasma concentration to fall by half after reaching the maximum concentration (C_{max}). Data are expressed as mean ± SEM.

	AUC (μM*h)	C_{max} (μM)	T_{max} (h)	$T_{1/2}$ (h)
δTE	43.6 ± 7.7	16.0 ± 2.3	2 ± 0	1.4 ± 0.1
γTE	8.9 ± 1.6	2.2 ± 0.4	2 ± 0	1.7 ± 0.1
SO3-δ-CEHC	4.6 ± 0.8	0.5 ± 0.1	3.3 ± 0.7	5.1 ± 1.5
SO3-γ-CEHC	1.3 ± 0.3	0.1 ± 0.0	4 ± 2	14.1 ± 3.7
δTE-9'	0.04 ± 0.0	0.01 ± 0.0	4 ± 1.6	4.7 ± 2.8
δTE-9'S	0.3 ± 0.1	0.1 ± 0.0	5.3 ± 0.7	3.4 ± 0.7
γTE-9'S	0.6 ± 0.1	0.1 ± 0.0	6 ± 1.2	6.6 ± 2.4
δTE-11'S	2.1 ± 0.2	0.3 ± 0.1	4.7 ± 0.7	4.1 ± 1.2
γTE-11'S	2.6 ± 0.3	0.2 ± 0.0	7.3 ± 0.7	13.9 ± 4.1
δTE-13'	0.1 ± 0.1	0.02 ± 0.0	2 ± 0	3.5 ±0.2
δTE-13'S	0.1 ± 0.0	0.03 ± 0.0	4 ± 0	2.6 ± 0.4
δTE-13'-OH	0.2 ± 0.1	0.04 ± 0.0	3.3 ± 0.7	1.9 ± 0.2

Table 2.3 Fecal excretion of vitamin E forms increased in rats at 0-24 h after supplementation of γTmT or δTE/γTE.

A single gavage of 46 mg/kg of γTmT is equivalent to intake of γT, δT and αT at 17.3, 6.73 and 3.16 μmoles and 35 mg/kg δTE/γTE is equivalent to intake of δTE and γTE at 19.6 and 2.4 μmol, respectively. Data are expressed as mean ± SEM (% excretion after subtracting baseline). * $P< 0.05$, ** $P< 0.01$, and *** $P< 0.001$: difference between control and tocopherol/tocotrienol supplementation. n.d. – not detectable

	Total amount excreted (nmol)	Baseline	γTmT nmol (%)	δTE/γTE nmol (%)
Study 1 (8-24 h)	δTE	12.5 ± 6.2	n.d	3909.5 ± 1552.6 ** (19.9%)
	γTE	123.6 ± 5.9	n.d	828.0 ± 181.7 ** (31.1%)
	δT	125.2 ± 13.3	1747.7 ± 200.6 ** (24.7%)	n.d
	γT	492.8 ± 49.8	4780.4 ± 832.5 ** (26.0%)	n.d
	αT	967.9 ± 138.4	1492.2 ± 146.0 * (26.5%)	n.d
Study 2 (0-8 h)	δTE	9.5 ± 0.8	n.d	40.4 ± 35.3
	γTE	403.3 ± 37.1	n.d	206.7 ± 23.3
	δT	263.4 ± 33.1	249.0 ± 208.4	n.d
	γT	878.6 ± 100.9	644.0 ± 510.1	n.d
	αT	1863.8 ± 197.4	408.6 ± 130.7 *	n.d
Study 2 (8-24 h)	δTE	9.5 ± 0.8	n.d	3367.3 ± 770.5 * (17.8%)
	γTE	403.3 ± 37.1	n.d	1013.3 ± 162.4 * (31.0%)
	δT	263.4 ± 33.1	3226.7 ± 341.7 ** (45.3%)	n.d
	γT	878.6 ± 100.9	8420.0 ± 681.3 ** (45.3%)	n.d
	αT	1863.8 ± 197.4	3336.7 ± 124.4 * (65.4%)	n.d
Study 2 (24-48 h)	δTE	9.5 ± 0.8	n.d	55.9 ± 5.7 **
	γTE	403.3 ± 37.1	n.d	723.3 ± 44.1 **
	δT	263.4 ± 33.1	299.7 ± 15.5	n.d
	γT	878.6 ± 100.9	867.2 ± 21.8	n.d
	αT	1863.8 ± 197.4	1587.9 ± 60	n.d

Table 2.4 Metabolites detected in the fecal samples of rats at 8-24 h after given a single gavage of 46 mg/kg of γTmT.

A single gavage of γTmT is equivalent to intake of γT, δT and αT at 17.3, 6.73 and 3.16 μmoles. Data are expressed as mean ± SEM (% excretion after subtracting baseline). # $P< 0.1$, * $P< 0.05$, ** $P< 0.01$, and *** $P< 0.001$: difference between control and tocopherol/tocotrienol supplementation. n.d. – not detectable

Total amount excreted (nmol)	Study 1: γTmT		Study 2: γTmT		
	0 h	24 h	0 h	8 h	24 h
γ-CEHC	16.7 ± 2.5	35.5 ± 4.2 **	56.7 ± 10.7	33.0 ± 7.5	71.5 ± 22.6
δ-CEHC	1.0 ± 0.2	5.4 ± 0.2 ***	5.5 ± 1.5	7.7 ± 1.5	20.3 ± 4.6 *
γT-5'	0.4 ± 0.2	2.7 ± 0.5 **	n.d	n.d	n.d
γT-7'	5.2 ± 1.5	61.6 ± 14.6 **	14.8 ± 4.7	19.1 ± 3.5	63.5 ± 15.9 *
δT-7'	0.8 ± 0.1	11.0 ± 2.5 *	n.d	n.d	n.d
γT-9'	2.0 ± 0.5	21.1 ± 3.5 ***	4.8 ± 0.6	6.3 ± 1.3	18.4 ± 2.5 **
δT-9'	0.7 ± 0.1	8.9 ± 1.6 ***	1.3 ± 0.3	2.1 ± 0.4	12.6 ± 6.0 *
γT-11'	4.1 ± 1.5	66.9 ± 12.6 **	8.8 ± 1.9	16.0 ± 3.4	135.1 ± 25.3 **
δT-11'	1.8 ± 0.7	49.2 ± 12.9 *	3.9 ± 1.1	5.5 ± 1.6	47.9 ± 21.3 *
γT-13'	14.1 ± 5.5	480.4 ± 121.9 **	33.4 ± 4.5	155.4 ± 22.9 **	362.0 ± 78.9 *
δT-13'	8.0 ± 2.2	244.9 ± 55.7 **	19.9 ± 2.1	38.3 ± 10.6	337.7 ± 188.8 *
γT-13'-OH	1.6 ± 0.6	137.2 ± 43.1 **	6.9 ± 1.8	25.2 ± 11.0	114.6 ± 35.2 *
δT-13'-OH	0.7 ± 0.2	44.1 ± 6.9 ***	1.4 ± 0.3	3.3 ± 0.4 *	70.6 ± 54.7 *
γT-11'S	1.4 ± 0.5	81.6 ± 40.1 **	1.5 ± 0.5	4.1 ± 0.7 *	10.7 ± 3.4 #
γT-13'S	10.6 ± 2.3	131.0 ± 31.7 ***	18.0 ± 1.2	15.9 ± 4.0	108.4 ± 1.2 ***
δT-13'S	2.7 ± 0.3	45.7 ± 8.4 ***	4.3 ± 0.2	8.1 ± 1.3 *	25.5 ± 4.2 **
δ-metabolites	15.7 ± 2.8	423.5 ± 87.8 ** (6.5%)	36.3 ± 4.1	64.9 ± 14.3 (0.42%)	514.7 ± 272.6 ** (7.65%)
γ-metabolites	56.0 ± 10.4	1018.0 ± 229.5 * (6.0%)	144.8 ± 20.0	275.0 ± 45.8 # (0.75%)	884.1 ± 183.5 * (5.1%)

Table 2.5 Metabolites detected in the fecal samples of rats at 0-24 h after given a single gavage of 35 mg/kg δTE/γTE.

A single gavage of δTE/γTE is equivalent to intake of δTE and γTE at 19.6 and 2.4 μmol, respectively. Data are expressed as mean ± SEM (% excretion after subtracting baseline). # $P < 0.1$, * $P < 0.05$, and ** $P < 0.01$: difference between control and tocopherol/tocotrienol supplementation. n.d. – not detectable

Total amount excreted (nmol)	Study 1: δTE/γTE		Study 2: δTE/γTE		
	0 h	24 h	0 h	8 h	24 h
δ-CEHC	1.1 ± 0.6	26.1 ± 9.1 #	2.2 ± 0.1	1.5 ± 0.4	28.1 ± 7.0 *
γTE-7'	4.9 ± 0.2	15.5 ± 1.9 **	n.d	n.d	n.d
δTE-7'	Low	14.2 ± 0.8 **	Low	Low	4.6 ± 1.9 #
γTE-9'	4.8 ± 0.9	25.4 ± 5.0 **	5.0 ± 0.6	2.0 ± 0.3 **	13.3 ± 2.9 *
δTE-9'	Low	33.4 ± 3.7 **	Low	Low	20.6 ± 4.9 *
γTE-11' (2DB)	13.7 ± 2.7	50.2 ± 1.5 **	14.5 ± 1.7	6.8 ± 1.1 *	46.4 ± 12.2 *
δTE-11' (2DB)	0.4 ± 0.0	167.2 ± 6.0 **	0.4 ± 0.0	0.2 ± 0.0	141.8 ± 37.1 *
γTE-13' (2DB)	19.1 ± 6.0	36.1 ± 10.3	39.6 ± 6.5	16.1 ± 2.6 *	138.2 ± 28.0 *
γTE-13' (3DB)	8.9 ± 3.5	60.2 ± 19.2 #	4.6 ± 0.8	1.1 ± 0.3 *	13.1 ± 1.7 *
δTE-13' (2DB)	1.2 ± 0.4	351.4 ± 87.9 **	1.7 ± 0.2	0.9 ± 0.3	551.3 ± 72.9 **
δTE-13' (3DB)	1.0 ± 0.4	449.8 ± 70.7 **	0.1 ± 0.1	0.1 ± 0.1	451.1 ± 119.5 **
γTE-13'OH	6.4 ± 1.6	22.2 ± 3.8 *	6.6 ± 0.9	2.6 ± 0.2 *	20.6 ± 3.2 **
δTE-13'OH	0.6 ± 0.1	251.8 ± 27.9 **	0.7 ± 0.0	0.5 ± 0.3	237.2 ± 50.5 **
γTE-13'S	1.6 ± 0.5	18.0 ± 2.5 *	n.d	n.d	n.d
δTE-13'S	Low	177.1 ± 25.7 **	Low	Low	17.3 ± 3.1 *
δ-metabolites (nmol)	4.4 ± 0.4	1489.1 ± 159.8 * (7.6%)	5.9 ± 0.4	3.9 ± 1.1	1468.9 ± 290.2 * (7.5%)
γ-metabolites (nmol)	82.1 ± 19.3	279.6 ± 37.2 ** (8.3%)	73.9 ± 8.7	30.6 ± 4.2	239.9 ± 49.2 * (8.3%)

Table 2.6 Predominant metabolites detected in the urine samples of rats at 8-24 h after given a single gavage of γTmT or δTE/γTE. A single gavage of 46 mg/kg of γTmT is equivalent to intake of γT, δT and αT at 17.3, 6.73 and 3.16 μmoles and 35 mg/kg δTE/γTE is equivalent to intake of δTE and γTE at 19.6 and 2.4 μmol, respectively. Data are expressed as mean ± SEM (% excretion after subtracting baseline). * $P< 0.05$, ** $P< 0.01$, *** $P< 0.001$ and, # $P< 0.1$: difference between control and tocopherol/tocotrienol supplementation.

Study 1: Total amount (nmol)	γTmT at 46 mg/kg		δTE/γTE at 35 mg/kg	
	0hr	24hr	0hr	24hr
δ-CEHC	0.03 ± 0.02	0.7 ± 0.1 **	0.2 ± 0.2	2.6 ± 1.6 **
SO3-δ-CEHC	1.0 ± 0.5	10.8 ± 1.6 **	3.13 ± 0.9	52.0 ± 13.8 *
Conjugated-δ-CEHC	13.6 ± 0.3	103.9 ± 18.3 *	4.0 ± 1.3	65.9 ± 25.3 **
γ-CEHC	0.1 ± 0.02	0.3 ± 0.03 **	0.3 ± 0.1	0.3 ± 0.1
SO3-γ-CEHC	6.5 ± 2.1	37.2 ± 3.4 **	12.4 ± 3.8	31.0 ± 2.1 *
Conjugated-γ-CEHC	167.4 ± 11.8	506.4 ± 72.8 *	18.7 ± 0.4	19.1 ± 7.2
δ-metabolites (nmol)	14.7 ± 0.7	115.4 ± 19.8 ** (1.1%)	7.4 ± 2.3	120.5 ± 38.0 ** (0.6%)
γ-metabolites (nmol)	174.0 ± 13.9	543.9 ± 75.7 ** (2.0%)	31.3 ± 3.7	50.4 ± 8.3 * (0.8%)

Study 2: Total amount (nmol)	γTmT at 46 mg/kg			δTE/γTE at 35 mg/kg		
	0hr	8hr	24hr	0hr	8hr	24hr
δ-CEHC	0.1 ± 0.03	0.2 ± 0.01 *	1.9 ± 0.4 **	0.1 ± 0.04	0.5 ± 0.2	6.4 ± 2.1 *
SO3-δ-CEHC	0.7 ± 0.1	5.1 ± 0.6 **	9.7 ± 1.8 **	0.8 ± 0.4	18.7 ± 5.5 *	37.1 ± 6.1 **
Conjugated-δ-CEHC	2.2 ± 0.7	27.2 ± 9.1 **	71.3 ± 30.6 **	3.8 ± 0.9	32.3 ± 12.5 *	48.3 ± 27.2 *
γ-CEHC	0.1 ± 0.03	0.03 ± 0.01 #	1.0 ± 0.3 *	0.2 ± 0.1	0.1 ± 0.1	1.4 ± 0.2 **
SO3-γ-CEHC	8.0 ± 0.8	14.7 ± 3.8	34.4 ± 5.4 **	13.1 ± 3.4	9.6 ± 2.3	26.8 ± 4.8 **
Conjugated-γ-CEHC	9.4 ± 4.3	69 ± 23.3 *	274.8 ± 45.7 **	16.2 ± 5.2	13.1 ± 4.6	23.2 ± 13.8
δ-metabolites (nmol)	2.9 ± 0.6	32.5 ± 9.3 ** (0.35%)	82.8 ± 30.6 ** (0.90%)	4.6 ± 1.2	51.5 ± 18.2 ** (0.20%)	91.7 ± 31.9 ** (0.5%)
γ-metabolites (nmol)	17.5 ± 4.4	83.7 ± 20.4 ** (0.36%)	310.2 ± 50.4 ** (1.72%)	29.6 ± 8.5	22.8 ± 6.9	51.3 ± 18.3 * (0.9%)

Table 2.7 Percent (%) of vitamin E forms and metabolites recovered in the plasma, urine, and feces.

The values were calculated by the ratio of AUCs (plasma) or total amount of 24-h urinary or fecal excretion to the amount of γT or δTE intake.

%	Plasma vitE forms	Plasma metabolites	Fecal vitE forms	Fecal metabolite	Urine metabolite	Total recovery
γT	18.6	1.3	26.0-45.3	5.6	1.9	53.4-72.7
δT	11.2	0.6	24.7-45.3	7.1	1.0	44.6-65.2
γTE	5.9	3	30.6	8.3	0.9	48.7
δTE	3.5	0.66	18.6	7.6	0.6	31.0

Table 2.8 Metabolites from γT in plasma of subjects supplemented with 2 γT-enriched gel tab every 12 hours for 3 doses.

Blood samples were collected from 10 healthy volunteers at baseline, 24 hours (before receiving dose 3) and 30 hours (6 hours after receiving dose 3). Data are expressed as mean ± SEM. # $P < 0.1$, * $P < 0.05$, ** $P < 0.01$, and *** $P < 0.001$ significant different compared to baseline.

Conc. (μM)	Baseline	24hr	30hr
γ-SO3-CEHC	0.001 ± 0.0001	0.02 ± 0.005 ***	0.02 ± 0.004 ***
γ-CEHC	0.2 ± 0.04	6.8 ± 1.4 ***	6.9 ± 1.3 ***
α-CEHC	0.01 ± 0.002	0.03 ± 0.01 *	0.03 ± 0.01 *
γT-11'S	0.002 ± 0.001	0.04 ± 0.01 *	0.03 ± 0.01 **
γT-13'S	0.001 ± 0.0004	0.04 ± 0.02 #	0.03 ± 0.02
γT-11'	Low	0.01 ± 0.002 #	0.004 ± 0.002 *
γT-13'	0.001 ± 0.0004	0.02 ± 0.004 ***	0.02 ± 0.01 **
γT-13'-OH	0.004 ± 0.0004	0.06 ± 0.011 ***	0.05 ± 0.01 ***
αT-13'-OH	0.013 ± 0.0013	0.01 ± 0.002	0.01 ± 0.001

CHAPTER 3. ALPHA- AND GAMMA-TOCOPHEROL ATTENUATED DSS-INDUCED BARRIER DYSFUNCTION AND MODULATED MICROBIAL COMPOSITION

3.1 Abstract

Inflammatory bowel diseases (IBD) are chronic idiopathic inflammatory conditions characterized by disruption of intestinal barrier integrity and affect 3 million people in the United States. We investigated the potential protective effect of vitamin E forms, i.e., α-tocopherol (αT) and γ-tocopherol (γT), on intestinal barrier function in a cellular model and a mouse colitis model. In Caco-2 colon epithelial cells, we evaluated the effect of αT (25μM) or γT (25μM) on cytokine (10 ng/mL TNF-α/IFN-γ)-induced impairment of trans-epithelial electrical resistance (TEER). In male BALB/c mice, we examined the effect of αT or γT-rich mixed tocopherols at 0.05% diet on dextran sodium sulfate (DSS)-induced colitis and fecal microbiota using paired-end sequencing of 16S rRNA amplicon. Cytokine treatment led to a reduction of Caco-2 cell barrier resistance. Both αT and γT were able to preserve Caco-2 barrier integrity. Similarly, αT and γT attenuated DSS induced fecal bleeding and diarrhea in mice and reduced colon inflammation and colitis-associated damages based on histological analysis. Additionally, αT and γT supplementation attenuated colitis associated loss of tight junction protein, occludin. Gut microbiota data showed that DSS treatment reduced the relative abundance of Lachnospiraceae compared to healthy mice, and supplementation of αT and γT partially reversed this effect. Interestingly, the family Lachnospiraceae has been reported to decrease in IBD patients. Our study demonstrated protective effects of vitamin E forms on intestinal barrier integrity in a cell-based model and a colitis model in mice. Furthermore, we demonstrated that these

vitamin E forms caused favorable changes in intestinal microbial population under colitis condition.

3.2 Introduction

Inflammatory bowel diseases (IBD) are chronic inflammatory disorders of the gastrointestinal tracts that consist of two major types known as Crohn's Disease (CD) and Ulcerative Colitis (UC). An estimation of 3 million adults in the U.S. is reported being diagnosed with IBD [104]; this number not only increases in the U.S. but worldwide [106]. Although the pathoetiology of IBD remains unclear, inappropriate inflammatory response, defect in the gastrointestinal epithelial barrier, and disturbed gut microbial population are some of the major characteristics identified in patients with IBD [108].

Generally, intestinal microorganisms are viewed as symbionts by establishing a mutual relationship with the host. The host provides a nutritious environment and residence for the gut microbes, and as return, the microbes produce short-chain fatty acids and essential vitamins for the host [122]. However, some diseases will disrupt microbial communities, reduce microbial diversity and give rise to detrimental microorganisms that could negatively affect host health [122-124]. This perturbance in gut microbial population is referred to as "dysbiosis", which is a pattern often observed in patients with IBD. The relative abundance of certain bacterial taxa correlates with established markers of disease activity such as enriched *Enterobacteriaceae* and depleted *Lachnospiraceae* [124]. Increased penetration of bacteria in mucosa and decreased bacterial species richness are observed in IBD patients [124]. These changes in microbial patterns leading to dysbiosis are critical for the pathogenesis of IBD.

Accumulating evidence suggests that a defect in the gastrointestinal epithelial barrier is an important factor for the development of IBD. Many studies have demonstrated that patients with IBD suffer from inflammation-induced leak flux diarrhea due to impaired intestinal barrier [145-147]. One important component of intestinal barrier integrity are tight junctions (TJ). Tight junctions are protein complexes that consist of transmembrane proteins, cytosolic scaffold proteins and the cytoskeleton. TJ proteins regulate the passage of ions, water, and molecules through the paracellular pathway [151,152,243]. The interaction of TJ proteins on cell membrane of the epithelial cells forms a barrier that protects against the permeation of harmful molecules cross the intestinal lumen [148]. TJ strands are critical for the maintenance of TJ integrity, and Schulzke et al found that patients with CD or UC had increased intestinal epithelial leaks due to reduced tight junction (TJ) complexity, with lower TJ strands and increased frequency of strand discontinuities [147].

Some of transmembrane proteins involved in TJ's include occludin, claudins and junctional adhesion molecules (JAM). These transmembrane proteins form the backbone of TJ strands creating a semipermeable barrier in the epithelium [244].Besides the transmembrane proteins, the cytosolic scaffold protein, zonula occluden-1 (ZO-1), also plays a critical role in barrier formation in the epithelium. ZO-1 anchors the transmembrane proteins to the cytoskeletal molecules, which is important for tight junction assembly [245]. Factors such as pro-inflammatory cytokines and dextran sodium sulfate (DSS) treatment can impair intestinal barrier function via modification of TJ assembly and expression in cells [157] and animals [149]. The increased permeation of intestinal antigens to the body activates inflammatory response and accelerates the progression of IBD [150].

Vitamin E is generally referred to eight structurally related lipophilic antioxidants, i.e., α-, β-, γ-, and δ-tocopherol (αT, βT, γT, and δT) and corresponding tocotrienols [1]. Among the different isoforms of vitamin E, αT is the predominant vitamin E in plasma and tissues due to the high binding affinity to hepatic α-tocopherol transfer protein (αTTP) that transports αT and prevents it from being metabolized in the liver [1,35,225]. Unlike αT, other vitamin E forms, such as γT, are substantially metabolized in the liver by cytochrome P450-4F2 via ω-hydroxylation and oxidation to generate 13'-hydroxychromanol (13'-OH) and 13'-carboxychromanol (13'-COOH), which are further metabolized via β-oxidation to various shorter-chain carboxychromanols [1,24,54].

Although αT is the predominant form of vitamin E in tissues, γT is the major vitamin E form in the U.S. diet and possesses unique biological properties that may be beneficial against chronic diseases [11]. For instance, γT with an un-substituted 5-position can trap reactive nitrogen species that are enhanced during inflammation, but not αT with a methyl group at the 5-position [1]. We also demonstrated that 13'-COOHs derived from γT are potent dual inhibitors of pro-inflammatory enzymes, cyclooxygenases [52] and 5-lipoxygenase [54]. Consistent with these mechanistic studies, γT [32] and γT rich mixed tocopherol (γTmT) supplementation [160] attenuated colon inflammation induced by DSS in mice. Although γT possesses anti-inflammatory activities that may be beneficial against IBD, IBD is a multi-factorial disease involving intestinal barrier dysfunction and microbial dysbiosis. Here, we investigated and compared the effect of γT and αT against cytokine-induced barrier dysfunction in Caco-2 monolayer, as well as the effect of γTmT (containing γT, δT and αT at 58, 22, and 11%) and αT supplementation at 0.05% diet on DSS-induced colitis in male Balb/c mice.

3.3 Materials and methods

3.3.1 Reagents and diets

αT (>90%) and γT (~95%) used for cellular treatment were obtained from Sigma-Aldrich (St. Louis, MO). Cytokines, TNF-α and IFN-γ, were obtained from Cell Signaling (Denver, MA) and R&D Systems (Minneapolis, MN), respectively. Dextran sodium sulfate (DSS, molecular weight 36-50kDa) was obtained from MP Biomedicals (Solon, OH). Vitamin E metabolites including γ-CEHC (≥98%), α-CEHC, and (±)-αT-5'-COOH (α-CMBHC) were purchased from Cayman Chemicals (Ann Arbor, MI). δT-13'-COOH and δTE-13'-COOH, which are long-chain metabolites from δT and δTE, respectively, were synthesized according to a published procedure [246]. All other chemicals were purchased from Sigma.

AIN93G diet was the control diet obtained from Dyets Inc. (Bethlehem, PA). αT (~96%) and γT enriched mixed tocopherols (γTmT, ~92%, γT:δT:αT, 58:22:11) were obtained from BASF Inc. (Ludwigshafen, Germany) and Yasoo Health Inc. (Johnson City, TN), respectively. The αT- and γTmT-supplemented diets contain 0.05% of αT and γTmT in AIN93G-based diet.

3.3.2 Cell cultures and treatments

Caco-2 cells were maintained at 37°C in a complete DMEM culture medium containing 4.5 mg/ml glucose, 50 U/ml penicillin, 50 U/ml streptomycin, 4 mM glutamine, 25 mM HEPES, and 10% FBS. The cells were plated on 0.4 μM transwell filters (Corning Life Sciences, Corning, NY) with a seeding density of 0.5×10^5 cells/cm^2 and kept at 37°C in a 5% CO_2 environment. Culture medium was changed every two days until 21 days after the cells become confluent. αT or γT were added to the apical membrane compartments of

Caco-2 monolayer. After 16 hours of αT and γT pre-incubation, 10 ng/ml of TNF-α and IFN-γ were added to the basolateral membrane compartment of the Caco-2 monolayer. Transepithelial electrical resistance (TEER) was measured at 48 hours post cytokine stimulation.

3.3.3 Determination of Caco-2 epithelial monolayer resistance

An epithelial voltohmmeter (World Precision Instruments, Sarasota, FL) was used for TEER measurement of the filter-grown Caco-2 intestinal monolayers as described previously [247]. Briefly, both apical and basolateral sides of the epithelium were bathed with complete cell culture medium. Electrical resistance was measured until similar values were recorded on three consecutive measurements. The resistances of monolayers were reported after subtraction of the resistance value of the filters alone. The relative epithelial resistance of Caco-2 monolayer was calculated based on the resistance of control Caco-2 monolayer without vitamin E and cytokine treatment.

3.3.4 DSS-induced colitis model

All animal studies were approved by Purdue Animal Use and Care Committee. Male BALB/c mice (3-4 week old) were obtained from Harlan (Indianapolis, IN) and maintained in the animal care facility at Purdue University under specific pathogen-free condition. DSS was added to drinking water at a final concentration of 2% (wt/vol) for 7 days to induce colitis. Mice were randomly divided into four groups, control AIN93G diet without DSS treatment (n=10), control AIN93G diet with 2% DSS treatment (n=10), 0.05% αT supplemented with 2% DSS (n=10), and 0.05% γTmT supplemented with 2% DSS (n=10). To reduce potential oxidation of αT and γTmT, diets were stored in 4^{o}C and food given to mice were changed once a week. All animals were adapted to the housing

environment for a week prior to the supplementation. To examine the protective effect of long-term vitamin E supplementation against colitis, animals were given their assigned diet for three weeks prior to the administration of DSS. After 3 weeks of pre-supplementation of αT and γTmT, 2% DSS was given in drinking water for 7 days to induce colitis. To examine short-term supplementation of vitamin E forms against colitis, mice started the supplementation diets on the same day as 2% DSS was given. Animals were observed, weighed, and monitored daily during DSS administration for fecal evaluation of bleeding and diarrhea symptoms. The severity of fecal bleeding and diarrhea was subjectively evaluated based on a scale of 0-3. The total fecal score ranges from 0 to a maximum of 6 points based upon the summation of rectal bleeding and diarrhea. Food intake was recorded once per week. After 7 days of DSS administration, animals were sacrificed for tissue collection.

3.3.5 Tissue harvest

During tissue collection, colons were removed, flushed with PBS. The weight and length of the colon were measured and then cut open longitudinally. Half of the colons were fixed flat in 4% formaldehyde. After divided into 3-4 sections, the colon samples were embedded in paraffin for histopathological assessment. The other half of the colons were frozen for Western blot and ELISA analysis of pro-inflammatory markers and barrier function. Plasma samples were collected and stored in -80^{o}C freezer. Fecal samples were collected before sacrifice for 16S rRNA Illunmia sequencing.

3.3.6 Western blot and ELISA

Colonic tissue was homogenized in radioimmunoprecipitation RIPA assay lysis buffer containing protease and phosphatase inhibitors, and total protein concentrations

were measured using Pierce BCA Protein Assay Kit (Thermo Fisher Scientific, Waltham, MA). Equal quantities of protein were separated by a 10% (w/v) SDS-PAGE gel and transferred to PVDF membrane. The membrane was blocked with 5% nonfat milk and incubated overnight (4ºC) with mouse anti-occludin (1:1000; Life Technology, Waltham, MA). After incubation with peroxidase-conjugated goat anti-mouse IgG (1:2000; Santa Cruz, Dallas, TX) for 1 hr at RT, enhanced chemiluminescence (PerkinElmer, Waltham, MA) was used for bioimaging detection. Bands were quantified using ImageJ 1.48v [248], and actin was used as loading control. According to the manufacturer's instruction, colonic IL-6 level was measured using ELISA kit (R&D systems, Minneapolis, MN). LPS-binding protein concentration in plasma was measured using ELISA kit (Novus Biologicals, Centennial, CO).

3.3.7 Histological analysis

Paraffin-embedded colon tissues were cut into 6-μm sections and stained with hematoxylin and eosin (H&E) for histological analysis via light microscopy. The degree of inflammation in cross-sections of the colon was assessed by an experienced pathologist blinded to treatment allocation. Colitis was assessed semi-quantitatively as previously described [249]. Briefly, the severity of the leukocyte infiltration into the mucosa layer was subjectively assessed as none, mild, moderate or severe (0–3). The distribution of inflammation as indicated by leukocyte infiltration was evaluated and denoted as focal/locally extensive, multifocal, or diffuse (0–3). The distribution of erosion/ulceration was assessed as none, focal, multifocal or diffuse (0–3). Necrosis was assessed as none, mild, moderate or severe (0–3). Total disease score ranges from 0 to a maximum of 12 points based upon the summation of each assigned criterion.

3.3.8 DNA extraction, sequencing and sequence analysis

Total genomic DNA was extracted from each fecal sample (~50 mg) using the Fast DNA Soil Spin kit (MP Biomedicals, Solon, OH) according to the manufacturer's instructions. The DNA concentration was determined using NanoDrop 3300 (Thermo Scientific, Wilmington, DE) fluorospectrometer and quality was assessed. MiSeq Illumina 2x250 paired-end sequencing was used to determine fecal bacterial sequences in the fecal samples collected from each mouse on the last day of DSS treatment. Primers that amplify the V3–V4 region of the 16S rRNA gene (forward TAC GGR AGG CAG CAG and reverse CTA CCR GGG TAT CTA ATC C) were used for better primer accuracy, and coverage of phylogenetic information for short sequencing reads [250]. Samples were tagged with a combination of 8-bp forward and reverse primer as to the manufacturer protocol (Illumina, San Diego, CA). PCR was performed using Q5 High Fidelity DNA Polymerase (New England Biolabs, Ipswich, MA). Primers and nucleotides were separated from PCR amplicon using Agencourt AMPure XP kit (Beckman Coulter, Brea, CA). Purified amplicons were quantified by fluorospectrometer with the Quantifluor dsDNA Assay Kit (Promega, Madison, WI). Amplicons from each sample were combined in equimolar quantities and sent to the Purdue Genomics facilities for sequencing using a MiSeq instrument (Illumina, San Diego, CA).

Primer tags and low-quality sequence reads (<Q30) were trimmed prior to DADA2 denoise [251]. Sequences were analyzed using the QIIME2 DADA2 pipeline [252], and SILVA 132 marker gene reference database was used to assign taxonomy to the representative ASV sequences [253]. All subsequent comparisons were performed using equivalent numbers of taxa per sample that were chosen by rarefaction of 26,700 sequences. Good's coverage was used to obtain an estimation of sequence coverage of the communities used in these

analyses [254]. Rarefied analyses of alpha diversity indices (observed OTUs [255], Pielou's evenness [256], Shannon [257]) were calculated to compare microbiota diversity within each sample. Beta diversity comparisons among microbial communities were made using phylogenetic distance matrices, unweighted and weighted Unifrac [258-260] and non-phylogenetic distance matrices using Bray Curtis distance and Jaccard.

3.3.9 Extraction of vitamin E forms and metabolites from plasma

Vitamin E forms and metabolites from plasma sample were extracted as previously described [33]. Briefly, plasma samples were extracted by a solvent mixture containing 6 volume of working methanol (containing 0.2 mg/mL ascorbic acid and 0.1 mg BHT; butylated hydroxytoluene) and 12 volume of hexane via vigorous vortexing for 1 minute. After centrifugation at 12,000 rpm for 2 min, the upper hexane layer was collected and dried under nitrogen gas. The methanol layer (90-95%) was transferred into another tube, and the residual pellet was extracted one more time with 4 volume of working methanol. After extraction of residual pellet, the combined methanol layers were dried under nitrogen gas. Both dried methanol- and hexane-extracted samples were resuspended in HPCL-grade ethanol before being analyzed by HPLC or LC/MS/MS.

3.3.10 Extraction of vitamin E forms and metabolites from feces

Approximately 30-50 mg of fecal samples was homogenized in 2 mL of methanol with ascorbate (0.2 mg/mL) and BHT (0.92 mg/mL). Residues in feces were removed by centrifugation, and 1.4 mL of methanol layer was mixed with 200 μL of PBS and 5 mL of hexane via vigorous vortexing for 1 minute. After centrifugation, 1.4 mL of methanol layer and 4 mL of hexane layer were collected and dried under nitrogen. The dried methanol-

and hexane-extracts were resuspended in 200ul of HPLC-grade ethanol and further diluted 10 times before being analyzed by HPLC or LC/MS/MS.

3.3.11 Analysis of vitamin E forms by HPLC with electrochemical detection

As previously described [25,32], tocopherols were separated on a 150 x 4.6 mm, 5 μm Supelcosil LC-18-DB column (Supelco, Bellefonte, PA), and eluted with 95/5 (v/v) methanol/0.1 M lithium acetate. Vitamin E forms were monitored by coulometric detection (Model Coulochem II, ESA Inc., Chelmsford, MA) at 300 (upstream) and 500 mV (downstream electrode) using a Model 5011 analytical cell.

3.3.12 Analysis of vitamin E metabolites by LC/MS/MS

Prior to LC/MS/MS analysis, α-CMBHC (5 μM) was added as IS to the reconstituted methanol layer. The LC/MS/MS analysis was done with an Agilent 1200 LC system coupled to an Agilent 6460 QQQ mass spectrometer equipped with a jet stream ESI source (Santa Clara, CA) as previously reported [33]. The chromatography used an Atlantis dC18 column (2.1 × 150 mm, 3 μm) from Waters Corporation (Milford, MA). Buffer A consisted of acetonitrile-ethanol-water (165:135:700, v/v/v), and buffer B was acetonitrile-ethanol-water (539:441:20, v/v/v), both of which contained 10 mM ammonium acetate with acetic acid to adjust pH to 4-4.3. The LC gradient was as follows: time 0 min, 0% B; time 1 min, 0% B; time 30 min, 99% B; time 40 min, 99% B; time 43 min, 0% B; time 48 min, 0% B. The flow rate was 0.3 mL/min with a total run time of 48 min. Multiple reaction monitoring was used to analyze each compound. Negative polarity ESI was used with the following source conditions: gas temperature, 325^{o}C; gas flow, 10 liters per min; nebulizer pressure, 30 psi; sheath gas temperature, 250^{o}C; sheath gas flow, 7 liter per min; capillary voltage, 4,000 V; nozzle voltage, 1,500 V; and an electron multiplier voltage of -300 V.

All data were evaluated with Agilent MassHunter Qualitative Analysis software, version B.06.00.

3.3.13 Statistical analysis

Comparisons of barrier function in Caco-2 cell model, colon length-to-weight ratio in colitis model, vitamin E and metabolite concentration were statistically analyzed by one-way ANOVA followed by post hoc analysis of Gabriel. General linear model with repeated measures was used for statistical analysis of fecal symptoms. For histological scores, occludin, IL-6, LBP level and alpha-diversity distances, Kruskal-Wallis analysis (non-parametric equivalent to ANOVA) was used followed by Mann-Whitney U test to determine the overall difference among each group and between treatment groups. Pearson correlation was used to assess the association between plasma LBP level and colonic occludin level. All data in bar graphs and tables are expressed as mean ± SEM. $P < 0.05$ was considered significant. Significant differences in beta diversity were determined using perMANOVA [261] non-parametric multivariate statistic and PERMDISP [262,263] permutational analysis of multivariate dispersions. PERMDISP was used to ensure that the significant differences were not due to differences in dispersion. ANCOM (analysis of composition of microbiomes) followed by Kruskal-Wallis pairwise comparison with false discovery rate (FDR) correction was used for comparison of average proportions of taxa in mice fecal samples between experimental groups. CCA (canonical correspondence analysis) [264] in PAST3 (Paleontological statistics) [265] was used to determine associations between non-DSS, DSS, αT, γTmT, fecal symptoms, histology score, and taxon relative abundance among communities in each fecal sample. Significance of the model for the correlations was calculated using a Monte Carlo test with 999 permutations.

3.4 Results

3.4.1 αT and γT pretreatment attenuated cytokine-induced epithelial barrier dysfunction in Caco-2 monolayer

Similar to previous findings from other investigators, the combination of TNF-α and IFN-γ disrupted intestinal barrier function in Caco-2 model, as indicated by the reduction in epithelial resistance measured by TEER and other permeability markers [156,266-270]. Here, we adopted this *in vitro* model by stimulating barrier dysfunction in human colonic Caco-2 epithelial cell monolayers with 10 ng/mL of TNF-α and IFN-γ to investigate the effect of vitamin E forms on intestinal barrier function. TEER measures epithelial paracellular permeability to ionic solutes, thus is often used to assess barrier function. In Figure 3.1A, cytokine mixture of 10 ng/mL TNF-α and IFN-γ significantly reduced the relative resistance of Caco-2 monolayer. Pre-treatment of αT or γT at 25 μM for 16 h prior to cytokine stimulation partially but significantly attenuated the reduction in Caco-2 epithelial resistance induced by the cytokine mixture. In this study, αT and γT alone did not alter the barrier resistance of Caco-2 monolayer.

To examine the potential mechanism underlying the protective effect of αT and γT, the level of tight junction protein was measured. In the current study, we found that cytokine treatment significantly reduced the protein level of occludin in Caco-2 monolayer (Figure 3.1B). However, both vitamin E forms did not attenuate this cytokine-induced loss of occludin protein in Caco-2 monolayer (Figure 3.1B). We also measured the level of ZO-1 in Caco-2 monolayer and found that cytokine treatment tended to reduce the level of ZO-1 ($P = 0.052$), and this reduction was attenuated by γT ($P = 0.02$), but not αT pre-treatment (Figure 3.1C).

3.4.2 Pre-supplementation of γTmT and αT attenuated DSS-induced colitis symptoms and colon inflammation in mice

In the Caco-2 model, αT and γT pre-treatment attenuated cytokine-induced barrier dysfunction. Here, we used a pre-supplementation model to evaluate whether γTmT and αT supplementations given 3 weeks prior to DSS can prevent colitis induced by 2% DSS in Balb/c mice (Figure 3.2A). DSS administration increased fecal symptoms of bleeding and diarrhea with time (Figure 3.2B). Pre-supplementation of αT and γTmT significantly ameliorated fecal symptoms induced by DSS (Figure 3.2B). Additionally, colon length-to-weight ratio is often used as an indicator of colon inflammation [271]. DSS treatment significantly reduced the colon length-to-weight ratio as compared to non-DSS treated control, but this reduction was attenuated by pre-supplementation of αT and γTmT (Figure 3.2C).

3.4.3 Supplementation of γTmT and αT given at the same time as DSS treatment showed protection against DSS-induced colon inflammation and intestinal barrier dysfunction in mice

γTmT and αT prevented DSS-induced colitis symptoms and colon inflammation in the pre-supplementation model. However, preventive intervention can be challenging to implement when people are not experiencing symptoms or exposed to risk factors. Here, we investigated the protective effect of γTmT and αT when these vitamin E forms were given at the same time as DSS induction (Figure 3.3A). One week supplementation of γTmT and αT significantly raised plasma level of γT (2.5-fold) and αT (2-fold), respectively (Figure 3.3B). Similar to the pre-supplementation study, 2% DSS in drinking water markedly induced colitis symptoms of bleeding and diarrhea time-dependently in mice, and γTmT and αT supplementation (given at the same time as DSS) mitigated colitis symptoms induced by DSS (Figure 3.3C) and attenuated colon inflammation as indicated

by colon length-to-weight ratio (Figure 3.3D). Additionally, histological analysis of colon tissues showed that DSS treatment significantly increased colon damages and immune cell infiltration compared to control non-DSS treated mice, which were attenuated by γTmT supplementation, but not αT (Figure 3.3E). The level of pro-inflammatory cytokine IL-6 in colon tissues was also elevated with DSS treatment and significantly reduced by γTmT and αT supplementation to the level of non-DSS treated control (Figure 3.3F).

Besides inflammation, intestinal epithelial barrier dysfunction is another major characteristic of IBDs. Here, we measured the level of tight junction protein occludin in colon tissues of mice, and found that γTmT and αT supplementation prevent the loss of tight junction protein induced by DSS treatment (Figure 3.4A). Additionally, the levels of lipopolysaccharide (LPS) and LPS-binding protein (LBP) in plasma are positively associated with gut leakiness of the intestinal barrier [272,273]. Similarly, we found that DSS treatment significantly elevated the level of LBP in plasma, which was attenuated by γTmT and αT supplementation (Figure 3.4B). The level of LBP in plasma is negatively correlated with the colonic level of occludin (Figure 3.4C).

3.4.4 DSS treatment and vitamin E supplementation contributed to differences in the composition of fecal microbiome

Comparisons of the rarefied 26700 sequences from each sample of different treatments indicated that there were significant differences in microbial diversity. Alpha-diversity measures the mean species diversity, including evenness and richness, within each fecal sample [249]. Pielou's Evenness index estimates how evenly distributed of the species in sample [256], which showed that DSS treatment significantly lowered the evenness of species distributed in mice compared to those without DSS treatment (Figure 3.5A). Both γTmT and αT did not reverse lowered evenness index caused by DSS treatment

(Figure 3.5A). Another alpha diversity index, observed operational taxonomic units (OTUs), for estimating species richness within samples, indicated that neither DSS treatment nor vitamin E supplementation altered species richness (Figure 3.5B). Alternative alpha diversity metric, Shannon diversity (data not shown), which incorporates species evenness as well as richness, showed a similar trend as Pielou's Evenness index, suggesting that DSS treatment caused changes in species evenness rather than richness.

Beta diversity was measured using a variety of algorithms for distance measures (Jaccard, Bray Curtis, unweighted Unifrac, and weighted Unifrac) to determine the difference in diversity among samples [274]. Principal coordinate analysis (PCoA) is used to visualize dissimilarities in a dataset (Figure 3.5C-D). In each PCoA plot, the percentage on each axis represents the percent variation in the data explained by that axis. PCoA of unweighted Unifrac and weighted Unifrac metrics showed separation of microbial communities between non-DSS treated (Diamond ♦) and DSS treated (Square ■) animals (Figure 3.5C-D). Among DSS-treated animals, PCoA of unweighted Unifrac matrix showed that the microbial communities of animals receiving γTmT supplementation (Sphere ●) were significantly different from those of animals without supplementation (Figure 3.5C). On the other hand, PCoA of weighted Unifrac showed no difference between the microbial communities of DSS-treated and DSS with αT supplemented mice (Figure 3.5D). PERMDISP analysis confirmed that these significances were not due to dispersion difference [262].

ANCOM was used to determine taxa that were significantly different among different treatment groups [275]. At the species level, DSS treatment significantly increased the relative abundance of unclassified *Bacteroides* and *Parabacteroides goldsteinii*

CL02T12C30, and reduced the relative abundance of *Roseburia* uncultured bacterium, uncultured Lachnospiraceae mouse gut metagenomes, and unclassified uncultured Lachnospiraceae (Table 3.1). Interestingly, both γTmT and αT supplementation raised the relative abundance of *Roseburia* uncultured bacterium reduced by DSS treatment (Table 3.1), but only γTmT attenuated the reduction of uncultured Lachnospiraceae mouse gut metagenome induced by DSS in mice. Additionally, αT supplementation increased the relative abundance of *Bacteroides acidifaciens* in fecal sample of mice compared to those without vitamin E supplementation (Table 3.1).

Canonical Correspondence Analysis (CCA) is a constrained ordination method to identify the relationship between the abundance of microbial species and environmental factors. The CCA model indicated that variation in species abundance was significantly correlated with DSS treatment, αT/γTmT supplementation, and fecal symptoms (P=0.001; Figure 3.6). The relative orientation of arrows in this plot shows the direction of the corresponding environmental factor and the arrow length indicates the magnitude of the respective variable in the model. In our CCA, non-DSS control is negatively associated with DSS control treatment and fecal symptoms on axis 1, which explains 70% of the total constrained variation in this model. Vitamin E supplementation, on the other hand, is negatively associated with DSS control treatment and fecal symptom on axis 2, which explains 18% of the total constrained variation in this model.

3.4.5 Concentration of tocopherols and metabolites in the feces

Based on the microbiome analysis, intestinal microbial composition can be influenced by vitamin E forms. Thus, we measured the level of tocopherols and their metabolites presented in the feces of mice. Supplementation with αT and γTmT led to a

significant increase of αT (4-fold) and γT (2-fold) in the feces, respectively (Figure 3.7A). Despite the higher fecal excretion of αT (3759.2 ± 304.4 nmol/g) than γT (938.2 ± 36.6 nmol/g) from supplemented mice ($P < 0.05$), the level of metabolites excreted from γTmT supplementation was higher than αT supplementation (727.2 ± 76.4 vs 260.6 ± 34.4 nmol/g, respectively, $P < 0.05$; Figure 3.7B).

3.4.6 Correlation between the abundance of specific taxa and different experimental measures

Using Spearman correlation, we identified specific taxa that are associated with other experimental measures in this study (Table 3.2). The fecal level of αT metabolites was positively associated with the relative abundance of uncultured Acidobacteriales bacterium and *Eggerthellaceae Enterorhabdus* mouse gut metagenome. The level of γT metabolites excreted from feces was negatively correlated with the relative abundance of *Solibacteraceae (Subgroup 3) Bryobacter*, and the level of δT metabolites from feces of γTmT supplemented mice was positively associated with the relative abundance of uncultured Chitinophagaceae bacterium. The un-metabolized γT and δT were negatively associated with the relative abundance of Clostridiales vadinBB60 group uncultured bacterium and Ruminococcaceae UCG-014 uncultured bacterium, respectively. Additionally, colonic level of IL-6 was positively correlated with the relative abundance of Lachnospiraceae NK4A136 group *Clostridiales bacterium CIEAF 020*, and negatively correlated with the relative abundance of Lachnospiraceae and Ruminococcaceae family. Lastly, systemic LBP level was negatively associated with uncultured Lachnospiraceae mouse gut metagenome.

3.5 Discussion

To our knowledge, our study is the first to show that αT and γT at a supplemental dose can protect against cytokine-induced barrier dysfunction in Caco-2 cells, alleviate fecal symptoms of diarrhea and bleeding, prevent intestinal barrier dysfunction, and modulate microbial composition caused by DSS treatment in mice. Both αT and γT achieved these beneficial effects at 0.05% of diet which is equivalent to a daily supplement of 350-400 mg αT and γT to a human adult with body weight of 70 kg (calculation based on [32,276]). Animals receiving the supplemental dose of αT and γT, either long-term (4 weeks) or short-term (1 week), did not show any adverse effect. Thus, our study indicates that supplementation of αT and γT can be a safe and effective therapeutic option for colon inflammation.

Our study demonstrates that mice with DSS treatment exhibited severe fecal symptoms of bleeding and diarrhea, and inflammation-associated colon damages that are similar to clinical and histopathological diagnosis in human IBD [277]. Patients with IBD reported having bloody stools and diarrhea as a result of inflammatory damage of the digestive tract [278]. During inflammation, neutrophil infiltration of lamina propria and submucosa resulting in cryptitis and crypt abscesses, as well as epithelial degeneration and necrosis leading to the disappearance of epithelial cells, are common histological changes during acute DSS-colitis [131,190,277]. Additionally, elevated pro-inflammatory cytokines, such as TNF-α, IL-1β, and IL-6, are observed in the acute phase of DSS colitis [131,190] and had been shown previously to be associated with human IBD [66,277]. Our study showed that the supplementation of αT and γTmT significantly alleviated fecal symptoms of bleeding and diarrhea, attenuated colon inflammation and damages, and reduced elevated IL-6 level

in the colon induced by DSS, suggesting that supplementation of these vitamin E forms may be a beneficial therapeutic option for IBD.

As previously reported [32,160,161], we found that supplementation of 0.05% αT and γTmT significantly attenuated DSS-induced fecal symptoms of bleeding and diarrhea, as well as colon inflammation in Balb/c mice. Similar protection of αT and γTmT were observed in mice with and without pre-supplementation. Consistent with our current findings, Li et al. [160] reported that γTmT (γT/δT/αT~57/24/13) at 0.03%, 0.1%, and 0.3% dose-dependently attenuated DSS-induced colon inflammation WT mice (C57BL/6 J; 1.0% DSS) and Nrf2 knockout mice (C57BL/SV129; 0.5% DSS), suggesting that the protective effect of γTmT is independent of Nrf2. However, we previously showed that 0.1% γT but not 0.1% γTmT alleviate moderate but not severe colitis induced by 1.5% DSS in mice [32]. In that study, the ratio of γT/δT/αT in the γTmT diet was 45/45/10, whereas for this current study, the ratio of γT/δT/αT was 58/22/11. The ratio of γT is higher in the current study than the previous study, although the overall amount of γT given to the animals was still lower in the current study. Higher γT-to-δT ratio or γT alone appears to have better protection against DSS-induced colitis.

Inflammation-induced leak flux diarrhea is a common symptom in patients with IBD [147]. Elevated pro-inflammatory cytokines in these patients also reported having an impaired barrier function [66,147]. Thus, pro-inflammatory cytokines, such as TNF-α [156,157] and IFN-γ [266], are commonly used in various cellular models to induced epithelial barrier dysfunction for mechanistic studies and drug discovery. Consistent with the previous observations [266], our study showed that the combination of TNF-α and IFN-γ caused Caco-2 epithelial barrier dysfunction as indicated by reduced TEER. αT and γT pre-treatment

partially, but significantly attenuated Caco-2 epithelial barrier dysfunction induced by cytokines. Additionally, cytokine treatments reduced the level of tight junction proteins, occludin and ZO-1, in Caco-2 epithelium. γT, but not αT, attenuated cytokine-induced reduction in ZO-1, but not occludin. Although the protein level of tight junction proteins in Caco-2 epithelium can provide information regarding the status of the barrier function, the assembly of tight junction proteins is more insightful for the determination of barrier function [245,279]. In our study, αT and γT did not alter occludin level after cytokine treatment in Caco-2 cells. Similar observations were reported in another study [266] that treatments did not change the protein level of ZO-1 and occludin, but significantly affected the assembly of these proteins in the membrane of Caco-2 epithelium. This suggested that the assembly of these tight junction proteins is very critical for Caco-2 barrier function, and may explain the potential protection of αT and γT against cytokine-induced barrier dysfunction showed by TEER in our study.

Consistent with the findings from Caco-2 model, αT and γTmT supplementation prevented the loss of tight junction protein, occludin, in the colon, and attenuated increased gut permeability induced by DSS treatment, as indicated by reduced LBP in plasma. Previous study reported that elevated LPS level in plasma is associated with impaired barrier function as a result of bacterial translocation from the intestinal lumen to mesenteric lymph nodes or the circulation in patients with chronic bowel diseases [280]. LPS is endotoxin derived from the cell walls of gram-negative bacteria that can trigger an inflammatory response by innate immune cells [273]. In order to stimulate an inflammatory response, LBP binding to LPS is required for the recognition and binding to CD14, a cellular receptor on myeloid cells, to activate LPS-mediated immune response [281]. A recent study reported that

increase LPS in the circulation markedly elevated LBP level for clearance of endotoxin [282]. Additionally, our data showed that the level of occludin in the colon is inversely correlated with plasma level of LBP, suggesting that circulating LBP can be a predictor for intestinal barrier function. These results indicated that αT and γTmT could protect the intestinal barrier *in vitro* and *in vivo*.

Intestinal microbiota as a key factor for the pathogenesis of IBD can be modulated by DSS treatment and γTmT supplementation. DSS treatment significantly reduced species evenness in mice. Species evenness is one of the alpha-diversity measures, which compares the similarity of the relative abundance of different species present. Previous studies reported a decrease in alpha diversity associated with IBD patients [283,284]. However, alpha-diversity reported in these studies were mostly referred to as species richness. In an animal model, 5% DSS treatment for 5 days significantly reduced species richness and evenness in C57Bl/6 mice [285]. However, our study showed that DSS treatment did not alter species richness instead significantly decreased species evenness, suggesting that DSS treatment is diminishing the abundance of certain species, but not completely deplete them from the environment.

Beta-diversity comparisons revealed that the most significant difference in communities was due to DSS treatment. Based on weighted Unifrac matrix, a phylogenetic matrix based incorporating the abundance of taxa, αT and γTmT supplementation showed no modification on the microbial composition in DSS treated mice. Interestingly, unweighted Unifrac, a phylogenetic matrix based on presence and absence of species, showed that only γTmT, but not αT supplementation, significantly changed microbial composition in mice with DSS treatment. These results suggest that the difference in

microbial communities between DSS and γTmT mice is dependent on the changes in low abundance taxa.

DSS treatment and vitamin E supplementation increased the relative abundance of species in the family of Bacteroidaceae and Tannerellaceae in mice. Previous study reported that the relative abundance of Bacteroidaceae increased in mice with DSS treatment [286]. With more advanced sequencing and sequence analysis techniques, we are able to identify unclassified *Bacteroides* and *Bacteroides acidifaciens* that were significantly increased by DSS treatment and αT supplementation, respectively. Earlier studies using conventional fecal based or mucosal bacterial isolation had often shown an increased concentration of *Bacteroides* species in patients with CD and UC [287]. However, a meta-analysis of the currently available data showed that the mean level of *Bacteroides* in IBD patients with active disease was lower than healthy control [288]. Additionally, a recent study has shown that *Bacteroides thetaiotaomicron*, a species of *Bacteroides*, either actively growing or retained by freeze-dried cells ameliorated colon inflammation induced by 3% DSS in C57BL/6 mice [289]. A recent review summarized that *Bacteroides* is one of the most predominant genera of Gram-negative bacteria that can flexibility adapt to the nutritional condition of the intestinal environment depending on the nutrient availability [290]. The relative abundance of unclassified *Bacteroides* is highest in γTmT-supplemented mice showed in our study, suggesting that some of these *Bacteroides* species are adapted to and can utilize γTmT. Similarly, we found that the relative abundance of *Parabacteroides goldsteinii CL02T12C30* increased with DSS treatment and highest in mice with γTmT supplementation. Neyrinck et al. reported that *Parabacteroides goldsteinii* might have anti-inflammatory properties against hepatic inflammation in

alcoholic liver disease model [291]. Additionally, we found that the relative abundance of *Bacteroides acidifaciens* increased with αT supplementation in mice. Although the role of *Bacteroides acidifaciens* on IBD is not clear, Yang et al. showed that oral administration of *Bacteroides acidifaciens* could prevent obesity and improve insulin sensitivity in B6 mice fed a high-fat diet [292]. Currently, the role of *Bacteroides* and *Parabacteroides* in IBD has not been well established yet; our data suggest that some of these species are responsive to vitamin E supplementation.

DSS treatment significantly reduced the relative abundance of Lachnospiraceae members in mice, which was attenuated by vitamin E supplementation. The depletion of Lachnospiraceae is shown in patients with IBD [122,124]. Consistent with a previous study reporting that the relative abundance of Lachnospiraceae is negatively associated with DSS treatment [285,286], our study showed that the relative abundance of Lachnospiraceae is negatively associated with IL6 and LBP level, which are markers elevated with DSS treatment. A number of unclassified Lachnospiraceae and *Roseburia* are known butyrate producers [293], that contains anti-inflammatory properties against IBD. In our study, αT and γTmT supplementation attenuated DSS-induced depletion of uncultured *Roseburia* and Lachnospiraceae in mice, especially γTmT showing stronger potency for preserving these bacteria, suggesting vitamin E supplementations can modulate DSS-induced dysbiosis in mice.

Based on the microbiota analysis, γTmT supplementation is more effective than αT in modulating microbial dysbiosis caused by DSS, which is likely due to higher metabolites generated from γTmT. Unlike αT, γT and δT are substantially metabolized by hepatic enzyme, cytochrome P450 4F2 (CYP450 4F2) in the body via ω-hydroxylation and

oxidation to generate 13'-hydroxychromanol (13'-OH) and 13'-carboxychromanol (13'-COOH), which can further metabolize via β-oxidation to various shorter-chain carboxychromanols [1,24,54]. We have shown that the fecal level of αT and γT increased in mice after αT and γTmT supplementation, respectively. With higher level of αT given in the diet than γT, the fecal excretion of αT is ~3-fold higher than γT in mice. Interestingly, the level of γT metabolites found in feces is ~3-fold higher in γTmT-supplemented mice than αT metabolites in αT-supplemented mice despite less γTmT given to the animals. This result is consistent with our previous finding that γTmT supplementation significantly increased the levels of metabolites in the feces of mice [32]. More importantly, we observed correlations between some microbial taxa and the different vitamin E forms and metabolites, suggesting that these vitamin E forms and their metabolites can modulate gut microbiota.

Our current study is the first to demonstrate that vitamin E supplementation could alleviate DSS-induced colitis by reducing colon damages associated with inflammation, preserving intestinal barrier function, and modulating intestinal microbial composition in mice. However, our current study did not provide enough evidence to support whether vitamin E forms or their metabolites can be utilized by intestinal microbiota or direct evidence to prove that the anti-colitic properties of vitamin E forms are dependent on the modulation of intestinal microbiota. Therefore, future study research using antibiotic or germ-free model will provide more information regarding the protective effect of vitamin E forms on DSS-induced colitis be due to the modulation of gut microbiota. Also, anaerobic cultivation of vitamin E forms and metabolites with human or animal feces may

discover microbes that can utilize vitamin E forms and metabolites. Nevertheless, our study indicates that vitamin E supplementation can be a safe and effective treatment for IBD.

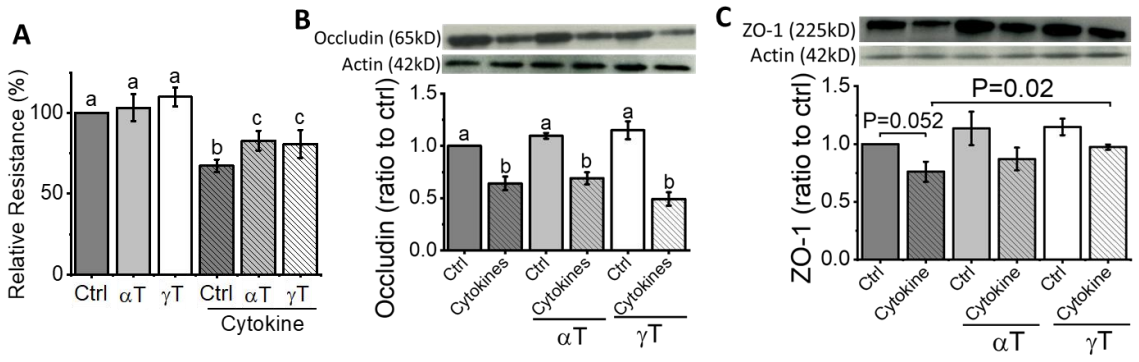

Figure 3.1 The effect of αT and γT pre-treatment on cytokine-induced barrier dysfunction in Caco-2 monolayer.

Caco-2 monolayer was pre-treated without or with 25 μM αT and γT for 16 h, then stimulated without or with 10ng/ml TNF-α/IFN-γ for 48 h. Caco-2 monolayer resistance was measured by TEER. A: αT and γT pre-treatment at 25μM attenuated cytokine-induced barrier dysfunction in Caco-2 monolayer as indicated by reduced in relative monolayer resistance. After TEER measurement, Caco-2 monolayer was collected after 48hr of mixed cytokine treatment for Western blot analysis. B: Mixed cytokine treatment significantly reduced transmembrane protein, occludin, in Caco-2 monolayer. However, αT and γT pre-treatment did not protect against cytokine-induced loss of occludin. C: Mixed cytokine treatment also showed a tendency to reduced cytosolic scaffold protein, ZO-1, in Caco-2 monolayer, and γT but not αT attenuated the loss of ZO-1 induced by cytokine treatment. Data are presented as mean ± SEM (n=3). Different letters represent significant different.

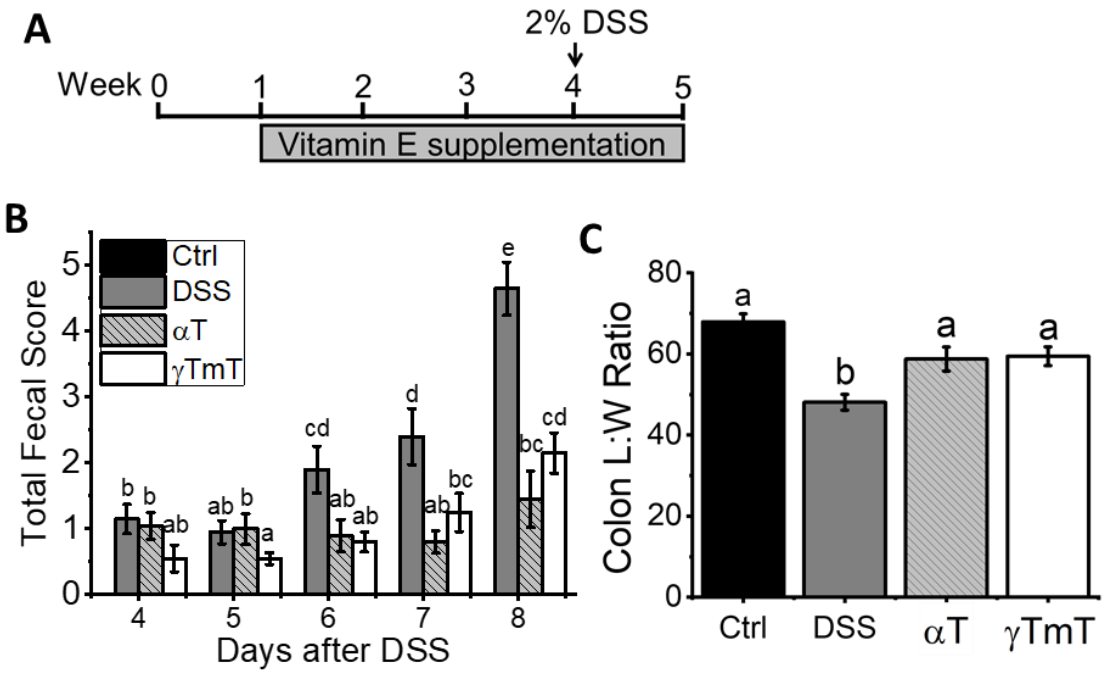

Figure 3.2 The effect of γTmT and αT pre-supplementation on DSS-induced colitis in BALB/c mice.

A: The design of DSS study. B: DSS administration markedly induced colon damage time-dependently as indicated by total fecal score (rectal bleeding and stool consistency). Both αT and γT supplementation attenuated the disease progression of DSS-induced colitis as indicated by total fecal score. C: DSS administration markedly reduced the colon length-to-weight ratio, and was attenuated by supplementation of αT and γT. Mean ± SEM (n= 9-10); different letters represent significant different.

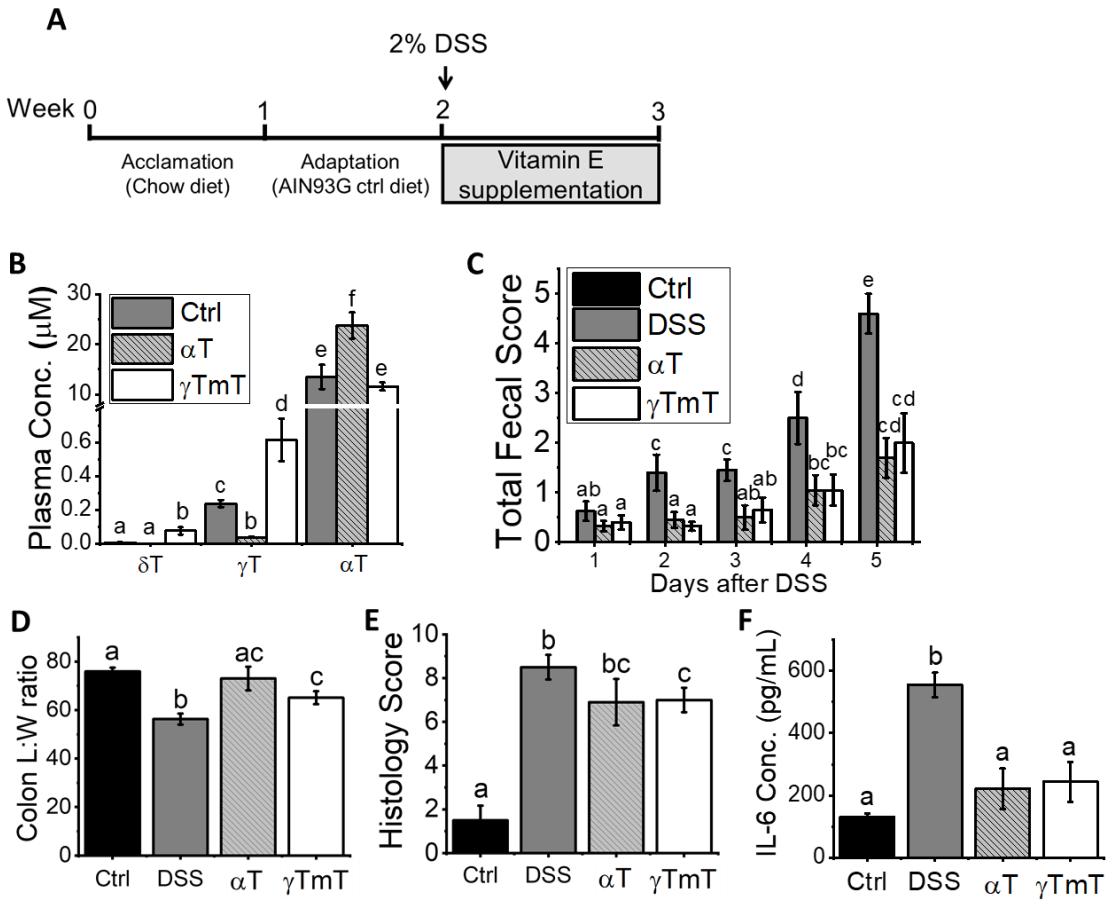

Figure 3.3 The effect of short-term γTmT and αT supplementation on DSS-induced colitis in BALB/c mice.

A: The design of DSS study. B: One week γTmT and αT supplementation increased plasma level of γT and αT, respectively. C-F: DSS (2%) in drinking water markedly induced colitis symptoms time-dependently, and αT and γTmT treatments stabilized disease progression (C), and also alleviated colon inflammation and colitis-associated damages induced by DSS as indicated by colon length-to-weight ratio (D), histological analysis of colon tissues (E) and colonic IL-6 level (F). Mean ± SEM (n=10), different letters represent significant different.

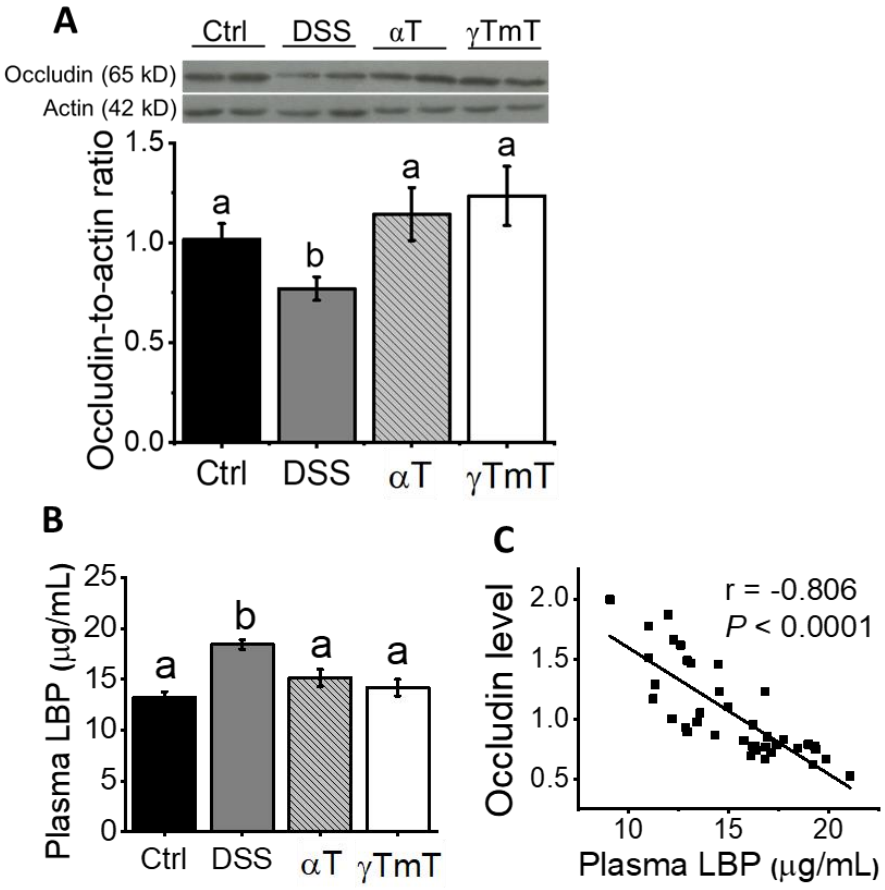

Figure 3.4 The effect of short-term γTmT and αT supplementation on intestinal barrier function induced by DSS in BALB/c mice.

A: Both αT and γT supplementation attenuated DSS-induced lost of tight junction protein, occludin, in colon epithelium of mice. B: αT and γT supplementation reduced systemic LPS binding protein level induced by DSS. C: Colonic occludin level is negatively associated with LPS binding protein level in plasma. Mean ± SEM (n=10), different letters represent significant different. Pearson correlation $p<0.001$.

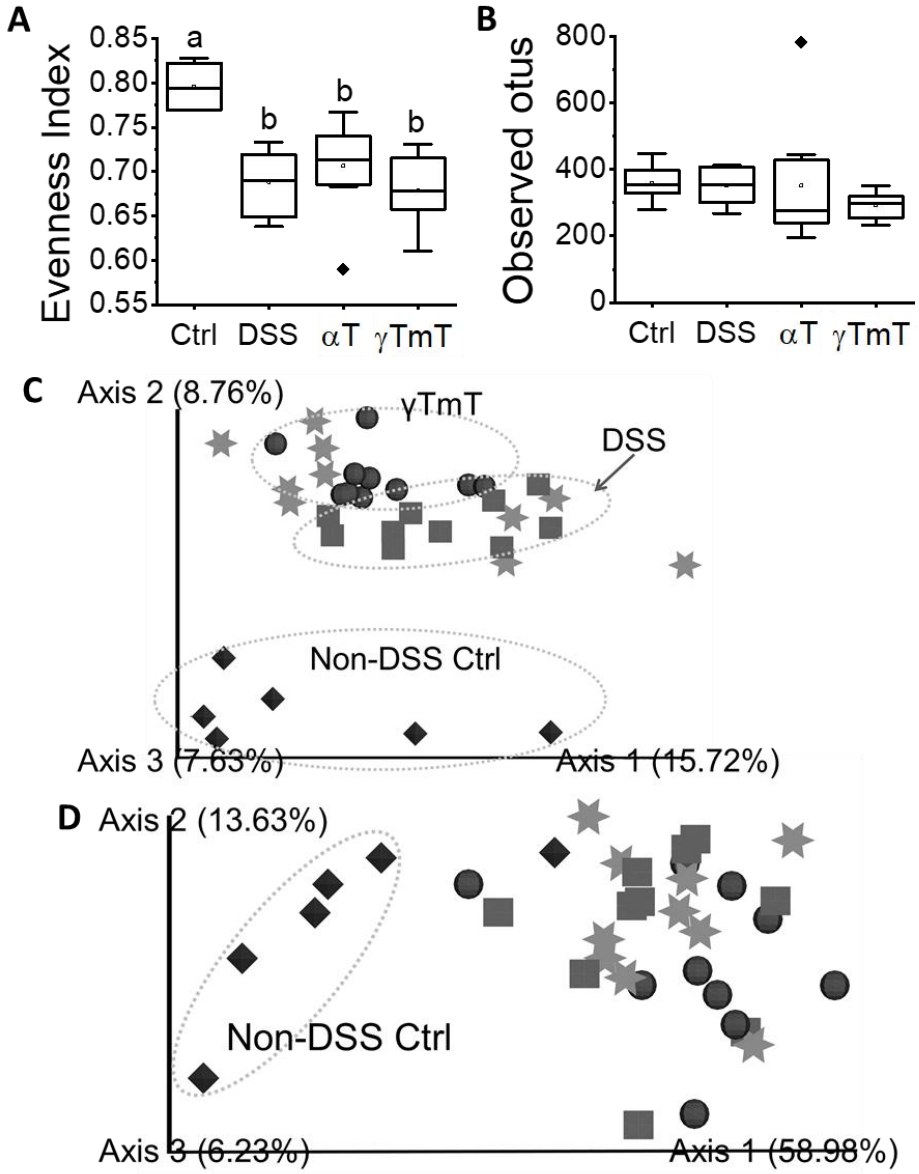

Figure 3.5 The effect of DSS and vitamin E supplementation on microbial diversity in mice. A-B: Mice with DSS treatment had significantly lower Evenness index than mice without DSS (A), but did not change species richness as indicated by Observed otus index (B). Significant differences at P=0.001 were determined using Kruskal-Wallis with 999 Monte Carlo permutations and Bonferroni correction. Data rarefied to a maximum depth of 26700 reads per samples. C-D: DSS contributed to the major differences in microbial communities present in PCoA of the Unweighted Unifrac (C) and Weighted Unifrac (D). Non-DSS control (Diamond ♦); DSS control (Square ■); αT (Star ★); γTmT (Sphere ●). Overall differences were determined using Permanova followed by pairwise permanova test to determine differences among each treatment group (P<0.05). Permdisp indicated that dispersion does not contribute to significance.

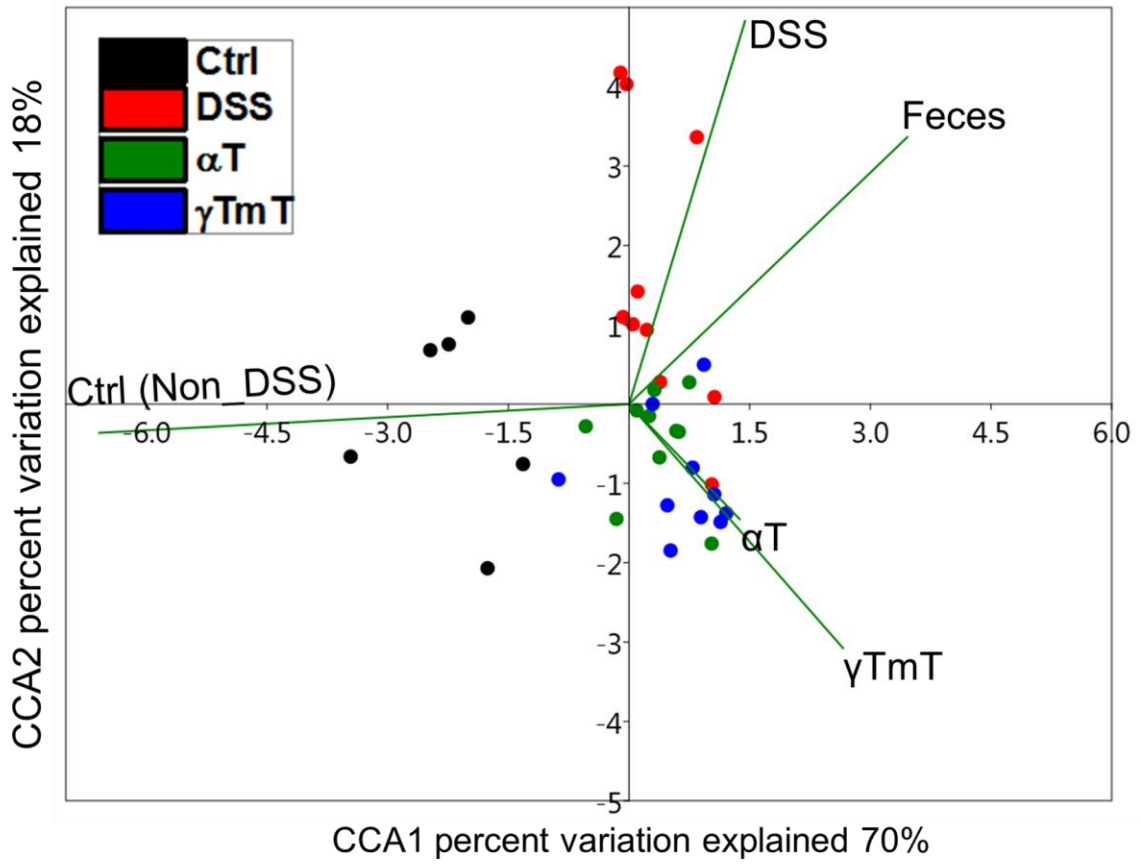

Figure 3.6 The relationship between the relative abundance of microbial species and experimental factors.

CCA model was performed with the relative abundance of fecal microbiome at the genus level as species matrix and the experimental variables of DSS treatments, vitamin E supplementations, fecal symptoms, and histological analysis of colon inflammation as the environmental matrix. Variable biplot arrows indicate the direction of environmental gradients. Angles between arrows corresponds to the relationship of the experimental variables to one another based on the relative abundance of fecal microbiome. The relative length of arrows corresponds to the importance of the respective variables in the model. The fecal microbiome of mice without DSS treatment (non-DSS) is negatively associated with those treated with DSS, as well as the severity of fecal symptoms and colon inflammation by histological analysis on CCA1. Vitamin E supplementations are oppositely associated with DSS and severity of fecal and histological analysis on CCA2. γTmT supplementation showed a strong negative association with DSS than αT based on arrow length. Overall significance of the model is P= 0.001. CCA1 and 2 explained the majority of the total constrained variation of 70% and 18%, respectively.

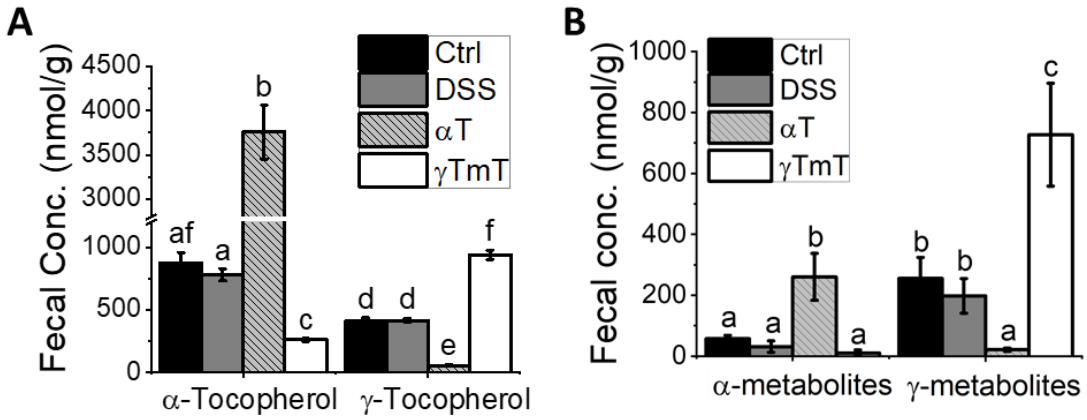

Figure 3.7 γTmT supplementation increases metabolite excretion in feces than αT.

Vitamin E forms and metabolites were extracted from feces of mice receiving different diets. Panel A: αT supplementation significantly increases the parental vitamin E form extraction than γT. Panel B: The metabolites from γT were found significantly higher in feces of mice with γTmT supplementation compared to αT metabolites excreted from mice with αT supplementation. Mean ± SEM (n = 6), different letters represent significant different.

Table 3.1 Relative proportion (%) of bacterial species that significantly differed between treatments.

Overall significance was tested using analysis of composition (ANCOM) with W-value range between 394-478. Differences among the treatment groups were confirmed and tested using Kruskal-Wallis followed by Mann-Whitney U with Bonferroni correction. Unclassified taxa are species that are yet to be classified with a species name. Uncultured taxa are those has yet to be cultured. n = 6 -10 for each treatment..

Genus	Species	Ctrl	DSS	αT	γTmT
Bacteroides	unclassified	3.3 ± 0.8 a	18.5 ± 2.6 b	12.9 ± 1.4 ab	22.8 ± 2.2 b
Bacteroides	acidifaciens	4.2 ± 1.5 a	4.6 ± 0.8 a	11.6 ± 2.7 b	6.8 ± 2.0 ab
Parabacteroides	Parabacteroides goldsteinii CL02T12C30	0.6 ± 0.2 a	10.6 ± 2.2 b	9.2 ± 2.0 b	12.6 ± 2.3 b
Roseburia	uncultured bacterium	0.6 ± 0.1 a	0.01 ± 0.01 b	0.05 ± 0.02 a	0.12 ± 0.04 a
uncultured	mouse gut metagenome	0.2 ± 0.1 a	0.0 ± 0.0 b	0.03 ± 0.02 bc	0.13 ± 0.1 ac
uncultured	Unclassified	0.7 ± 0.1 a	0.2 ± 0.03 b	0.3 ± 0.2 b	0.4 ± 0.1 ab

Table 3.2 Correlation between the abundance of gut microbiome and levels of vitamin E forms, vitamin E metabolites, IL-6, and LPB.

Spearman correlation was used with FDR correction (n = 6-10 for each treatment).

Factors	Taxa	Correlation coefficient	p-value
αT-metabolites	uncultured Acidobacteriales bacterium	0.87	0.001
	Eggerthellaceae Enterorhabdus mouse gut metagenome	0.85	0.001
γT-metabolites	Solibacteraceae (Subgroup 3) Bryobacter	-0.78	0.004
δT-metabolites	uncultured Chitinophagaceae bacterium	0.79	0.004
γT	Clostridiales vadinBB60 group uncultured bacterium	-0.82	0.002
δT	Ruminococcaceae UCG-014 uncultured bacterium	-0.8	0.003
IL-6	Lachnospiraceae NK4A136 group Clostridiales bacterium CIEAF 020	0.63	0.000
	Lachnospiraceae	-0.59	0.000
	Ruminococcaceae	-0.54	0.001
LBP	Lachnospiraceae uncultured mouse gut metagenome	-0.56	0.001

CHAPTER 4. THE COMBINATION OF ASPIRIN AND GAMMA-TOCOPHEROL INHIBITS COLITIS-ASSOCIATED TUMORIGENESIS IN MICE

4.1 Abstract

The chemopreventive effect of aspirin has been evaluated in numerous clinical and pre-clinical model of colorectal cancer (CRC). However, the outcomes are not very impressive instead along with various gastric complications. γ-Tocopherol (γT), a vitamin E form, has been shown to prolong the anti-inflammatory activity of aspirin while alleviating aspirin-induced adverse effect. Herein, we investigated the anticancer efficacy of the combination of aspirin and γT on HCT-116 human colon cancer cells and azoxymethane (AOM)-induced dextran sodium sulfate (DSS) promoted colon tumorigenesis in Balb/c mice. In HCT-116 cells, the combination of aspirin and γT synergistically suppressed the growth of colon cancer cell. Similarly, the combination of 0.025% aspirin and 0.05% γT, but not 0.025% aspirin or 0.05% γT alone, significantly reduced the number of total and large-size tumor by 40% and 50% ($P < 0.05$), respectively. Also, the combination of aspirin and γT reduced the overall size of the tumor by 60% ($P < 0.05$). Stomach lesion caused by aspirin treatment was alleviated by γT supplementation. Interestingly, we found that supplementation of γT, with or without aspirin, modulated intestinal microbiota and increased the relative abundance of butyrate producer, Roseburia, as compared to those without γT supplementation. As recent research reveals the importance of gut microbiota on CRC development, the modulation of gut microbial composition by γT may play a critical role in the antitumor effect of the combination of aspirin and γT in this model. Our data showed that the combination of aspirin and γT has

better anticancer efficacy than aspirin or γT alone, and the supplementation of γT alleviated aspirin-induced side effect as well as modulated gut microbiota.

4.2 Introduction

Colorectal cancer (CRC) is one of the leading causes of cancer death in developed countries with the anticipated death of newly diagnosed patients estimated to be 27,640 in men and 23,380 in women [162], despite advances in detection, surgery, and chemotherapy. The trend of death from colorectal cancer is still increasing in the United States in the last few decades, suggesting that there is no effective treatment for this fatal disease at this point of time. Therefore, the development of a non-toxic and simple to apply drug, that is effective for the prevention and treatment of colorectal cancer requires more attention.

It is well established that prostaglandins and leukotrienes synthesized by COX-1/COX-2 and 5-LOX, respectively, are important in the initiation, progression, and invasion of colon carcinogenesis [79]. Therefore, COX-2 inhibitors, such as aspirin, are proposed as chemoprevention agents for colon cancer [217]. However, long-term use of aspirin can cause many undesirable outcomes in the gastrointestinal tract [216,294]. Additionally, the chemoprotective effect of aspirin was very modest, and some of the outcomes are inconsistent in some clinical trials [213]. To this end, the dual inhibition of COX and 5-LOX has been shown to enhance the anticancer activity of COX-inhibitor alone via the suppression of multiple cancer-promoting pathways [187], suggesting that targeting both COX- and 5-LOX-mediated reactions may improve the chemopreventive activity of aspirin.

Vitamin E contains eight naturally occurring and structurally related fat-soluble antioxidants, i.e., α, β, γ, δ-tocopherol (αT, βT, γT, and δT) and corresponding tocotrienols. The non-αT forms of vitamin E, such as γT, are metabolized by hepatic CYP4F2 via ω-

hydroxylation and oxidation of the side-chain to various long-chain, medium-chain, and short-chain metabolites. Mechanistic studies and pre-clinical models of CRC demonstrated that γT and its long-chain metabolite 13'-carboxychromanol (13'-COOH) have anti-inflammatory properties that are beneficial against colon tumorigenesis. γT has been shown to inhibit the production of prostaglandins and leukotrienes in intact cells assays, and 13'-COOH from γT is a competitive inhibitor of COX-1 [52,54]. Ju et al. demonstrated that the supplementation of γT-rich mixed tocopherol (γTmT) reduced prostaglandin E2 (PGE_2) and leukotriene B4 (LTB_4) level and suppressed azoxymethane (AOM)/dextran sodium sulfate (DSS) induced colon tumorigenesis in mice. Based on these anti-inflammatory and anticancer properties, γT may enhance the anticancer activity of aspirin. We have previously shown that the combination of γT and aspirin prolonged the anti-inflammatory activity of aspirin and also attenuated aspirin-associated adverse effects on carrageenan-induced inflammation in rats [239]. Here, we investigated the anticancer efficacy of the combination of aspirin and γT compared to aspirin or γT alone in HCT-116 human colon cancer cells and on AOM-induced DSS-promoted colon tumorigenesis in male Balb/c mice. We also examined whether the combination of γT with aspirin would attenuate aspirin-induced gastric injury.

4.3 Materials and Methods

4.3.1 Reagents and diets

γT (~95%) and aspirin (>99.5%) was obtained from Sigma (St. Louis, MO). Azoxymethane (AOM) and dextran sodium sulfate (DSS, MW 36,000-50,000) were obtained from Sigma and MP Biochemicals (Solon, Ohio), respectively. Dimethyl

sulfoxide (DMSO) and [3-(4,5)-dimethylthiazol-2-yl]-2,5-diphenyl tetrazolium bromide (MTT) and all other chemicals were from Sigma.

Mice in the control group were fed AIN93G diet from Dyets Inc (Bethlehem, PA), and those in aspirin, γT, and combination group were fed 0.025% aspirin, 0.05% γT (95%, Yasoo Health Inc. Johnson City, TN), and combination of 0.025% aspirin and 0.05% γT-supplemented AIN93G diet, respectively. The dose of aspirin is equivalent to ~175 mg, and the dose of γT is equivalent to ~350 mg daily intake for a 70 kg person (calculation based on [276]). Both dosages represent a medium supplement dose. To minimize potential oxidation of vitamin E, diets were stored in 4^{o}C and food given to mice were changed weekly.

4.3.2 Cell culture and MTT assay

HCT-116 human colon cancer cells were obtained from American Type Culture Collection (Manassas, VA) and routinely cultured in McCoy's 5A modified medium containing 10% fetal bovine serum (FBS) at 37^{o}C in 5% CO_2. Subconfluent HCT-116 cells were treated with different doses of γT, aspirin, and their combination for 24 h, 48 h, and 72 h. Cell viability was examined by MTT assay by estimation of mitochondrial dehydrogenase activity as previously described [100].

4.3.3 AOM-DSS-induced colorectal cancer mode

All animal studies were approved by Purdue Animal Use and Care Committee. Male BALB/c mice (4-5 week old) were obtained from Harlan (Indianapolis, IN) and maintained in the animal care facility at Purdue University under a specific pathogen-free condition with ad libitum water and diets. After a week of acclimatization, mice were randomly divided into non-AOMDSS control (nonAD) and AOMDSS-treated groups.

Mice in the AOMDSS group were injected with 9.5 mg/kg body weight of AOM in 0.1 mL phosphate buffered saline (PBS) intraperitoneally. One week later, AOM-injected mice were further randomized into control (AD), aspirin, γT, and combination (Comb) group. Meanwhile, 1.5% DSS was given to the mice in drinking water for 7 days to induce colitis. The DSS cycle was repeated after two weeks to promote chronic inflammation (Figure 4.2A). Animals were monitor and weighed daily after AOM injection and during DSS administration. Fecal symptoms of bleeding and diarrhea were monitor during DSS administration. The severity of fecal bleeding and diarrhea was subjectively evaluated based on a scale of 0-3. Total fecal score ranges from 0 to a maximum of 6 points based upon the summation of rectal bleeding and diarrhea. Food intake was recorded once per week. After that, animals were being monitored and weighed weekly until the end of the study period.

4.3.4 Tissue harvest and tumor analysis

During tissue collection, colons were removed, flushed with PBS. The weight and length of the colon were measured and then cut open longitudinally from rectum to cecum. Tumors along the colon were examined, recorded, and counted. Half of the colons were fixed flat in 4% formaldehyde. After divided into 3-4 sections, the colon samples were embedded in paraffin for histopathological assessment. The other half of the colons were frozen for future analysis of pro-inflammatory markers and barrier function. Stomach was also removed, rinsed and examined for ulcerative lesion. Scoring criteria for stomach lesion as follows: 0 for no visible lesion; 0.5 for redness and hyperemia in the mucosa; 1 for 1-2 erosion or lesion; 2 for 3-6 erosion or lesion; 3 for > 6 erosion or ulcer. Plasma samples

were collected and stored in -80^{o}C freezer. Fecal samples were collected 24hr before sacrifice for 16S rRNA Illunmia sequencing.

4.3.5 Histological analysis

Colon tissues were embedded in paraffin and stained with hematoxylin and eosin (H&E) for histological analysis via microscopy. Briefly, the degree of inflammation in cross-sections of the colon was assessed by an experienced pathologist blinded to treatment allocation. The inflammation status was assessed semi-quantitatively in non-tumorous tissues and tumorous tissue as described under Materials and Method section in Chapter 3.

4.3.6 DNA extraction, sequencing and sequence analysis

Total genomic DNA was extracted, quantified, amplified, and sequenced as described in DNA extraction, sequencing and sequence analysis under the Materials and Methods section in Chapter 2. Briefly, total genomic DNA was extracted from each fecal sample (~30-40 mg) using the Fast DNA Soil Spin kit and quantified using NanoDrop 3300 (Thermo Scientific, Wilmington, DE) fluorospectrometer, and quality was assessed. MiSeq Illumina 2x250 paired-end sequencing was used to sequence the amplified the V3–V4 region of the 16S rRNA gene in the fecal samples collected from each mouse on the last day of the study period. Amplicons from each sample were combined in equimolar quantities and sent to the Purdue Genomics facilities for sequencing using a MiSeq instrument (Illumina, San Diego, CA).

Primer tags and low-quality sequence reads (<Q30) were trimmed prior to DADA2 denoise [251]. Sequences were analyzed using the QIIME2 DADA2 pipeline [252], and SILVA 132 marker gene reference database was used to assign taxonomy to the representative OTU sequences [253]. All subsequent comparisons were performed based on rarefaction of

21495 sequences per samples. Good's coverage was used to obtain an estimation of sequence coverage of the communities used in these analyses [254]. Rarefied analyses of alpha diversity indices (observed OTUs [255], Pielou's evenness [256], Shannon [257]) were calculated to compare microbiome community diversity within each sample. Beta diversity comparisons among microbial communities were made using phylogenetic distance matrices, unweighted and weighted Unifrac [258-260] and non-phylogenetic distance analysis using Bray Curtis distance and Jaccard.

4.3.7 Statistical analysis

The anticancer efficacy of the combination of aspirin and γT on HCT-116 human colon cancer cells is calculated by comparing the relative cancer cell death induced by the combination γT and aspirin treatment vs. the sum of relative cancer cell death induced by aspirin alone and γT alone using student's t-test. General linear model with repeated measures was used for statistical analysis of fecal symptoms and animal body weight changes. Colon length-to-weight ratio, spleen weight, and stomach lesion were statistically analyzed by one-way ANOVA followed by post hoc analysis of Gabriel. For tumor multiplicity and tumor area, Kruskal-Wallis analysis (non-parametric equivalent to ANOVA) was used followed by Mann-Whitney U test to determine the overall difference among each group and between treatment groups. All data are expressed as mean ± SEM. $P < 0.05$ was considered significant. Significant differences in beta diversity were determined using perMANOVA [261] non-parametric multivariate statistic and PERMDISP [262,263] permutational analysis of multivariate dispersions. PERMDISP was used to ensure significant differences were not due to differences in dispersion. ANCOM (analysis of composition of microbiome) followed by a pairwise comparison of Kruskal-Wallis test

corrected by false discovery rate (FDR) was used for comparison of average proportions of taxa in mice fecal samples between experimental groups. CCA (canonical correspondence analysis) [264] in PAST3 (Paleontological statistics) [265] was used to determine associations between experimental factors, such as non-AOMDSS (nonAD), AOMDSS (AD), aspirin, γT, the combination (Comb), large tumor multiplicity (Ltumor), and taxon relative abundance among communities in each fecal sample. The significance of the model for the correlations was calculated using a Monte Carlo test with 999 permutations.

4.4 Results

4.4.1 The combination of aspirin and γT inhibited proliferation of HCT-116 human colon cancer cells

Cianchi et al. [187] demonstrated that dual inhibition of 5-LOX and COX-2 effectively suppressed the growth of various colon cancer cells. Here, we investigated whether the combination of aspirin and γT has better anti-proliferative activity against cancer growth than aspirin or γT alone using HCT-116 colon cancer cells. Aspirin treatment alone at different dosages did not affect cell viability, while 50 μM γT treatment alone showed a weak reduction in HCT-116 cell viability time-dependently (Figure 4.1). When adding γT to aspirin, γT sensitized HCT-116 cells to respond to aspirin treatment, which the combination of γT and aspirin significantly reduced the relative cell viability of HCT-116 cells time- and dose-dependently (Figure 4.1). The relative cell death induced by the combination of γT and aspirin was ~50% higher than the combined relative cell death induced by γT alone and aspirin alone.

4.4.2 The combination of γT and aspirin, but not aspirin or γT alone, significantly reduced the number of total and large tumors as well as tumor surface area induced by AOMDSS

To investigate the anticancer activity of γT and aspirin compared to aspirin or γT alone in a whole body environment, supplementations of 0.025% aspirin, 0.05% γT or the combination of the two were given to male Balb/c mice with AOM/DSS induction for colon tumorigenesis (Figure 4.2A). Supplementation of aspirin, γT, and their combination did not change body weight of mice compared to the control diet (Figure 4.2B). AOMDSS treatment led to a marked induction of tumors developed in the middle to distal colon (Figure 4.2C) as observed in previous study [32]. Based on histopathological analyses, these tumors were identified as adenomas (Figure 4.2C). The combination of γT and aspirin, but not γT or aspirin alone, significantly reduced total tumor and large-size tumor multiplicity by ~50% in mice as compared to those in AOMDSS control mice (Figure 4.2D). Additionally, the number of total and large size tumor of combination-fed animals was 60-70% lower than those of aspirin-fed mice. Furthermore, the overall tumor surface area of combination-fed animals was 60% lower compared to AOMDSS control mice (Figure 4.2E). Noteworthy, the overall tumor surface area of aspirin-fed mice was 77% higher than combination-fed mice and 65% higher than γT-fed mice (Figure 4.2E). It is also worth to mention that the incidence of 3D tumor is 12 out of 16 in control AOMDSS group, 9 out of 14 in the aspirin group, 9 out of 16 in the γT group, and 7 out of 15 in the combination group (data not shown). These 3D tumors and large size tumor have a higher tendency to become carcinomas. Inconsistent with the higher tumor counts in mice fed aspirin-supplemented diet, histopathological analyses revealed that lower necrosis in tumor tissues of mice with aspirin supplementation (Figure 4.2F).

4.4.3 Aspirin-exacerbated stomach lesion and AOMDSS-induced colitis symptoms and inflammation were attenuated by γT supplementation

Clinical symptoms of colitis such as bleeding and diarrhea were evaluated during each cycle of DSS treatment and presented as total fecal score (Figure 4.3A-B). During the first DSS cycle, AOMDSS treatment induced moderate fecal symptoms of bleeding and diarrhea with time, which was exacerbated by aspirin supplementation on day 7 of DSS treatment, which was attenuated by combination with γT (Figure 4.3A). Supplementation of γT, not the combination, significantly attenuated AOMDSS-induced colitis symptoms on day 6 but not day 7 of DSS treatment. Similar to the first DSS cycle, the second cycle of DSS treatment significantly induced colitis symptoms in mice with time (Figure 4.3B). The fecal symptoms induced during second DSS cycle is more robust than first DSS cycle in the AD control group. Supplementation of γT and the combination significantly attenuated DSS-induced symptoms on day 5 of the second DSS cycle and promoted recovery on day 8 after the removal of DSS treatment from drinking water (Figure 4.3B).

Aspirin supplementation also exacerbated colon and systemic inflammation as well as stomach lesion in mice. Colon length-to-weight ratio is a common marker for colon inflammation. During inflammation, the length of the colon tends to shorten and the weight of colon increases due to infiltration of immune cells [131,190,271]. Here, we showed that aspirin supplementation significantly reduced colon length-to-weight ratio in AOMDSS-treated mice as compared to non-AOMDSS control mice, which was attenuated by the combination of aspirin and γT (Figure 4.3C). Additionally, aspirin supplementation also significantly increase the spleen weight in animals compared to non-AOMDSS control (Figure 4.3D). An increase in spleen weight is another indicator of chronic inflammation [295]. Most importantly, we found that consistent with previous report [216], aspirin

supplementation promoted stomach lesion in mice, which was alleviated by the combined supplementation with γT (Figure 4.3E).

4.4.4 Diets and large tumor multiplicity contributed to differences in mouse fecal microbiota

Comparison of the rarefied 21,495 sequences from each sample of different treatments indicated that there were significant differences in microbial diversity. Alpha-diversity measures the mean species diversity, including evenness and richness, within each fecal sample [249]. Observed operational taxonomic units (Observed OTUs), for estimating species richness within samples, indicated that γT supplementation either alone or combined with aspirin significantly reduced species richness in mice compared to those without γT supplementation (Figure 4.4A). Another alpha diversity index, Pielou's Evenness index estimates how evenly distributed of the species in sample [256], revealed that more than three large tumors significantly decreased species evenness as compared to having less three large size tumor (Figure 4.4B).

Beta-diversity matrices, such as unweighted and weighted Unifrac, were measured to compare the microbial diversity among samples. Principal coordinate analysis (PCoA) plot is used to visualize dissimilarities in a dataset, and the percentage on each axis represents the percent variation in the data was explained by that axis (Figure 4.4C-D). PCoA of unweighted Unifrac matrix showed separation of microbial communities between γT-supplemented (alone or combined with aspirin) mice and those without γT supplementation (Figure 4.4C). Large tumor multiplicity also contributed to the separation of microbial communities as indicated by PCoA of weighted Unifrac matrix (Figure 4.4D). The microbial communities of mice with no large tumor is separated from those with more than three large tumors, while having 1-3 large tumor is intermediate between the two

groups (Figure 4.4D). Permdisp analyses confirmed that the significance observed in these models was not due to dispersion differences [262].

4.4.5 AOMDSS treatment and dietary supplementations altered the microbial composition in mice

ANCOM was used to determine taxa that were significantly different among different treatment groups as shown in Table 4.1 [275]. At the family level, AOMDSS significantly reduced the relative abundance of Bifidobacteriaceae compared to non-AOMDSS control in mice, but was attenuated by the supplementation of aspirin and the combination, but not γT. At the genus level, the combination of aspirin and γT significantly reduced the relative abundance of *Ruminococcaceae UCG-014* in mice as compared to those of AOMDSS control and aspirin. At the species level, the supplementation of γT with or without aspirin significantly increased the relative abundance of *Enterorhabdus* uncultured bacterium and unclassified *Roseburia*, and reduced the relative abundance of uncultured *Clostridia bacterium* in Clostridiales vadinBB60 group. Additionally, *Alistipes obesi* was depleted, and *Candidatus Saccharimonas* uncultured bacterium was enriched in mice with AOMDSS treatment. Supplementation of aspirin, γT, and their combination, significantly reduced the relative abundance of *Candidatus Saccharimonas* uncultured bacterium in mice that was enriched by AOMDSS treatment.

4.4.6 Correlation of gut microbiota and experimental factors

Canonical Correspondence Analysis (CCA) is a constrained ordination method to identify the relationship between the abundance of microbial species and experimental factors. The CCA model indicated that variation in species abundance was significantly correlated with AOMDSS treatment, dietary supplementations of aspirin, γT, and

combination, as well as the multiplicity of large tumors ($P = 0.001$; Figure 4.5). The relative orientation of arrows in this plot shows the direction of the corresponding experimental factors based on microbial composition and the arrow length indicates the magnitude of the respective variable in the model. CCA1 is separated by tumor multiplicity, whereas CCA2 separates based on γT supplementation, which explains 34.9% and 31.7% of the total constrained variation in this model, respectively. Based on the tumor count data, combination-fed mice had lower total and large tumors than mice in other treatment groups, suggesting that microbial composition correlates with large tumor multiplicity on CCA1. Both supplementation of γT and combination contains 0.05% γT in the diet, which influences microbial composition and contributes to the separation on CCA2.

4.5 Discussion

We have demonstrated that the combination of aspirin and γT has better anticancer efficacy than aspirin or γT alone against HCT-116 human colon cancer cells and AOM-induced DSS promoted colon tumorigenesis in mice. The supplementation of γT also attenuated colon and systemic inflammation, as well as stomach lesion exacerbated by aspirin supplementation. Based on microbial analyses, γT supplementation in the diet and large tumor multiplicity are the major contributors in modulating microbial composition. Our study by far demonstrated that by combining aspirin with γT, improves anticancer efficacy of aspirin and alleviates aspirin-induced gastric lesion, in addition to modulation of intestinal microbiota.

Evidence from epidemiological studies reveals an inverse association between the use of aspirin and relative risk for CRC development [217,296]. However, long-term use of aspirin is not plausible as it may lead to upper gastrointestinal (GI) complications such as

gastric ulcers [216]. Most importantly, the chemopreventive efficacy of aspirin shown in some clinical trials is very modest [213]. As shown in our study, aspirin was ineffective in reducing the proliferation of HCT-116 human colon cancer cells, which is also reflected in the AOMDSS-induced tumorigenesis model. Consistent with others[297-299], aspirin treatment neither decreases the tumor multiplicity nor reduces tumor size in AOMDSS-induced colon tumorigenesis. Although one study [300] showed that aspirin inhibits colon carcinogenesis in AOMDSS-induced CF-1 mice, this group of scientists was not able to repeat this finding in their work published the following year [298]. As indicated in the present study, aspirin is ineffective in reducing tumor loads and tumor size in AOMDSS-induced Balb/c mice.

Previous studies also reported that aspirin did not attenuate DSS-induced colitis symptoms and colon inflammation [297,298], which is consistent with our findings. In our study, aspirin not only did not attenuate DSS-induced colitis but also further exacerbated DSS-induced colitis symptoms in the first DSS cycle and increase inflammatory markers as indicated by colon length-to-weight ratio and spleen weight. Furthermore, our study demonstrated that aspirin treatment induced gastric lesion, although this was not reported in the other two studies. This may due to a slightly higher aspirin dose used in our study than the other two studies (0.025% vs. 0.02% respectively) [297,298]. Nevertheless, the exacerbation of colitis symptoms and gastric lesion may due to reduced cytoprotective prostaglandins caused by aspirin [301]. Interestingly, the combination treatment significantly alleviated aspirin-induced gastric lesion and attenuated aspirin-exacerbated colitis symptom during the first DSS cycle.

Mechanistic studies indicate that γT inhibits prostaglandin and leukotriene productions [52,54,83], which are essential for inflammation and cancer progression. Dual

inhibition of 5-LOX and COX-2 has been shown effectively suppresses tumorigenesis in various colon cancer cells [187] and $APC^{min/+}$ mouse model [302]. In HCT-116 human colon cancer cells, we have demonstrated that γT treatment enhanced aspirin's anticancer efficacy by sensitizing HCT-116 to response to aspirin treatment. Consistent with the findings from the cell study, we have shown that the combination of γT and aspirin reduced tumor formation and enhanced tumor necrosis in AOMDSS-induced mice. The anticancer efficacy of the combination of aspirin and γT is better than aspirin or γT alone. Studies by others and us [32,94,219] have shown that γT supplementation suppresses colon tumorigenesis in pre-clinical animal models. Although the reduced number and size of tumor in γT-supplemented mice is not statistically significant compared to those in AD group in the present study, it is worth to mention that the amount of γT supplemented in the current study is at least 50% lower than γT supplemented in the previous studies [32,94,219].

γT supplementation not only enhanced the anticancer efficacy of aspirin, it also alleviated aspirin-caused side effects, which is consistent with our observation in carrageenan-induced inflammation in rats [239]. Long-term use of aspirin is known to cause GI related problems [294]. Previous study showed that 5-LOX inhibitor effectively reduced gastric damages induced by NSAIDs [303], dual inhibition of 5-LOX and COX-2 not only enhances anticancer efficacy but also reduced associated side effect as demonstrated in our study.

Accumulating evidence suggests that intestinal microbiota is critical in the development of CRC. We found that higher number of large tumors decrease species evenness and changes microbial composition. Additionally, we have shown that γT- and comb-supplemented mice have lower species richness compared to animals without γT

supplementation, i.e., nonAD, AD, and aspirin, while the species richness is not significantly different between AD and nonAD group. Species richness is an alpha-diversity index to evaluate microbial stability under certain health condition. Traditionally, lower species richness represents unstable microbiome associated with illness, which is not always concomitant as discussed by Johnson and Burnet [304].

Additionally, we found that γT supplementation alone or in combination with aspirin significantly influence the microbial composition in mice as the supplementation of γT and combination of aspirin and γT increased the relative abundance of unclassified *Roseburia* species, which are depleted in patients with CRC [305,306]. *Roseburia* contains butyrate producers that exert pro-inflammatory activities against inflammation-induced colorectal cancer [207,307]. Additionally, AOMDSS treatment increased the relative abundance of *Candidatus Saccharimonas* in the TM7 phylum in feces compared to nonAD mice. Bacteria in the TM7 phylum are associated with active inflammatory bowel disease [308]. Interestingly, our data indicated that aspirin, γT, and their combination reduced the relative abundance of *Candidatus Saccharimonas* compared to AD mice. Furthermore, we found the relative abundance of Bifidobacteriaceae family reduced within the feces of AD mice as compared to nonAD mice, and the supplementation of aspirin alone or with γT attenuated the loss of Bifidobacteriaceae induced by AOMDSS treatment. Species in the Bifidobacteriaceae family exhibit anticancer activities in AOM-induced colon carcinogenesis in rats [309-311]. However, only the combination treatment, but not aspirin suppressed tumorigenesis in our study, suggesting that γT may have symbiotic activity with Bifidobacteriaceae to promote the anticancer activity.

Our study demonstrated that the combination of γT with aspirin enhanced the anticancer efficacy of aspirin in human colon cancer cells and colitis-associated colon tumorigenesis in mice, as well as attenuated aspirin-induced side effects. Further analyses on colon inflammation markers such as pro-inflammatory cytokines, specifically IL-6 and transcription factors STAT3 are needed as IL-6/STAT3 signaling cascade is a critical regulator for the proliferation and survival of colon carcinogenesis [312]. A previous study showed that aspirin down-regulated the IL-6/STAT3 pathway and activated apoptosis in colon tumor tissues but it was not sufficient in reducing the tumor load [297]. It is possible that γT enhanced aspirin's apoptotic activity by modulating sphingolipid metabolism in our study. Additionally, the level of eicosanoids from 5-LOX and COX-2 should be measured in the tumor tissue as the combination of aspirin and γT can inhibit both enzymes, which may be contributed to the tumor suppression observed in this study. Intestinal microbiota also plays a critical role in the development and progression of CRC. The results from microbial analysis also revealed that tumor multiplicity and γT supplementation are the major contributors to the alteration of microbial composition in this model. Unfortunately, we do not have enough evidence to show whether these changes in microbial composition is contributed to the tumor suppression in this model.

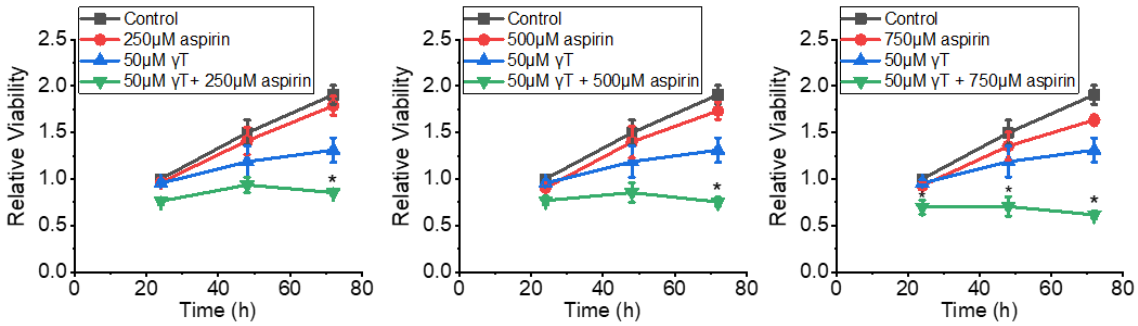

Figure 4.1 The effect of aspirin, γT, and their combination on cell viability of human colon HCT-116 cells.

The relative cell viability was measured by MTT assay after cells were treated with aspirin, γT, and aspirin/γT combination at indicated concentrations and times compared to DMSO controls. Data are presented as mean ± SEM (n=4). * represents $P < 0.05$ using student's t-test by comparing the relative cell death induced by the combination treatment of aspirin and γT vs. the combine relative cell death induced by aspirin alone and γT alone.

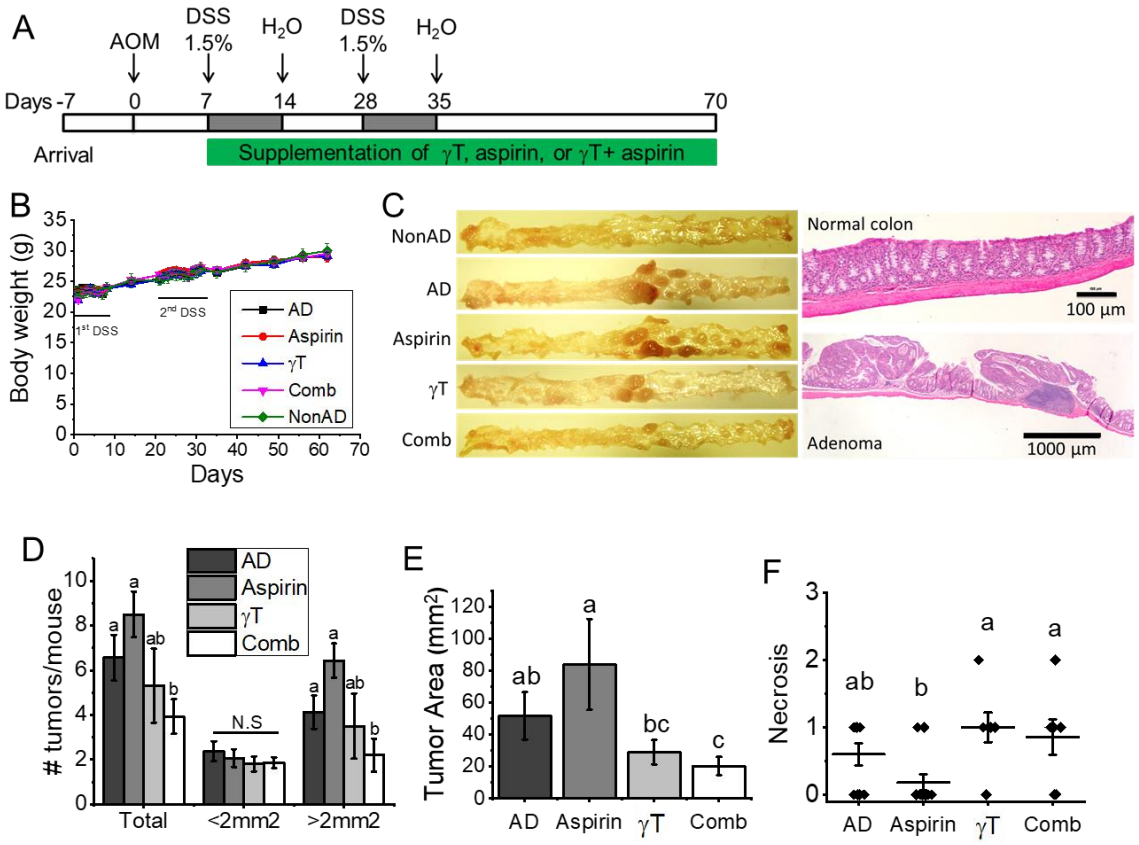

Figure 4.2 The effects of aspirin, γT, and their combination (Comb) on AOM-induced DSS promoted colon tumorigenesis.

A: The study design. B: The body weight of mice during the entire experiment after supplementation started. C: Polyps were counted macroscopically and identified histopathologically as adenomas. D-F: The effect of aspirin, γT, and their combination on colon tumor multiplicity (D), tumor area (E), and necrosis in tumor tissues (F). Data are presented as mean ± SEM (n=5-16). Different letters represent significant different.

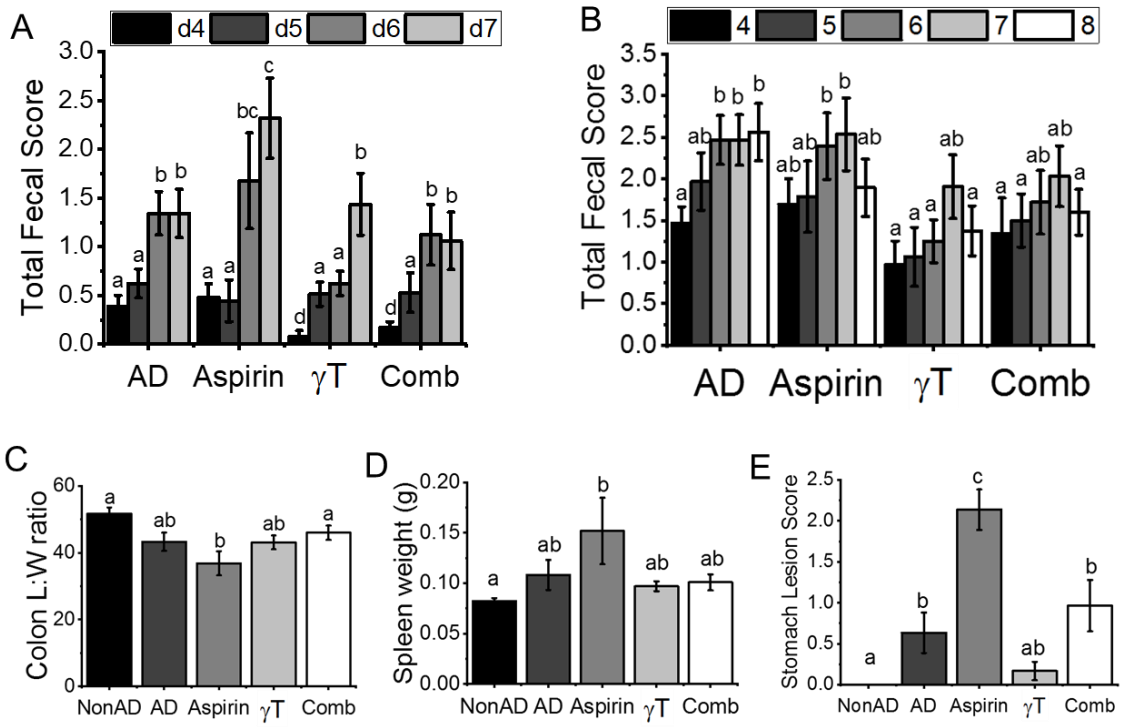

Figure 4.3 The effects of aspirin, γT, and their combination (Comb) on colitis symptoms and inflammation induced by AOM/DSS.

A-B: The effect of aspirin, γT, and their combination on total fecal score of bleeding and diarrhea symptoms during first (A) and second (B) DSS cycle, and colon length-to-weight (L:W) ratio (C), and spleen weight (D), as well as stomach lesion (E). Data are presented as mean ± SEM (n=5-16). Different letters represent significant different.

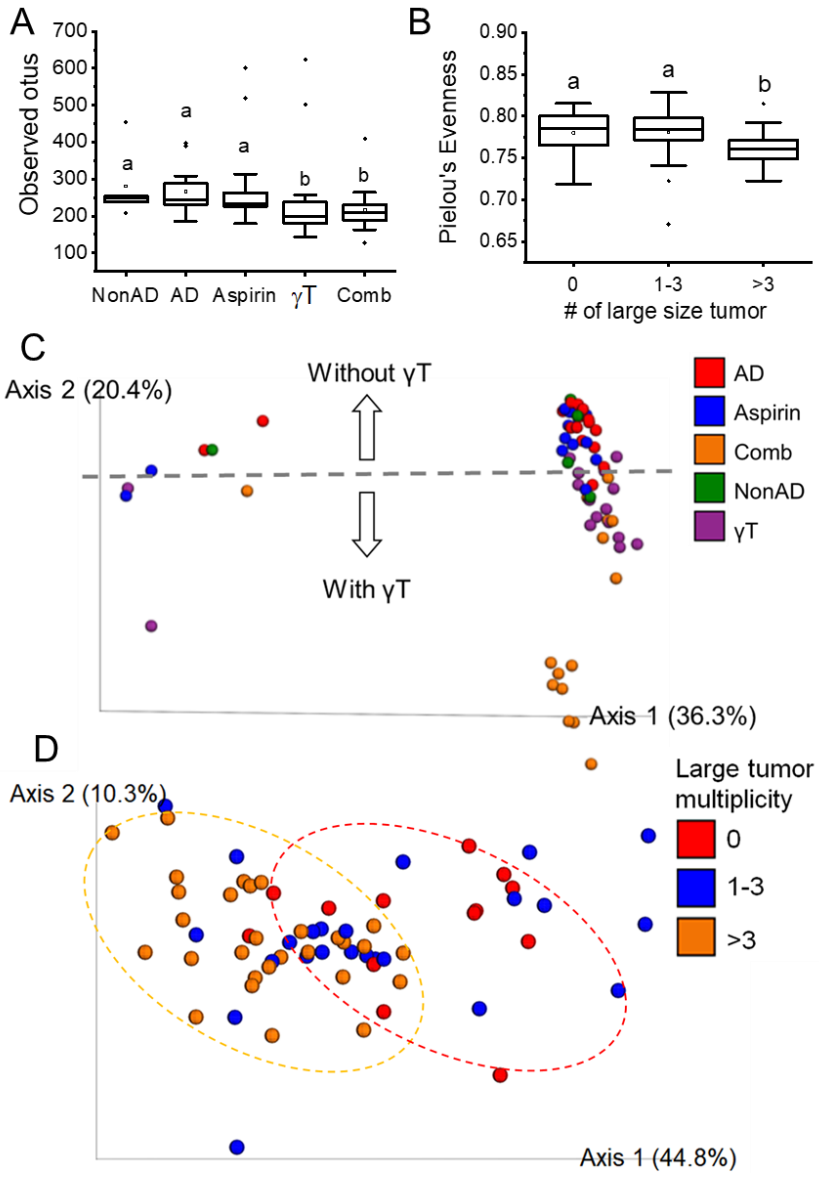

Figure 4.4 The effects of AOMDSS, aspirin, γT, and their combination (Comb) on microbial diversity in mice.

A-B: The effect of different treatments (A) and large tumor multiplicity (B) on alpha-diversity index of richness (A) and evenness (B), respectively. Significant differences at P=0.001 were determined using Kruskal-Wallis with 999 Monte Carlo permutations and Bonferroni correction. Data rarefied to a maximum depth of 21495 reads per samples. C: PCoA of beta-diversity comparison using unweighted Unifrac distances to reveal the significant separation of microbial communities based on different treatment groups. D: PCoA of beta-diversity comparison using weighted Unifrac distances to reveal a significant separation of microbial communities based on large tumor multiplicity. Overall differences were determined using Permanova followed by pairwise permanova test to determine differences among each treatment group ($P<0.05$). Permdisp indicated that dispersion dose does not contribute to significance.

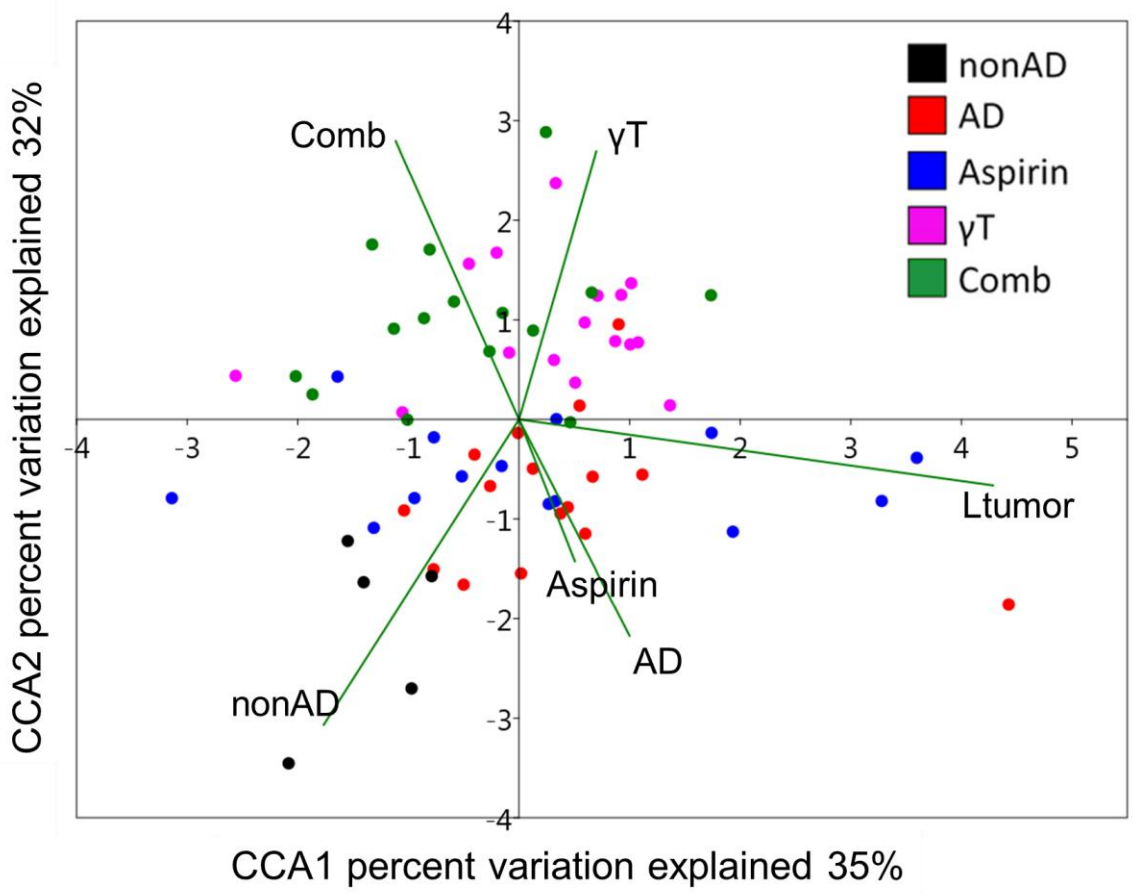

Figure 4.5 Canonical correspondence analysis (CCA) of fecal bacterial composition and experimental variables.

CCA model was performed with the relative abundance of fecal microbiome at species level as species matrix and the experimental variables of AOMDSS treatment, supplementation of aspirin, γT, and their combination, as well as large tumor multiplicity as the environmental matrix. Variable biplot arrows indicate the direction of environmental gradients. Angles between arrows corresponds to the relationship of the experimental variables to one another based on the relative abundance of fecal microbiome. The relative length of arrows corresponds to the importance of the respective variables in the model. The overall significance of the model is P= 0.001. CCA1 and CCA2 explained the majority of the total constrained variation of 34.9% and 31.7%, respectively.

Table 4.1 Relative proportion (%) of bacterial species that significantly differed between treatment groups.

n = 5-16 for each treatment. Overall significance was tested using analysis of composition (ANCOM) with W-value range between 211-508. Differences among treatment groups were confirmed and tested using pairwise comparison of Kruskal-Wallis with Bonferroni correction. Unclassified taxa are species that are yet to be classified with a species name. Uncultured taxa are those has yet to be cultured.

Family	Genus	Species	nonAD	AD	Aspirin	γT	Comb
Bifidobacteriaceae			0.2 ± 0.04 a	0.0 ± 0.0 b	0.7 ± 0.3 a	0.05 ± 0.03 b	0.7 ± 0.4 a
Ruminococcaceae	Ruminococcaceae UCG-014		0.2 ± 0.2 ab	0.6 ± 0.1 a	0.3 ± 0.1 a	0.2 ± 0.1 ab	0.0 ± 0.0 b
Clostridiales vadinBB60 group	uncultured Clostridia bacterium	uncultured Clostridia bacterium	0.2 ± 0.2 a	0.4 ± 0.1 a	0.6 ± 0.2 a	0.0 ± 0.0 b	0.0 ± 0.0 b
Eggerthellaceae	Enterorhabdus	uncultured bacterium	0.04 ± 0.01 ab	0.03 ± 0.0 a	0.02 ± 0.0 a	0.07 ± 0.01 b	0.09 ± 0.01 b
Lachnospiraceae	Roseburia	unclassified	0.05 ± 0.03 a	0.05 ± 0.03 a	0.01 ± 0.01 a	0.2 ± 0.1 b	0.5 ± 0.2 b
Rikenellaceae	Alistipes	Alistipes obesi	0.04 ± 0.01 a	0.0 ± 0.0 b	0.0 ± 0.0 b	0.0 ± 0.0 b	0.0 ± 0.0 b
Saccharimonadaceae	Candidatus Saccharimonas	uncultured bacterium	0.02 ± 0.01 a	0.1 ± 0.02 b	0.03 ± 0.01 a	0.01 ± 0.01 a	0.01 ± 0.01 a

CHAPTER 5. SUMMARY AND FUTURE DIRECTIONS

5.1 The pharmacokinetics, bioavailability, and excretion of vitamin E and metabolites

Our first study characterizes the time-course formation of short- and long-chain vitamin E metabolites following a single dose supplementation of tocopherols or tocotrienols. Sulfated carboxychromanols appeared to be the major metabolites detected in the plasma of rats, whereas unconjugated 13'-COOHs are the predominant metabolites in the feces of rats. In the plasma, 13'-COOHs and 13'-OH take less time to reach maximum concentration as compared to shorter chain or conjugated counterparts, which is likely due to 13'-COOHs and 13'-OH are the initially-formed metabolites as a result of ω-oxidation [1,24]. Tocotrienols also appear to have more rapid turnover rate than tocopherols as indicated by the shorter time to reach maximum concentration. Based on the ratio of the overall exposure of the vitamers in the body to the intake of each vitamer, the relative bioavailability of vitamin E forms in the plasma follows the order of $\gamma T > \delta T > \gamma TE > \delta TE$, whereas the relative bioavailability of metabolites in plasma follows the order of $\gamma TE > \gamma T > \delta TE \approx \delta T$. These results suggest that the bioavailability of metabolites does not depend on the bioavailability of vitamin E forms. Furthermore, our study reveals new and interesting aspects of fecal and urinary excretion of tocopherols, tocotrienols, and metabolites. The excretion of unmetabolized tocopherols is higher than tocotrienol in the feces, while the level of metabolites from δTE is higher than γT in the feces. Nevertheless, the overall recovery rate of γT is much higher than δTE. Previous studies reported that a considerable amount of tocotrienols was found in adipose tissue or skin of rodents after

administration [23,232,313]. In the future, adipose tissues and skin should be analyzed to determine the levels of vitamin E forms and their metabolites remain in these tissues.

We also found a distinction in metabolite formation between human and rats. As observed in rats, various conjugated and unconjugated metabolites were detected in the plasma. However, the major metabolite in human plasma is unconjugated γ-CEHC, rather than sulfated CEHC in rats. Due to the limitation of the human study, the time-course formation of vitamin E metabolites is not determined. Future study should be carried out to characterize the pharmacokinetics formation of vitamin E metabolites as well as the excretion in human.

5.2 The effect of vitamin E forms on barrier function and colitis

In the second study, we demonstrated that both αT and γT could preserve intestinal barrier function disturbed by cytokine treatment in Caco-2 cells as well as attenuate DSS-induced colitis in Balb/c mice. In Caco-2 cell study, pre-treatment of αT and γT attenuated cytokine-induced barrier dysfunction. Intestinal barrier dysfunction is one of the major characteristics of IBD [147]. This led to the hypothesis that αT and γT can protect against DSS-induced colitis in mice. In this study, we have shown that αT and γT supplementation given at the same time as DSS or pre-supplemented for 3 weeks before DSS treatment alleviated DSS-induced colitis symptoms as well as reduced colon inflammation. We also found that both αT and γT supplementation preserved tight junction protein in the colon and attenuated intestinal barrier dysfunction induced by DSS treatment. Additionally, we have shown that Intestinal microbiota as a critical factor for the pathogenesis of IBD can be modulated by DSS treatment and γTmT supplementation. Previous studies reported that

patients with IBD have different microbial composition compared to healthy individuals [283,284]. We have also shown that DSS-treated mice have a very different microbial composition as compared those of non-DSS control mice. However, γT, but not αT, further modulate the microbial composition that is different from those of DSS control mice. Additionally, we found that DSS reduced the relative abundance of butyrate-producing bacteria, including uncultured Lachnospiraceae and Roseburia in the feces of mice. These bacteria are known butyrate producers [293], that contain anti-inflammatory properties against IBD. Both αT and γTmT supplementation attenuated DSS-induced depletion of uncultured Roseburia and Lachnospiraceae in mice, especially γTmT showing stronger potency for preserving these bacteria, suggesting vitamin E supplementations can modulate DSS-induced dysbiosis in mice. Interestingly, we found that the level of metabolites from γT is higher than αT, which coincides with the influence of intestinal microbial composition, suggesting that metabolites from γT may interact and modulate intestinal microbiota.

Overall, our study indicates that vitamin E supplementation can be a safe and effective treatment for IBD. However, our current study did not provide enough evidence to show whether vitamin E forms or their metabolites can be utilized by intestinal microbiota or direct evidence to prove that the anti-colitis effects of vitamin E forms are dependent on the modulation of intestinal microbiota. Therefore, future study research using antibiotic or germ-free model will provide more information on whether the protective effect of vitamin E forms on DSS-induced colitis is due to the modulation of gut microbiota. Also, anaerobic cultivation of vitamin E forms and metabolites with human or animal feces may reveal relative microbes that can utilize vitamin E forms and metabolites.

5.3 Anticancer efficacy of aspirin and γT combination on colon cancer

Our third project reveals that the combination of γT and aspirin is a more effective anticancer agent against CRC than aspirin or γT alone in a cellular and pre-clinical model. In HCT-116 colon cancer cells, γT treatment sensitized HCT-116 cells to respond to aspirin treatment, which enhanced the anticancer activity of aspirin. In a colitis-driven tumorigenesis mouse model, the combination of γT and aspirin reduced the multiplicity of the total and large-size tumor as well as tumor size compared to control AOM/DSS-treated mice. We also found that aspirin supplementation exacerbated DSS-induced colitis in mice, which was attenuated by the combination with γT. Consistent with the observations in human [216,294], long-term aspirin supplementation caused gastric lesion in mice, which also was alleviated by the combination with γT. Additionally, data from microbial analyses demonstrated that γT could influence microbial composition by reducing the relative abundance of potential inflammation-associated bacteria and increasing the relative abundance of butyrate-producing bacteria, which may contribute to the anticancer activity of the combination of aspirin and γT. To further investigate the mechanisms underlying improved anticancer efficacy of aspirin by combining with γT, the level of eicosanoids in the colon should be measured. As we know, prostaglandins and leukotrienes synthesized by COX-1/COX-2 and 5-LOX, respectively, are important in the initiation, progression, and invasion of colon carcinogenesis [79]. Dual inhibition of COXs and 5-LOX by γT may enhance the anticancer activity of aspirin. Additionally, further analyses on colon inflammation markers such as pro-inflammatory cytokines, specifically IL-6 and transcription factors STAT3 are needed as IL-6/STAT3 signaling cascade is a critical regulator for the proliferation and survival of colon carcinogenesis [312]. A previous study

showed that aspirin could down-regulate the IL-6/STAT3 pathway and activated apoptosis in colon tumor tissues, but it was not sufficient in reducing the tumor load [297]. It is possible that γT enhanced aspirin's apoptotic activity by modulating sphingolipid metabolism.

REFERENCES

1. Jiang Q. Natural forms of vitamin E: metabolism, antioxidant, and anti-inflammatory activities and their role in disease prevention and therapy. Free Radic Biol Med 2014;72:76-90.

2. Evans HM, Bishop KS. On the Existence of a Hitherto Unrecognized Dietary Factor Essential for Reproduction. Science 1922;56(1458):650-1.

3. Mene-Saffrane L, DellaPenna D. Biosynthesis, regulation and functions of tocochromanols in plants. Plant Physiol Biochem 2010;48(5):301-9.

4. Traber MG, Burton GW, Ingold KU, Kayden HJ. Rrr-Alpha-Tocopherol and Srr-Alpha-Tocopherol Are Secreted without Discrimination in Human Chylomicrons, but Rrr-Alpha-Tocopherol Is Preferentially Secreted in Very Low-Density Lipoproteins. J Lipid Res 1990;31(4):675-85.

5. Chun J, Lee J, Ye L, Exler J, Eitenmiller RR. Tocopherol and tocotrienol contents of raw and processed fruits and vegetables in the United States diet. Journal of Food Composition and Analysis 2006;19(2-3):196-204.

6. Sundl I, Murkovic M, Bandoniene D, Winklhofer-Roob BM. Vitamin E content of foods: comparison of results obtained from food composition tables and HPLC analysis. Clin Nutr 2007;26(1):145-53.

7. Thomas RG, Gebhardt SE. Nuts and seeds as sources of alpha- and gamma-tocopherols. J Nutr 2007;137(1):281S.

8. Irias-Mata A, Stuetz W, Sus N, Hammann S, Gralla K, Cordero-Solano A, et al. Tocopherols, Tocomonoenols, and Tocotrienols in Oils of Costa Rican Palm Fruits: A Comparison between Six Varieties and Chemical versus Mechanical Extraction. J Agric Food Chem 2017;65(34):7476-82.

9. Walde CM, Drotleff AM, Ternes W. Comparison of dietary tocotrienols from barley and palm oils in hen's egg yolk: transfer efficiency, influence of emulsification, and effect on egg cholesterol. J Sci Food Agric 2014;94(4):810-8.

10. Zabot GL, Moraes MN, Meireles MAA. Process integration for producing tocotrienols-rich oil and bixin-rich extract from annatto seeds: A techno-economic approach. Food Bioprod Process 2018;109:122-38.

11. Jiang Q, Christen S, Shigenaga MK, Ames BN. gamma-tocopherol, the major form of vitamin E in the US diet, deserves more attention. Am J Clin Nutr 2001;74(6):714-22.

12. Tan B. Palm carotenoids, tocopherols and tocotrienols. Journal of The Amerian Oil Chemists Society 1989;66(6):770-6.

13. Traber MG. Vitamin E Inadequacy in Humans: Causes and Consequences. Advances in Nutrition 2014;5(5):503-14.

14. Drevon CA. Absorption, transport and metabolism of vitamin E. Free Radic Res Commun 1991;14(4):229-46.

15. Reboul E, Klein A, Bietrix F, Gleize B, Malezet-Desmoulins C, Schneider M, et al. Scavenger receptor class B type I (SR-BI) is involved in vitamin E transport across the enterocyte. J Biol Chem 2006;281(8):4739-45.

16. Goncalves A, Roi S, Nowicki M, Niot I, Reboul E. Cluster-determinant 36 (CD36) impacts on vitamin E postprandial response. Mol Nutr Food Res 2014;58(12):2297-306.

17. Reboul E, Soayfane Z, Goncalves A, Cantiello M, Bott R, Nauze M, et al. Respective contributions of intestinal Niemann-Pick C1-like 1 and scavenger receptor class B type I to cholesterol and tocopherol uptake: in vivo v. in vitro studies. Br J Nutr 2012;107(9):1296-304.

18. Reboul E, Trompier D, Moussa M, Klein A, Landrier JF, Chimini G, et al. ATP-binding cassette transporter A1 is significantly involved in the intestinal absorption of alpha- and gamma-tocopherol but not in that of retinyl palmitate in mice. Am J Clin Nutr 2009;89(1):177-84.

19. Goncalves A, Roi S, Nowicki M, Dhaussy A, Huertas A, Amiot MJ, et al. Fat-soluble vitamin intestinal absorption: absorption sites in the intestine and interactions for absorption. Food Chem 2015;172:155-60.

20. Reboul E. Vitamin E intestinal absorption: Regulation of membrane transport across the enterocyte. IUBMB Life 2018.

21. Traber MG. Vitamin E regulatory mechanisms. Annu Rev Nutr 2007;27:347-62.

22. Burton GW, Traber MG, Acuff RV, Walters DN, Kayden H, Hughes L, et al. Human plasma and tissue alpha-tocopherol concentrations in response to supplementation with deuterated natural and synthetic vitamin E. Am J Clin Nutr 1998;67(4):669-84.

23. Ikeda S, Niwa T, Yamashita K. Selective uptake of dietary tocotrienols into rat skin. J Nutr Sci Vitaminol (Tokyo) 2000;46:141-3.

24. Sontag TJ, Parker RS. Cytochrome P450 omega-hydroxylase pathway of tocopherol catabolism. Novel mechanism of regulation of vitamin E status. J Biol Chem 2002;277(28):25290-6.

25. Jiang Q, Freiser H, Wood KV, Yin X. Identification and quantitation of novel vitamin E metabolites, sulfated long-chain carboxychromanols, in human A549 cells and in rats. J Lipid Res 2007;48(5):1221-30.

26. Freiser H, Jiang Q. Gamma-tocotrienol and gamma-tocopherol are primarily metabolized to conjugated 2-(beta-carboxyethyl)-6-hydroxy-2,7,8-trimethylchroman and sulfated long-chain carboxychromanols in rats. J Nutr 2009;139(5):884-9.

27. Chiku S, Hamamura K, Nakamura T. Novel urinary metabolite of d-delta-tocopherol in rats. J Lipid Res 1984;25(1):40-8.

28. Swanson J, Ben R, Burton G, Parker R. Urinary excretion of 2,7, 8-trimethyl-2-(beta-carboxyethyl)-6-hydroxychroman is a major route of elimination of gamma-tocopherol in humans. J Lipid Res 1999;40(4):665-71.

29. Stahl W, Graf P, Brigelius-Flohé R, Wechter W, Sies H. Quantification of the alpha- and gamma-tocopherol metabolites 2,5,7, 8-tetramethyl-2-(2'-carboxyethyl)-6-hydroxychroman and 2,7, 8-trimethyl-2-(2'-carboxyethyl)-6-hydroxychroman in human serum. Anal Biochem 1999;275(2):254-9.

30. Bardowell SA, Ding X, Parker RS. Disruption of P450-mediated vitamin E hydroxylase activities alters vitamin E status in tocopherol supplemented mice and reveals extra-hepatic vitamin E metabolism. J Lipid Res 2012;53(12):2667-76.

31. Bardowell SA, Duan F, Manor D, Swanson JE, Parker RS. Disruption of mouse cytochrome p450 4f14 (Cyp4f14 gene) causes severe perturbations in vitamin E metabolism. J Biol Chem 2012;287(31):26077-86.

32. Jiang Q, Jiang Z, Hall YJ, Jang Y, Snyder PW, Bain C, et al. Gamma-tocopherol attenuates moderate but not severe colitis and suppresses moderate colitis-promoted colon tumorigenesis in mice. Free Radic Biol Med 2013;65:1069-77.

33. Jiang Q, Xu T, Huang J, Jannasch AS, Cooper B, Yang C. Analysis of vitamin E metabolites including carboxychromanols and sulfated derivatives using LC/MS/MS. J Lipid Res 2015;56(11):2217-25.

34. Hosomi A, Arita M, Sato Y, Kiyose C, Ueda T, Igarashi O, et al. Affinity for α-tocopherol transfer protein as a determinant of the biological activities of vitamin E analogs. FEBS Lett 1997;409(1):105-8.

35. Manor D, Morley S. The α-Tocopherol Transfer Protein. 2007;76:45-65.

36. Qian J, Morley S, Wilson K, Nava P, Atkinson J, Manor D. Intracellular trafficking of vitamin E in hepatocytes: the role of tocopherol transfer protein. J Lipid Res 2005;46(10):2072-82.

37. Schuelke M, Elsner A, Finckh B, Kohlschutter A, Hubner C, Brigelius-Flohe R. Urinary alpha-tocopherol metabolites in alpha-tocopherol transfer protein-deficient patients. J Lipid Res 2000;41(10):1543-51.

38. Traber MG, Elsner A, Brigelius-Flohé R. Synthetic as compared with natural vitamin E is preferentially excreted as α-CEHC in human urine: studies using deuterated α-tocopheryl acetates. FEBS Lett 1998;437(1-2):145-8.

39. Stahl W, Graf P, Brigelius-Flohe R, Wechter W, Sies H. Quantification of the alpha- and gamma-tocopherol metabolites 2,5,7, 8-tetramethyl-2-(2'-carboxyethyl)-6-hydroxychroman and 2,7, 8-trimethyl-2-(2'-carboxyethyl)-6-hydroxychroman in human serum. Anal Biochem 1999;275(2):254-9.

40. Birringer M, Pfluger P, Kluth D, Landes N, Brigelius-Flohe R. Identities and differences in the metabolism of tocotrienols and tocopherols in HepG2 cells. J Nutr 2002;132(10):3113-8.

41. Hasemann CA, Kurumbail RG, Boddupalli SS, Peterson JA, Deisenhofer J. Structure and function of cytochromes P450:a comparative analysis of three crystal structures. Structure 1995;3(1):41-62.

42. Halkier BA. Catalytic reactivities and structure/function relationships of cytochrome P450 enzymes. Phytochemistry 1996;43(1):1-21.

43. Freiser H, Jiang Q. Optimization of the enzymatic hydrolysis and analysis of plasma conjugated gamma-CEHC and sulfated long-chain carboxychromanols, metabolites of vitamin E. Anal Biochem 2009;388(2):260-5.

44. Mustacich DJ, Leonard SW, Patel NK, Traber MG. Alpha-tocopherol beta-oxidation localized to rat liver mitochondria. Free Radic Biol Med 2010;48(1):73-81.

45. Zhao Y, Lee MJ, Cheung C, Ju JH, Chen YK, Liu B, et al. Analysis of multiple metabolites of tocopherols and tocotrienols in mice and humans. J Agric Food Chem 2010;58(8):4844-52.

46. Lodge J, Ridlington J, Leonard S, Vaule H, Traber M. Alpha- and gamma-tocotrienols are metabolized to carboxyethyl-hydroxychroman derivatives and excreted in human urine. Lipids 2001;36(1):43-8.

47. Saito H, Kiyose C, Yoshimura H, Ueda T, Kondo K, Igarashi O. Gamma-tocotrienol, a vitamin E homolog, is a natriuretic hormone precursor. J Lipid Res 2003;44(8):1530-5.

48. Yamashita K, Takeda N, Ikeda S. Effects of various tocopherol-containing diets on tocopherol secretion into bile. Lipids 2000;35(2):163-70.

49. Traber MG. Mechanisms for the prevention of vitamin E excess. J Lipid Res 2013;54(9):2295-306.

50. Jiang Q. Natural forms of vitamin E and metabolites-regulation of cancer cell death and underlying mechanisms. IUBMB Life 2018.

51. Jiang Q. Natural Forms of Vitamin E as Effective Agents for Cancer Prevention and Therapy. Adv Nutr 2017;8(6):850-67.

52. Jiang Q, Yin X, Lill MA, Danielson ML, Freiser H, Huang J. Long-chain carboxychromanols, metabolites of vitamin E, are potent inhibitors of cyclooxygenases. Proc Natl Acad Sci U S A 2008;105(51):20464-9.

53. Wallert M, Schmolz L, Koeberle A, Krauth V, Glei M, Galli F, et al. alpha-Tocopherol long-chain metabolite alpha-13'-COOH affects the inflammatory response of lipopolysaccharide-activated murine RAW264.7 macrophages. Mol Nutr Food Res 2015;59(8):1524-34.

54. Jiang Z, Yin X, Jiang Q. Natural forms of vitamin E and 13'-carboxychromanol, a long-chain vitamin E metabolite, inhibit leukotriene generation from stimulated neutrophils by blocking calcium influx and suppressing 5-lipoxygenase activity, respectively. J Immunol 2011;186(2):1173-9.

55. Jang Y, Park NY, Rostgaard-Hansen AL, Huang J, Jiang Q. Vitamin E metabolite 13'-carboxychromanols inhibit pro-inflammatory enzymes, induce apoptosis and autophagy in human cancer cells by modulating sphingolipids and suppress colon tumor development in mice. Free Radic Biol Med 2016;95:190-9.

56. Christen S, Woodall AA, Shigenaga MK, Southwell-Keely PT, Duncan MW, Ames BN. γ-Tocopherol traps mutagenic electrophiles such as NOx and complements α-tocopherol: Physiological implications. Proceedings of the National Academy of Sciences 1997;94(7):3217-22.

57. Cooney RV, Franke AA, Harwood PJ, Hatch-Pigott V, Custer LJ, Mordan LJ. Gamma-tocopherol detoxification of nitrogen dioxide: superiority to alpha-tocopherol. Proceedings of the National Academy of Sciences 1993;90(5):1771-5.

58. Cooney R. Products of γ-tocopherol reaction with NO2 and their formation in rat insulinoma (RINm5F) cells. Free Radical Biol Med 1995;19(3):259-69.

59. Christen S, Jiang Q, Shigenaga MK, Ames BN. Analysis of plasma tocopherols α, γ, and 5-nitro-γ in rats with inflammation by HPLC coulometric detection. J Lipid Res 2002;43(11):1978-85.

60. Packer L, Weber SU, Rimbach G. Molecular aspects of alpha-tocotrienol antioxidant action and cell signalling. J Nutr 2001;131(2):369S-73S.

61. Wong RS, Radhakrishnan AK. Tocotrienol research: past into present. Nutr Rev 2012;70(9):483-90.

62. Terashima K, Takaya Y, Niwa M. Powerful antioxidative agents based on garcinoic acid from Garcinia kola. Bioorganic & Medicinal Chemistry 2002;10(5):1619-25.

63. Murdoch JR, Lloyd CM. Chronic inflammation and asthma. Mutat Res 2010;690(1-2):24-39.

64. Hanauer SB. Inflammatory bowel disease: Epidemiology, pathogenesis, and therapeutic opportunities. Inflammatory Bowel Diseases 2006;12:S3-S9.

65. Sartor RB. Mechanisms of disease: pathogenesis of Crohn's disease and ulcerative colitis. Nat Clin Pract Gastroenterol Hepatol 2006;3(7):390-407.

66. Szkaradkiewicz A, Marciniak R, Chudzicka-Strugala I, Wasilewska A, Drews M, Majewski P, et al. Proinflammatory cytokines and IL-10 in inflammatory bowel disease and colorectal cancer patients. Arch Immunol Ther Exp (Warsz) 2009;57(4):291-4.

67. Khor B, Gardet A, Xavier RJ. Genetics and pathogenesis of inflammatory bowel disease. Nature 2011;474(7351):307-17.

68. Corridoni D, Arseneau KO, Cominelli F. Inflammatory bowel disease. Immunol Lett 2014;161(2):231-5.

69. Grivennikov SI, Greten FR, Karin M. Immunity, inflammation, and cancer. Cell 2010;140(6):883-99.

70. Li Q, Withoff S, Verma IM. Inflammation-associated cancer: NF-kappaB is the lynchpin. Trends Immunol 2005;26(6):318-25.

71. Geremia A, Biancheri P, Allan P, Corazza GR, Di Sabatino A. Innate and adaptive immunity in inflammatory bowel disease. Autoimmun Rev 2014;13(1):3-10.

72. Belardelli F. Role of interferons and other cytokines in the regulation of the immune response. Apmis 1995;103(1-6):161-79.

73. Williams JA, Shacter E. Regulation of macrophage cytokine production by prostaglandin E2. Distinct roles of cyclooxygenase-1 and -2. J Biol Chem 1997;272(41):25693-9.

74. Yokomizo T, Izumi T, Shimizu T. Leukotriene B4: metabolism and signal transduction. Arch Biochem Biophys 2001;385(2):231-41.

75. Ricciotti E, FitzGerald GA. Prostaglandins and inflammation. Arterioscler Thromb Vasc Biol 2011;31(5):986-1000.

76. Funk CD. Prostaglandins and leukotrienes: advances in eicosanoid biology. Science 2001;294(5548):1871-5.

77. Stenson WF. Role of Eicosanoids as Mediators of Inflammation in Inflammatory Bowel Disease. Scandinavian Journal of Gastroenterology 2009;25(sup172):13-8.

78. Moreno JJ. Eicosanoid receptors: Targets for the treatment of disrupted intestinal epithelial homeostasis. Eur J Pharmacol 2017;796:7-19.

79. Wang D, Dubois RN. Eicosanoids and cancer. Nat Rev Cancer 2010;10(3):181-93.

80. Gupta RA, Dubois RN. Colorectal cancer prevention and treatment by inhibition of cyclooxygenase-2. Nat Rev Cancer 2001;1(1):11-21.

81. Fanning LB, Boyce JA. Lipid mediators and allergic diseases. Ann Allergy Asthma Immunol 2013;111(3):155-62.

82. Gilberto Poggioli SL, Massimo Campieri, Filippo Pierangeli, Paolo Gionchetti, Federica Ugolini, Lorenzo Gentilini, Piero Bazzi, Fernando Rizzello, and Maurizio Coscia. Infliximab in the treatment of Crohn's disease. Ther Clin Risk Manag 2007;3(2):301-8.

83. Jiang Q, Elson-Schwab I, Courtemanche C, Ames BN. gamma-tocopherol and its major metabolite, in contrast to alpha-tocopherol, inhibit cyclooxygenase activity in macrophages and epithelial cells. Proc Natl Acad Sci U S A 2000;97(21):11494-9.

84. Wang Y, Jiang Q. gamma-Tocotrienol inhibits lipopolysaccharide-induced interlukin-6 and granulocyte colony-stimulating factor by suppressing C/EBPbeta and NF-kappaB in macrophages. J Nutr Biochem 2013;24(6):1146-52.

85. Yang C, Jiang Q. Vitamin E delta-tocotrienol inhibits TNF-alpha-stimulated NF-kappaB activation by up-regulation of anti-inflammatory A20 via modulation of sphingolipid including elevation of intracellular dihydroceramides. J Nutr Biochem 2019;64:101-9.

86. Yam ML, Abdul Hafid SR, Cheng HM, Nesaretnam K. Tocotrienols suppress proinflammatory markers and cyclooxygenase-2 expression in RAW264.7 macrophages. Lipids 2009;44(9):787-97.

87. Qureshi AA, Reis JC, Papasian CJ, Morrison DC, Qureshi N. Tocotrienols inhibit lipopolysaccharide-induced pro-inflammatory cytokines in macrophages of female mice. Lipids Health Dis 2010;9:143.

88. Wang Y, Moreland M, Wagner JG, Ames BN, Illek B, Peden DB, et al. Vitamin E forms inhibit IL-13/STAT6-induced eotaxin-3 secretion by up-regulation of PAR4, an endogenous inhibitor of atypical PKC in human lung epithelial cells. J Nutr Biochem 2012;23(6):602-8.

89. Ahn KS, Sethi G, Krishnan K, Aggarwal BB. Gamma-tocotrienol inhibits nuclear factor-kappaB signaling pathway through inhibition of receptor-interacting protein and TAK1 leading to suppression of antiapoptotic gene products and potentiation of apoptosis. J Biol Chem 2007;282(1):809-20.

90. Wang Y, Park NY, Jang Y, Ma A, Jiang Q. Vitamin E gamma-Tocotrienol Inhibits Cytokine-Stimulated NF-kappaB Activation by Induction of Anti-Inflammatory A20 via Stress Adaptive Response Due to Modulation of Sphingolipids. J Immunol 2015;195(1):126-33.

91. Rajendran P, Li F, Manu KA, Shanmugam MK, Loo SY, Kumar AP, et al. gamma-Tocotrienol is a novel inhibitor of constitutive and inducible STAT3 signalling pathway in human hepatocellular carcinoma: potential role as an antiproliferative, pro-apoptotic and chemosensitizing agent. Br J Pharmacol 2011;163(2):283-98.

92. Ju J, Picinich SC, Yang Z, Zhao Y, Suh N, Kong AN, et al. Cancer-preventive activities of tocopherols and tocotrienols. Carcinogenesis 2010;31(4):533-42.

93. Moya-Camarena SY, Jiang Q. The Role of Vitamin E Forms in Cancer Prevention and Therapy – Studies in Human Intervention Trials and Animal Models. In: Sarkar FH, editor. Nutraceuticals and Cancer. Mexico: Springer Science Business Media; 2011. p. pp 323-54.

94. Guan F, Li G, Liu AB, Lee MJ, Yang Z, Chen YK, et al. delta- and gamma-tocopherols, but not alpha-tocopherol, inhibit colon carcinogenesis in azoxymethane-treated F344 rats. Cancer Prev Res (Phila) 2012;5(4):644-54.

95. Coussens LM, Werb Z. Inflammation and cancer. Nature 2002;420(6917):860-7.

96. Jiang Q, Rao X, Kim CY, Freiser H, Zhang Q, Jiang Z, et al. Gamma-tocotrienol induces apoptosis and autophagy in prostate cancer cells by increasing intracellular dihydrosphingosine and dihydroceramide. Int J Cancer 2012;130(3):685-93.

97. Jang Y, Rao X, Jiang Q. Gamma-tocotrienol profoundly alters sphingolipids in cancer cells by inhibition of dihydroceramide desaturase and possibly activation of sphingolipid hydrolysis during prolonged treatment. J Nutr Biochem 2017;46:49-56.

98. Hannun YA, Obeid LM. Many ceramides. J Biol Chem 2011;286(32):27855-62.

99. Hannun YA, Obeid LM. Principles of bioactive lipid signalling: lessons from sphingolipids. Nat Rev Mol Cell Biol 2008;9(2):139-50.

100. Jiang Q, Wong J, Fyrst H, Saba JD, Ames BN. gamma-Tocopherol or combinations of vitamin E forms induce cell death in human prostate cancer cells by interrupting sphingolipid synthesis. Proc Natl Acad Sci U S A 2004;101(51):17825-30.

101. Shah SJ, Sylvester PW. γ-Tocotrienol Inhibits Neoplastic Mammary Epithelial Cell Proliferation by Decreasing Akt and Nuclear Factor κB Activity. Exp Biol Med 2016;230(4):235-41.

102. Hiura Y, Tachibana H, Arakawa R, Aoyama N, Okabe M, Sakai M, et al. Specific accumulation of gamma- and delta-tocotrienols in tumor and their antitumor effect in vivo. J Nutr Biochem 2009;20(8):607-13.

103. Husain K, Francois RA, Hutchinson SZ, Neuger AM, Lush R, Coppola D, et al. Vitamin E delta-tocotrienol levels in tumor and pancreatic tissue of mice after oral administration. Pharmacology 2009;83(3):157-63.

104. Nguyen GC, Chong CA, Chong RY. National estimates of the burden of inflammatory bowel disease among racial and ethnic groups in the United States. J Crohns Colitis 2014;8(4):288-95.

105. Dahlhamer J, Zammitti E, Ward B, Wheaton A, Croft J. Prevalence of Inflammatory Bowel Disease Among Adults Aged ≥18 Years - United States, 2015. MMWR 2016;65(42):1166-9.

106. Molodecky NA, Soon IS, Rabi DM, Ghali WA, Ferris M, Chernoff G, et al. Increasing incidence and prevalence of the inflammatory bowel diseases with time, based on systematic review. Gastroenterology 2012;142(1):46-54 e42; quiz e30.

107. Basson A, Trotter A, Rodriguez-Palacios A, Cominelli F. Mucosal Interactions between Genetics, Diet, and Microbiome in Inflammatory Bowel Disease. Front Immunol 2016;7:290.

108. Kaplan GG. Global variations in environmental risk factors for IBD. Nature Reviews: Gastroenterology and Hepatology 2014;11:708-9.

109. Manichanh O, Borruel N, Casellas F, Guarner F. The gut microbiota in IBD. Nature Reviews: Gastroenterology and Hepatology 2012;9:599-608.

110. Kanauchi O, Mitsuyama K, Andoh A. The new prophylactic strategy for colon cancer in inflammatory bowel disease by modulating microbiota. Scand J Gastroenterol 2013;48(4):387-400.

111. Malik TA. Inflammatory Bowel Disease: Historical Perspective, Epidemiology, and Risk Factors. Surg Clin North Am 2015;95(6):1105-22, v.

112. Calkins B. A meta-analysis of the role of smoking in inflammatory bowel disease. Digestive Diseases and Science 1989;34(12):1841-54.

113. Benjamin JL, Hedin CR, Koutsoumpas A, Ng SC, McCarthy NE, Prescott NJ, et al. Smokers with active Crohn's disease have a clinically relevant dysbiosis of the gastrointestinal microbiota. Inflamm Bowel Dis 2012;18(6):1092-100.

114. Coward S, Heitman SJ, Clement F, Negron M, Panaccione R, Ghosh S, et al. Funding a smoking cessation program for Crohn's disease: an economic evaluation. Am J Gastroenterol 2015;110(3):368-77.

115. Ananthakrishnan AN, Khalili H, Konijeti GG, Higuchi LM, de Silva P, Korzenik JR, et al. A prospective study of long-term intake of dietary fiber and risk of Crohn's disease and ulcerative colitis. Gastroenterology 2013;145(5):970-7.

116. Wong C, Harris PJ, Ferguson LR. Potential Benefits of Dietary Fibre Intervention in Inflammatory Bowel Disease. Int J Mol Sci 2016;17(6).

117. Devkota S, Wang Y, Musch MW, Leone V, Fehlner-Peach H, Nadimpalli A, et al. Dietary-fat-induced taurocholic acid promotes pathobiont expansion and colitis in Il10-/- mice. Nature 2012;487(7405):104-8.

118. Hlavaty T, Toth J, Koller T, Krajcovicova A, Oravcova S, Zelinkova Z, et al. Smoking, breastfeeding, physical inactivity, contact with animals, and size of the family influence the risk of inflammatory bowel disease: A Slovak case-control study. United European Gastroenterol J 2013;1(2):109-19.

119. Xu L, Lochhead P, Ko Y, Claggett B, Leong RW, Ananthakrishnan AN. Systematic review with meta-analysis: breastfeeding and the risk of Crohn's disease and ulcerative colitis. Aliment Pharmacol Ther 2017.

120. Soon I, Molodecky NA, Rabi DM, Ghali WA, Barkema HW, Kaplan GG. The relationship between urban environment and the inflammatory bowel diseases: a systematic review and meta-analysis. BMC Gastroenterology 2012;12:51.

121. Ungaro R, Bernstein CN, Gearry R, Hviid A, Kolho KL, Kronman MP, et al. Antibiotics associated with increased risk of new-onset Crohn's disease but not ulcerative colitis: a meta-analysis. Am J Gastroenterol 2014;109(11):1728-38.

122. Matsuoka K, Kanai T. The gut microbiota and inflammatory bowel disease. Semin Immunopathol 2015;37(1):47-55.

123. Dalal SR, Chang EB. The microbial basis of inflammatory bowel diseases. J Clin Invest 2014;124(10):4190-6.

124. Berry D, Reinisch W. Intestinal microbiota: a source of novel biomarkers in inflammatory bowel diseases? Best Pract Res Clin Gastroenterol 2013;27(1):47-58.

125. Forbes JD, Van Domselaar G, Bernstein CN. The Gut Microbiota in Immune-Mediated Inflammatory Diseases. Front Microbiol 2016;7:1081.

126. Jones-Hall YL, Nakatsu CH. The Intersection of TNF, IBD and the Microbiome. Gut Microbes 2016;7(1):58-62.

127. Du Z, Hudcovic T, Mrazek J, Kozakova H, Srutkova D, Schwarzer M, et al. Development of gut inflammation in mice colonized with mucosa-associated bacteria from patients with ulcerative colitis. Gut Pathog 2015;7:32.

128. Hernandez-Chirlaque C, Aranda CJ, Ocon B, Capitan-Canadas F, Ortega-Gonzalez M, Carrero JJ, et al. Germ-free and Antibiotic-treated Mice are Highly Susceptible to Epithelial Injury in DSS Colitis. J Crohns Colitis 2016;10(11):1324-35.

129. Balish E, Warner T. Enterococcus faecalis Induces Inflammatory Bowel Disease in Interleukin-10 Knockout Mice. The American Journal of Pathology 2002;160(6):2253-7.

130. Kiesler P, Fuss IJ, Strober W. Experimental Models of Inflammatory Bowel Diseases. Cell Mol Gastroenterol Hepatol 2015;1(2):154-70.

131. Kim JJ, Shajib MS, Manocha MM, Khan WI. Investigating intestinal inflammation in DSS-induced model of IBD. J Vis Exp 2012(60).

132. Mizoguchi A. Animal models of inflammatory bowel disease. Prog Mol Biol Transl Sci 2012;105:263-320.

133. Wirtz S, Neufert C, Weigmann B, Neurath MF. Chemically induced mouse models of intestinal inflammation. Nat Protoc 2007;2(3):541-6.

134. Kimoto H, Kurisaki J, Tsuji N, Ohmomo S, Okamoto T. Lactococci as probiotic strains adhesion to human enterocyte-like Caco-2 cells and tolerance to low pH and bile. Letters in Applied Microbiology 1999;29:313-6.

135. Song AA, In LLA, Lim SHE, Rahim RA. A review on Lactococcus lactis: from food to factory. Microb Cell Fact 2017;16(1):55.

136. Bermudez-Humaran LG, Motta JP, Aubry C, Kharrat P, Rous-Martin L, Sallenave JM, et al. Serine protease inhibitors protect better than IL-10 and TGF-beta anti-inflammatory cytokines against mouse colitis when delivered by recombinant lactococci. Microb Cell Fact 2015;14:26.

137. Steidler L. Lactococcus lactis, A Tool for the Delivery of Therapeutic Proteins Treatment of IBD. The Scientific World 2001;1:216-7.

138. Wong CC, Zhang L, Li ZJ, Wu WK, Ren SX, Chen YC, et al. Protective effects of cathelicidin-encoding Lactococcus lactis in murine ulcerative colitis. J Gastroenterol Hepatol 2012;27(7):1205-12.

139. Gyuraszova M, Kovalcikova A, Gardlik R. Association between oxidative status and the composition of intestinal microbiota along the gastrointestinal tract. Med Hypotheses 2017;103:81-5.

140. Ballal SA, Veiga P, Fenn K, Michaud M, Kim JH, Gallini CA, et al. Host lysozyme-mediated lysis of Lactococcus lactis facilitates delivery of colitis-attenuating superoxide dismutase to inflamed colons. Proc Natl Acad Sci U S A 2015;112(25):7803-8.

141. Shigemori S, Watanabe T, Kudoh K, Ihara M, Nigar S, Yamamoto Y, et al. Oral delivery of Lactococcus lactis that secretes bioactive heme oxygenase-1 alleviates development of acute colitis in mice. Microb Cell Fact 2015;14:189.

142. Toumi R, Soufli I, Rafa H, Belkhelfa M, Biad a, Touil-Boukoffa C. Probiotic bacteria lactobacillus and bifidobacterium attenuate inflammation in DSS-induced experimental colitis in mice. Int J Immunopath and Pharm 2014;27(4):615-27.

143. Suzuki T. Regulation of intestinal epithelial permeability by tight junctions. Cell Mol Life Sci 2013;70(4):631-59.

144. Capaldo CT, Nusrat A. Cytokine regulation of tight junctions. Biochim Biophys Acta 2009;1788(4):864-71.

145. Hering NA, Fromm M, Schulzke JD. Determinants of colonic barrier function in inflammatory bowel disease and potential therapeutics. J Physiol 2012;590(Pt 5):1035-44.

146. Gerova V, Stoynov S, Katsarov D, Svinarov D. Increased intestinal permeability in inflammatory bowel diseases assessed by iohexol test. World J Gastroenterol 2011;17(17):2211-5.

147. Schulzke JD, Ploeger S, Amasheh M, Fromm A, Zeissig S, Troeger H, et al. Epithelial tight junctions in intestinal inflammation. Ann N Y Acad Sci 2009;1165:294-300.

148. Tsukita S, Furuse M. Occludin and claudins in tight-junction strands leading or supporting players. Trends in Cell Biology 1999;9:268-73.

149. Poritz LS, Garver KI, Green C, Fitzpatrick L, Ruggiero F, Koltun WA. Loss of the tight junction protein ZO-1 in dextran sulfate sodium induced colitis. J Surg Res 2007;140(1):12-9.

150. Peterson LW, Artis D. Intestinal epithelial cells: regulators of barrier function and immune homeostasis. Nat Rev Immunol 2014;14(3):141-53.

151. Balda MS, Matter K. Tight junctions at a glance. J Cell Sci 2008;121(Pt 22):3677-82.

152. Gonzalezmariscal L. Tight junction proteins. Progress in Biophysics and Molecular Biology 2003;81(1):1-44.

153. Balda MS, Matter K. The tight junction protein ZO-1 and an interacting transcription factor regulate ErbB-2 expression. EMBO J 2000;19(9):2024-33.

154. Paris L, Tonutti L, Vannini C, Bazzoni G. Structural organization of the tight junctions. Biochim Biophys Acta 2008;1778(3):646-59.

155. Bergmann KR, Liu SX, Tian R, Kushnir A, Turner JR, Li HL, et al. Bifidobacteria stabilize claudins at tight junctions and prevent intestinal barrier dysfunction in mouse necrotizing enterocolitis. Am J Pathol 2013;182(5):1595-606.

156. Ma TY, Iwamoto GK, Hoa NT, Akotia V, Pedram A, Boivin MA, et al. TNF-alpha-induced increase in intestinal epithelial tight junction permeability requires NF-kappa B activation. Am J Physiol Gastrointest Liver Physiol 2004;286(3):G367-76.

157. Ye D, Ma I, Ma TY. Molecular mechanism of tumor necrosis factor-alpha modulation of intestinal epithelial tight junction barrier. Am J Physiol Gastrointest Liver Physiol 2006;290(3):G496-504.

158. Al-Sadi R, Ma T. IL-1β Causes an Increase in Intestinal Epithelial Tight Junction Permeability. J Immunol. 2007;178(7):4641–9.

159. Kim YH, Kwon HS, Kim DH, Shin EK, Kang YH, Park JH, et al. 3,3'-diindolylmethane attenuates colonic inflammation and tumorigenesis in mice. Inflamm Bowel Dis 2009;15(8):1164-73.

160. Li G, Lee MJ, Liu AB, Yang Z, Lin Y, Shih WJ, et al. The antioxidant and anti-inflammatory activities of tocopherols are independent of Nrf2 in mice. Free Radic Biol Med 2012;52(7):1151-8.

161. Bitiren M, Karakilcik AZ, Zerin M, Ozardali I, Selek S, Nazligul Y, et al. Protective effects of selenium and vitamin E combination on experimental colitis in blood plasma and colon of rats. Biol Trace Elem Res 2010;136(1):87-95.

162. Siegel RL, Miller KD, Jemal A. Cancer statistics, 2019. CA Cancer J Clin 2019;69(1):7-34.

163. Rustgi AK. The genetics of hereditary colon cancer. Genes Dev 2007;21(20):2525-38.

164. Fearon E, Vogelstein B. A Genetic Model of Colorectal Tumorigenesis. Cell 1990;61:759-67.

165. Terzic J, Grivennikov S, Karin E, Karin M. Inflammation and colon cancer. Gastroenterology 2010;138(6):2101-14 e5.

166. Hanahan D, Weinberg RA. Hallmarks of cancer: the next generation. Cell 2011;144(5):646-74.

167. Janakiram NB, Rao CV. The role of inflammation in colon cancer. Adv Exp Med Biol 2014;816:25-52.

168. Cannon J. Colorectal Neoplasia and Inflammatory Bowel Disease. Surg Clin North Am 2015;95(6):1261-9, vii.

169. LA F, Souza R, Spechler S. Carcinogenesis in IBD: potential targets for the prevention of colorectal cancer. Gastroenterol. Hepatol. 2009;6:297-305.

170. Jess T, Rungoe C, Peyrin-Biroulet L. Risk of colorectal cancer in patients with ulcerative colitis: a meta-analysis of population-based cohort studies. Clin Gastroenterol Hepatol 2012;10(6):639-45.

171. Triantafillidis J, GNasioulas G, Kosmidis P. Colorectal cancer and inflammatory bowel disease epidemiology, risk factors, mechanisms of carcinogenesis and prevention strategies. Anticancer Research 2009;29:2727-38.

172. Lennerz JK, van der Sloot KW, Le LP, Batten JM, Han JY, Fan KC, et al. Colorectal cancer in Crohn's colitis is comparable to sporadic colorectal cancer. Int J Colorectal Dis 2016;31(5):973-82.

173. Yu H, Pardoll D, Jove R. STATs in cancer inflammation and immunity: a leading role for STAT3. Nat Rev Cancer 2009;9(11):798-809.

174. Cooks T, Pateras IS, Tarcic O, Solomon H, Schetter AJ, Wilder S, et al. Mutant p53 prolongs NF-kappaB activation and promotes chronic inflammation and inflammation-associated colorectal cancer. Cancer Cell 2013;23(5):634-46.

175. Karin M. Nuclear factor-kappaB in cancer development and progression. Nature 2006;441(7092):431-6.

176. Fernandez-Majada V, Aguilera C, Villanueva A, Vilardell F, Robert-Moreno A, Aytes A, et al. Nuclear IKK activity leads to dysregulated notch-dependent gene expression in colorectal cancer. Proc Natl Acad Sci U S A 2007;104(1):276-81.

177. Richmond A. Nf-kappa B, chemokine gene transcription and tumour growth. Nat Rev Immunol 2002;2(9):664-74.

178. Karin M, Cao Y, Greten FR, Li ZW. NF-kappaB in cancer: from innocent bystander to major culprit. Nat Rev Cancer 2002;2(4):301-10.

179. De Simone V, Franze E, Ronchetti G, Colantoni A, Fantini MC, Di Fusco D, et al. Th17-type cytokines, IL-6 and TNF-alpha synergistically activate STAT3 and NF-kB to promote colorectal cancer cell growth. Oncogene 2015;34(27):3493-503.

180. Sakamoto K, Maeda S, Hikiba Y, Nakagawa H, Hayakawa Y, Shibata W, et al. Constitutive NF-kappaB activation in colorectal carcinoma plays a key role in angiogenesis, promoting tumor growth. Clin Cancer Res 2009;15(7):2248-58.

181. Corvinus FM, Orth C, Moriggl R, Tsareva SA, Wagner S, Pfitzner EB, et al. Persistent STAT3 Activation in Colon Cancer Is Associated with Enhanced Cell Proliferation and Tumor Growth. Neoplasia 2005;7(6):545-55.

182. Liang J, Nagahashi M, Kim EY, Harikumar KB, Yamada A, Huang WC, et al. Sphingosine-1-phosphate links persistent STAT3 activation, chronic intestinal inflammation, and development of colitis-associated cancer. Cancer Cell 2013;23(1):107-20.

183. Wang D, Dubois RN. The role of COX-2 in intestinal inflammation and colorectal cancer. Oncogene 2010;29(6):781-8.

184. Radmark O, Werz O, Steinhilber D, Samuelsson B. 5-Lipoxygenase, a key enzyme for leukotriene biosynthesis in health and disease. Biochim Biophys Acta 2015;1851(4):331-9.

185. Reddy BS, Hirose Y, Lubet R, Steele V, Kelloff G, Paulson S, et al. Chemoprevention of colon cancer by specific cyclooxygenase-2 inhibitor, celecoxib, administered during different stages of carcinogenesis. Cancer Res 2000;60(2):293-7.

186. Ihara A, Wada K, Yoneda M, Fujisawa N, Takahashi H, Nakajima A. Blockade of Leukotriene B4 Signaling Pathway Induces Apoptosis and Suppresses Cell Proliferation in Colon Cancer. Journal of Pharmacological Sciences 2007;103(1):24-32.

187. Cianchi F, Cortesini C, Magnelli L, Fanti E, Papucci L, Schiavone N, et al. Inhibition of 5-lipoxygenase by MK886 augments the antitumor activity of celecoxib in human colon cancer cells. Mol Cancer Ther 2006;5(11):2716-26.

188. Kitajima S, Takuma S, Morimoto M. Histological Analysis of Murine Colitis Induced by Dextran Sulfate Sodium of Different Molecular Weights. Experimental Animals 2000;49(1):9-15.

189. Suzuki R, Kohno H, Sugie S, Nakagama H, Tanaka T. Strain differences in the susceptibility to azoxymethane and dextran sodium sulfate-induced colon carcinogenesis in mice. Carcinogenesis 2006;27(1):162-9.

190. Yan Y, Kolachala V, Dalmasso G, Nguyen H, Laroui H, Sitaraman SV, et al. Temporal and spatial analysis of clinical and molecular parameters in dextran sodium sulfate induced colitis. PLoS One 2009;4(6):e6073.

191. Valatas V, Bamias G, Kolios G. Experimental colitis models: Insights into the pathogenesis of inflammatory bowel disease and translational issues. Eur J Pharmacol 2015;759:253-64.

192. Dieleman, Palmen, Akol, Bloemena, Pena, Meuwissen, et al. Chronic experimental colitis induced by dextran sulphate sodium (DSS) is characterized by Th1 and Th2 cytokines. Clin Exp Immunol 1998;114(3):385-91.

193. Sohn OS, Ishizaki H, Yang CS, Fiala ES. Metabolism of azoxymethane, methylazoxymethanol and N-nitrosodimethylamine by cytochrome P450IIE1. Carcinogenesis 1991;12(1):127-31.

194. Takahashi M, Wakabayashi K. Gene mutations and altered gene expression in azoxymethane-induced colon carcinogenesis in rodents. Cancer Sci 2004;95(6):475-80.

195. Davidson LA, Callaway ES, Kim E, Weeks BR, Fan YY, Allred CD, et al. Targeted Deletion of p53 in Lgr5-Expressing Intestinal Stem Cells Promotes Colon Tumorigenesis in a Preclinical Model of Colitis-Associated Cancer. Cancer Res 2015;75(24):5392-7.

196. Tanaka T, Kohno H, Suzuki R, Yamada Y, Sugie S, Mori H. A novel inflammation-related mouse colon carcinogenesis model induced by azoxymethane and dextran sodium sulfate. Cancer Sci 2003;94(11):965-73.

197. Chen J, Huang X-F. The signal pathways in azoxymethane-induced colon cancer and preventive implications. Cancer Biology & Therapy 2014;8(14):1313-7.

198. Rosenberg DW, Giardina C, Tanaka T. Mouse models for the study of colon carcinogenesis. Carcinogenesis 2009;30(2):183-96.

199. Riviere A, Selak M, Lantin D, Leroy F, De Vuyst L. Bifidobacteria and Butyrate-Producing Colon Bacteria: Importance and Strategies for Their Stimulation in the Human Gut. Front Microbiol 2016;7:979.

200. Zitvogel L, Ayyoub M, Routy B, Kroemer G. Microbiome and Anticancer Immunosurveillance. Cell 2016;165(2):276-87.

201. Sanapareddy N, Legge RM, Jovov B, McCoy A, Burcal L, Araujo-Perez F, et al. Increased rectal microbial richness is associated with the presence of colorectal adenomas in humans. ISME J 2012;6(10):1858-68.

202. Boleij A, Schaeps RM, Tjalsma H. Association between Streptococcus bovis and colon cancer. J Clin Microbiol 2009;47(2):516.

203. Boleij A, van Gelder MM, Swinkels DW, Tjalsma H. Clinical Importance of Streptococcus gallolyticus infection among colorectal cancer patients: systematic review and meta-analysis. Clin Infect Dis 2011;53(9):870-8.

204. Chen W, Liu F, Ling Z, Tong X, Xiang C. Human intestinal lumen and mucosa-associated microbiota in patients with colorectal cancer. PLoS One 2012;7(6):e39743.

205. Zitvogel L, Daillere R, Roberti MP, Routy B, Kroemer G. Anticancer effects of the microbiome and its products. Nat Rev Microbiol 2017;15(8):465-78.

206. Kostic AD, Chun E, Robertson L, Glickman JN, Gallini CA, Michaud M, et al. Fusobacterium nucleatum potentiates intestinal tumorigenesis and modulates the tumor-immune microenvironment. Cell Host Microbe 2013;14(2):207-15.

207. Patterson AM, Mulder IE, Travis AJ, Lan A, Cerf-Bensussan N, Gaboriau-Routhiau V, et al. Human Gut Symbiont Roseburia hominis Promotes and Regulates Innate Immunity. Front Immunol 2017;8:1166.

208. Kuugbee ED, Shang X, Gamallat Y, Bamba D, Awadasseid A, Suliman MA, et al. Structural Change in Microbiota by a Probiotic Cocktail Enhances the Gut Barrier and Reduces Cancer via TLR2 Signaling in a Rat Model of Colon Cancer. Dig Dis Sci 2016;61(10):2908-20.

209. Bishehsari F, Engen PA, Preite NZ, Tuncil YE, Naqib A, Shaikh M, et al. Dietary Fiber Treatment Corrects the Composition of Gut Microbiota, Promotes SCFA Production, and Suppresses Colon Carcinogenesis. Genes (Basel) 2018;9(2).

210. Chauhan D. Chemotherapeutic potential of curcumin for colorectal cancer. Current Pharmaceutical Design 2002;8:1695-706.

211. Flossmann E, Rothwell PM. Effect of aspirin on long-term risk of colorectal cancer: consistent evidence from randomised and observational studies. The Lancet 2007;369(9573):1603-13.

212. Chan AT, Arber N, Burn J, Chia WK, Elwood P, Hull MA, et al. Aspirin in the chemoprevention of colorectal neoplasia: an overview. Cancer Prev Res (Phila) 2012;5(2):164-78.

213. Drew DA, Cao Y, Chan AT. Aspirin and colorectal cancer: the promise of precision chemoprevention. Nat Rev Cancer 2016;16(3):173-86.

214. MB S, Suh N. Chemoprevention: an essential approach to controlling cancer. Nature Review: Cancer 2002;2:537.

215. Reddy B, Hirose Y, Lubet R, Steele V, Kelloff G, Paulson S, et al. Chemoprevention of colon cancer by specific cyclooxygenase-2 inhibitor, celecoxib, administered during different stages of carcinogenesis. Cancer Research 2000;60:293-7.

216. Dubois RW, Melmed GY, Henning JM, Bernal M. Risk of Upper Gastrointestinal Injury and Events in Patients Treated With Cyclooxygenase (COX)-1/COX-2 Nonsteroidal Antiinflammatory Drugs (NSAIDs), COX-2 Selective NSAIDs, and Gastroprotective Cotherapy: An Appraisal of the Literature. J Clin Rheumatol 2004;10(4):178-89.

217. Marnett LJ. Aspirin and the potential role of prostaglandins in colon cancer. Cancer Res 1992;52(20):5575-89.

218. Tsujii M, Kawano S, Tsuji S, Sawaoka H, Hori M, DuBois RN. Cyclooxygenase Regulates Angiogenesis Induced by Colon Cancer Cells. Cell 1998;93(5):705-16.

219. Ju J, Hao X, Lee MJ, Lambert JD, Lu G, Xiao H, et al. A gamma-tocopherol-rich mixture of tocopherols inhibits colon inflammation and carcinogenesis in azoxymethane and dextran sulfate sodium-treated mice. Cancer Prev Res (Phila) 2009;2(2):143-52.

220. Newmark HL, Huang MT, Reddy BS. Mixed tocopherols inhibit azoxymethane-induced aberrant crypt foci in rats. Nutr Cancer 2006;56(1):82-5.

221. Chen JX, Liu A, Lee MJ, Wang H, Yu S, Chi E, et al. delta- and gamma-tocopherols inhibit phIP/DSS-induced colon carcinogenesis by protection against early cellular and DNA damages. Mol Carcinog 2017;56(1):172-83.

222. Chung H, Wu D, Han SN, Gay R, Goldin B, Bronson RE, et al. Vitamin E supplementation does not alter azoxymethane-induced colonic aberrant crypt foci formation in young or old mice. J Nutr 2003;133(2):528-32.

223. Zhang JS, Zhang SJ, Li Q, Liu YH, He N, Zhang J, et al. Tocotrienol-rich fraction (TRF) suppresses the growth of human colon cancer xenografts in Balb/C nude mice by the Wnt pathway. PLoS One 2015;10(3):e0122175.

224. Prasad S, Gupta SC, Tyagi AK, Aggarwal BB. gamma-Tocotrienol suppresses growth and sensitises human colorectal tumours to capecitabine in a nude mouse xenograft model by down-regulating multiple molecules. Br J Cancer 2016;115(7):814-24.

225. Thakur V, Morley S, Manor D. Hepatic alpha-tocopherol transfer protein: ligand-induced protection from proteasomal degradation. Biochemistry 2010;49(43):9339-44.

226. Wechter WJ, Kantoci D, Murray ED, D'Amico DC, Jung ME, Wang WH. A new endogenous natriuretic factor: LLU-alpha. Proceedings of the National Academy of Sciences 1996;93(12):6002-7.

227. Burbank AJ, Duran CG, Almond M, Wells H, Jenkins S, Jiang Q, et al. A short course of gamma-tocopherol mitigates LPS-induced inflammatory responses in humans ex vivo. J Allergy Clin Immunol 2017.

228. Burbank AJ, Duran CG, Pan Y, Burns P, Jones S, Jiang Q, et al. Gamma tocopherol-enriched supplement reduces sputum eosinophilia and endotoxin-induced sputum neutrophilia in volunteers with asthma. J Allergy Clin Immunol 2018;141(4):1231-8 e1.

229. Gabrielsson J, Weiner D. Non-compartmental analysis. Methods Mol Biol 2012;929:377-89.

230. Persky A. Foundations in Pharmacokinetics. Book 2013:24, 77, 185.

231. Sontag TJ, Parker RS. Influence of major structural features of tocopherols and tocotrienols on their omega-oxidation by tocopherol-omega-hydroxylase. J Lipid Res 2007;48(5):1090-8.

232. Okabe M, Oji M, Ikeda I, Tachibana H, Yamada K. Tocotrienol levels in various tissues of Sprague-Dawley rats after intragastric administration of tocotrienols. Biosci Biotechnol Biochem 2002;66(8):1768-71.

233. Uchida T, Abe C, Nomura S, Ichikawa T, Ikeda S. Tissue distribution of alpha- and gamma-tocotrienol and gamma-tocopherol in rats and interference with their accumulation by alpha-tocopherol. Lipids 2012;47(2):129-39.

234. Mahipal A, Klapman J, Vignesh S, Yang CS, Neuger A, Chen DT, et al. Pharmacokinetics and safety of vitamin E delta-tocotrienol after single and multiple doses in healthy subjects with measurement of vitamin E metabolites. Cancer Chemother Pharmacol 2016;78(1):157-65.

235. Giusepponi D, Torquato P, Bartolini D, Piroddi M, Birringer M, Lorkowski S, et al. Determination of tocopherols and their metabolites by liquid-chromatography coupled with tandem mass spectrometry in human plasma and serum. Talanta 2017;170:552-61.

236. Drotleff AM, Bohnsack C, Schneider I, Hahn A, Ternes W. Human oral bioavailability and pharmacokinetics of tocotrienols from tocotrienol-rich (tocopherol-low) barley oil and palm oil formulations. Journal of Functional Foods 2014;7:150-60.

237. Qureshi AA, Khan DA, Silswal N, Saleem S, Qureshi N. Evaluation of Pharmacokinetics, and Bioavailability of Higher Doses of Tocotrienols in Healthy Fed Humans. J Clin Exp Cardiolog 2016;7(4).

238. Springett GM, Husain K, Neuger A, Centeno B, Chen DT, Hutchinson TZ, et al. A Phase I Safety, Pharmacokinetic, and Pharmacodynamic Presurgical Trial of Vitamin E delta-tocotrienol in Patients with Pancreatic Ductal Neoplasia. EBioMedicine 2015;2(12):1987-95.

239. Jiang Q, Moreland M, Ames BN, Yin X. A combination of aspirin and gamma-tocopherol is superior to that of aspirin and alpha-tocopherol in anti-inflammatory action and attenuation of aspirin-induced adverse effects. J Nutr Biochem 2009;20(11):894-900.

240. C.S. Y, N. S. Cancer Prevention by Different Forms of Tocopherols. In: J. P, N. S, editors. Natural Products in Cancer Prevention and Therapy. Topics in Current Chemistry: Springer, Berlin, Heidelberg; 2012. vol 329 p. 21-33.

241. Dolfi SC, Yang Z, Lee MJ, Guan F, Hong J, Yang CS. Inhibitory effects of different forms of tocopherols, tocopherol phosphates, and tocopherol quinones on growth of colon cancer cells. J Agric Food Chem 2013;61(36):8533-40.

242. Birringer M, Lington D, Vertuani S, Manfredini S, Scharlau D, Glei M, et al. Proapoptotic effects of long-chain vitamin E metabolites in HepG2 cells are mediated by oxidative stress. Free Radic Biol Med 2010;49(8):1315-22.

243. Shen L. Tight junctions on the move: molecular mechanisms for epithelial barrier regulation. Ann N Y Acad Sci 2012;1258:9-18.

244. Chiba H, Osanai M, Murata M, Kojima T, Sawada N. Transmembrane proteins of tight junctions. Biochim Biophys Acta 2008;1778(3):588-600.

245. Fanning AS. ZO proteins and Tight Junction Assembly. In: Gonzalez-Mariscal L, editor. Tight Junctions. Eurekah.com; 2005.

246. Maloney D, Hecht S. A stereocontrolled synthesis of delta-trans-tocotrienoloic acid. Org. Lett 2005;7:4297-300.

247. Hubatsch I, Ragnarsson EG, Artursson P. Determination of drug permeability and prediction of drug absorption in Caco-2 monolayers. Nat Protoc 2007;2(9):2111-9.

248. Schindelin J, Arganda-Carreras I, Frise E, Kaynig V, Longair M, Pietzsch T, et al. Fiji: an open-source platform for biological-image analysis. Nat Methods 2012;9(7):676-82.

249. Jones-Hall YL, Kozik A, Nakatsu C. Ablation of tumor necrosis factor is associated with decreased inflammation and alterations of the microbiota in a mouse model of inflammatory bowel disease. PLoS One 2015;10(3):e0119441.

250. Nossa CW. Design of 16S rRNA gene primers for 454 pyrosequencing of the human foregut microbiome. World Journal of Gastroenterology 2010;16(33):4135.

251. Jovel J, Patterson J, Wang W, Hotte N, O'Keefe S, Mitchel T, et al. Characterization of the Gut Microbiome Using 16S or Shotgun Metagenomics. Front Microbiol 2016;7:459.

252. Callahan BJ, McMurdie PJ, Rosen MJ, Han AW, Johnson AJ, Holmes SP. DADA2: High-resolution sample inference from Illumina amplicon data. Nat Methods 2016;13(7):581-3.

253. Quast C, Pruesse E, Yilmaz P, Gerken J, Schweer T, Yarza P, et al. The SILVA ribosomal RNA gene database project: improved data processing and web-based tools. Nucleic Acids Res 2013;41(Database issue):D590-6.

254. Good IJ. The Population Frequencies of Species and the Estimation of Population Parameters. Biometrika 1953;40(3/4):237.

255. Edgar RC. Accuracy of microbial community diversity estimated by closed- and open-reference OTUs. PeerJ 2017;5:e3889.

256. Pielou EC. The measurement of diversity in different types of biological collections. J Theor Biol 1966;13:131-44.

257. Shannon CE, Weaver W. The mathematical theory of communication. Champaign, Illonois.: University of Illonois Press; 1949.

258. Lozupone CA, Hamady M, Kelley ST, Knight R. Quantitative and qualitative beta diversity measures lead to different insights into factors that structure microbial communities. Appl Environ Microbiol 2007;73(5):1576-85.

259. Hamady M, Lozupone C, Knight R. Fast UniFrac: facilitating high-throughput phylogenetic analyses of microbial communities including analysis of pyrosequencing and PhyloChip data. ISME J 2010;4(1):17-27.

260. Lozupone C, Lladser ME, Knights D, Stombaugh J, Knight R. UniFrac: an effective distance metric for microbial community comparison. ISME J 2011;5(2):169-72.

261. Anderson MJ. Permutational Multivariate Analysis of Variance (PERMANOVA). 2017:1-15.

262. Anderson MJ. Distance-based tests for homogeneity of multivariate dispersions. Biometrics 2006;62(1):245-53.

263. Anderson MJ, Ellingsen KE, McArdle BH. Multivariate dispersion as a measure of beta diversity. Ecol Lett 2006;9(6):683-93.

264. ter Braak CJF, Verdonschot PFM. Canonical correspondence analysis and related multivariate methods in aquatic ecology. Aquat Sci 1995;57(3):255-89.

265. Hammer O, Harper D, D. RP. PAST: Paleontological Statistics Software Package for Education and Data Analysis. Palaeontologia Electronica 2001;4(1):1-9.

266. Cao M, Wang P, Sun C, He W, Wang F. Amelioration of IFN-gamma and TNF-alpha-induced intestinal epithelial barrier dysfunction by berberine via suppression of MLCK-MLC phosphorylation signaling pathway. PLoS One 2013;8(5):e61944.

267. Bruewer M, Luegering A, Kucharzik T, Parkos CA, Madara JL, Hopkins AM, et al. Proinflammatory Cytokines Disrupt Epithelial Barrier Function by Apoptosis-Independent Mechanisms. The Journal of Immunology 2003;171(11):6164-72.

268. Poritz LS, Garver KI, Tilberg AF, Koltun WA. Tumor necrosis factor alpha disrupts tight junction assembly. J Surg Res 2004;116(1):14-8.

269. Ma TY, Boivin MA, Ye D, Pedram A, Said HM. Mechanism of TNF-{alpha} modulation of Caco-2 intestinal epithelial tight junction barrier: role of myosin light-chain kinase protein expression. Am J Physiol Gastrointest Liver Physiol 2005;288(3):G422-30.

270. Al-Sadi R, Guo S, Ye D, Ma TY. TNF-alpha modulation of intestinal epithelial tight junction barrier is regulated by ERK1/2 activation of Elk-1. Am J Pathol 2013;183(6):1871-84.

271. Park YH, Kim N, Shim YK, Choi YJ, Nam RH, Choi YJ, et al. Adequate Dextran Sodium Sulfate-induced Colitis Model in Mice and Effective Outcome Measurement Method. J Cancer Prev 2015;20(4):260-7.

272. Ghanim H, Abuaysheh S, Sia CL, Korzeniewski K, Chaudhuri A, Fernandez-Real JM, et al. Increase in plasma endotoxin concentrations and the expression of Toll-like receptors and suppressor of cytokine signaling-3 in mononuclear cells after a high-fat, high-carbohydrate meal: implications for insulin resistance. Diabetes Care 2009;32(12):2281-7.

273. Rao R. Endotoxemia and gut barrier dysfunction in alcoholic liver disease. Hepatology 2009;50(2):638-44.

274. Tuomisto H. A diversity of beta diversities: straightening up a concept gone awry. Part 1. Defining beta diversity as a function of alpha and gamma diversity. Ecography 2010;33(1):2-22.

275. Mandal S, Van Treuren W, White RA, Eggesbø M, Knight R, Peddada SD. Analysis of composition of microbiomes: a novel method for studying microbial composition. Microbial Ecology in Health & Disease 2015;26(0).

276. Nair AB, Jacob S. A simple practice guide for dose conversion between animals and human. J Basic Clin Pharm 2016;7(2):27-31.

277. Perse M, Cerar A. Dextran sodium sulphate colitis mouse model: traps and tricks. J Biomed Biotechnol 2012;2012:718617.

278. Bernstein CN, Fried M, Krabshuis JH, Cohen H, Eliakim R, Fedail S, et al. World Gastroenterology Organization Practice Guidelines for the diagnosis and management of IBD in 2010. Inflamm Bowel Dis 2010;16(1):112-24.

279. Anderson JM, Van Itallie CM, Peterson MD, Stevenson BR, Carew EA, Mooseker MS. ZO-1 mRNA and protein expression during tight junction assembly in Caco-2 cells. J Cell Biol 1989;109(3):1047-56.

280. Dlugosz A, Nowak P, D'Amato M, Mohammadian Kermani G, Nystrom J, Abdurahman S, et al. Increased serum levels of lipopolysaccharide and antiflagellin antibodies in patients with diarrhea-predominant irritable bowel syndrome. Neurogastroenterol Motil 2015;27(12):1747-54.

281. Schumann RR. Function of lipopolysaccharide (LPS)-binding protein (LBP) and CD14, the receptor for LPS/LBP complexes: a short review. Res Immunol 1992;143(1):11-5.

282. Kopp F, Kupsch S, Schromm AB. Lipopolysaccharide-binding protein is bound and internalized by host cells and colocalizes with LPS in the cytoplasm: Implications for a role of LBP in intracellular LPS-signaling. Biochim Biophys Acta 2016;1863(4):660-72.

283. Rajilic-Stojanovic M, Shanahan F, Guarner F, de Vos WM. Phylogenetic analysis of dysbiosis in ulcerative colitis during remission. Inflamm Bowel Dis 2013;19(3):481-8.

284. Shaw KA, Bertha M, Hofmekler T, Chopra P, Vatanen T, Srivatsa A, et al. Dysbiosis, inflammation, and response to treatment: a longitudinal study of pediatric subjects with newly diagnosed inflammatory bowel disease. Genome Med 2016;8(1):75.

285. Munyaka PM, Rabbi MF, Khafipour E, Ghia J-E. Acute dextran sulfate sodium (DSS)-induced colitis promotes gut microbial dysbiosis in mice. J Basic Microbiol 2016;56(9):986-98.

286. Berry D, Schwab C, Milinovich G, Reichert J, Ben Mahfoudh K, Decker T, et al. Phylotype-level 16S rRNA analysis reveals new bacterial indicators of health state in acute murine colitis. ISME J 2012;6(11):2091-106.

287. Tamboli CP. Dysbiosis in inflammatory bowel disease. Gut 2004;53(1):1-4.

288. Zhou Y, Zhi F. Lower Level of Bacteroides in the Gut Microbiota Is Associated with Inflammatory Bowel Disease: A Meta-Analysis. Biomed Res Int 2016;2016:5828959.

289. Delday M, Mulder I, Logan ET, Grant G. Bacteroides thetaiotaomicron Ameliorates Colon Inflammation in Preclinical Models of Crohn's Disease. Inflamm Bowel Dis 2019;25(1):85-96.

290. Rios-Covian D, Salazar N, Gueimonde M, de Los Reyes-Gavilan CG. Shaping the Metabolism of Intestinal Bacteroides Population through Diet to Improve Human Health. Front Microbiol 2017;8:376.

291. Neyrinck AM, Etxeberria U, Taminiau B, Daube G, Van Hul M, Everard A, et al. Rhubarb extract prevents hepatic inflammation induced by acute alcohol intake, an effect related to the modulation of the gut microbiota. Mol Nutr Food Res 2017;61(1).

292. Yang JY, Lee YS, Kim Y, Lee SH, Ryu S, Fukuda S, et al. Gut commensal Bacteroides acidifaciens prevents obesity and improves insulin sensitivity in mice. Mucosal Immunol 2017;10(1):104-16.

293. Vital M, Karch A, Pieper DH. Colonic Butyrate-Producing Communities in Humans: an Overview Using Omics Data. mSystems 2017;2(6).

294. Huang ES, Strate LL, Ho WW, Lee SS, Chan AT. Long-term use of aspirin and the risk of gastrointestinal bleeding. Am J Med 2011;124(5):426-33.

295. Mercier S, Breuille D, Mosoni L, Obled C, Patureau Mirand P. Chronic inflammation alters protein metabolism in several organs of adult rats. J Nutr 2002;132(7):1921-8.

296. Garcia-Albeniz X, Chan AT. Aspirin for the prevention of colorectal cancer. Best Pract Res Clin Gastroenterol 2011;25(4-5):461-72.

297. Tian Y, Ye Y, Gao W, Chen H, Song T, Wang D, et al. Aspirin promotes apoptosis in a murine model of colorectal cancer by mechanisms involving downregulation of IL-6-STAT3 signaling pathway. Int J Colorectal Dis 2011;26(1):13-22.

298. Guo Y, Su ZY, Zhang C, Gaspar JM, Wang R, Hart RP, et al. Mechanisms of colitis-accelerated colon carcinogenesis and its prevention with the combination of aspirin and curcumin: Transcriptomic analysis using RNA-seq. Biochem Pharmacol 2017;135:22-34.

299. Chiu CH, McEntee MF, Whelan J. Discordant effect of aspirin and indomethacin on intestinal tumor burden in Apc(Min/+)mice. Prostaglandins Leukot Essent Fatty Acids 2000;62(5):269-75.

300. Guo Y, Liu Y, Zhang C, Su ZY, Li W, Huang MT, et al. The epigenetic effects of aspirin: the modification of histone H3 lysine 27 acetylation in the prevention of colon carcinogenesis in azoxymethane- and dextran sulfate sodium-treated CF-1 mice. Carcinogenesis 2016;37(6):616-24.

301. Robert A. Cytoprotection by prostaglandins. Gastroenterology 1979;77(4):761-7.

302. Mohammed A, Janakiram NB, Li Q, Choi CI, Zhang Y, Steele VE, et al. Chemoprevention of colon and small intestinal tumorigenesis in APC(Min/+) mice by licofelone, a novel dual 5-LOX/COX inhibitor: potential implications for human colon cancer prevention. Cancer Prev Res (Phila) 2011;4(12):2015-26.

303. Rainsford KD. Inhibition by Leukotriene Inhibitors, and Calcium and Platelet-activating Factor Antagonists, of Acute Gastric and Intestinal Damage in Arthritic Rats and in Cholinomimetic-treated Mice. J Pharm Pharmacol 1999;51(3):331-9.

304. Johnson KV, Burnet PW. Microbiome: Should we diversify from diversity? Gut Microbes 2016;7(6):455-8.

305. Omar Al-Hassi H, Ng O, Brookes M. Tumour-associated and non-tumour-associated microbiota in colorectal cancer. Gut 2018;67(2):395.

306. Tilg H, Adolph TE, Gerner RR, Moschen AR. The Intestinal Microbiota in Colorectal Cancer. Cancer Cell 2018;33(6):954-64.

307. Takahashi K, Nishida A, Fujimoto T, Fujii M, Shioya M, Imaeda H, et al. Reduced Abundance of Butyrate-Producing Bacteria Species in the Fecal Microbial Community in Crohn's Disease. Digestion 2016;93(1):59-65.

308. Kuehbacher T, Rehman A, Lepage P, Hellmig S, Folsch UR, Schreiber S, et al. Intestinal TM7 bacterial phylogenies in active inflammatory bowel disease. J Med Microbiol 2008;57(Pt 12):1569-76.

309. Singh J. Bifidobacterium longum, a lactic acid-producing intestinal bacterium inhibits colon cancer and modulates the intermediate biomarkers of colon carcinogenesis. Carcinogenesis 1997;18(4):833-41.

310. Femia AP. Antitumorigenic activity of the prebiotic inulin enriched with oligofructose in combination with the probiotics Lactobacillus rhamnosus and Bifidobacterium lactis on azoxymethane-induced colon carcinogenesis in rats. Carcinogenesis 2002;23(11):1953-60.

311. Le Leu RK, Hu Y, Brown IL, Woodman RJ, Young GP. Synbiotic intervention of Bifidobacterium lactis and resistant starch protects against colorectal cancer development in rats. Carcinogenesis 2010;31(2):246-51.

312. Grivennikov S, Karin E, Terzic J, Mucida D, Yu GY, Vallabhapurapu S, et al. IL-6 and Stat3 are required for survival of intestinal epithelial cells and development of colitis-associated cancer. Cancer Cell 2009;15(2):103-13.

313. Deng L, Peng Y, Wu Y, Yang M, Ding Y, Chen Q, et al. Tissue distribution of emulsified gamma-tocotrienol and its long-term biological effects after subcutaneous administration. Lipids Health Dis 2014;13:66.

VITA

Kilia Yun Liu

Ph.D. Candidate, Interdepartmental Nutrition Program, Purdue University, liu1173@purdue.edu

---

EDUCATION

Purdue University, West Lafayette, IN
Aug 2013 – present
Ph.D. Candidate in Interdepartmental Nutrition Program
Dissertation: The effect of vitamin E forms on colon inflammation and inflammation-associated carcinogenesis (Advisor: Dr. Qing Jiang)
Degree expected December 2018; Current GPA: 3.6/4.0

University of Illinois, Urbana-Champaign (UIUC), Urbana, IL
Aug 2010 – Aug 2012
Master of Science in Nutritional Sciences
Thesis: The effect of bioactive components found in human breast milk on natural killer cell activity and immune development in neonatal piglets (Advisor: Dr. Sharon Donovan)

University of Illinois, Urbana-Champaign (UIUC), Urbana, IL
Aug 2006 – Dec 2009
Bachelor of Science, Food Science and Human Nutrition, Minor in Chemistry

HONORS & AWARDS

- **Winner (3rd place) of Health and Disease: Science, Technology, Culture and Policy – Inflammation, Immunology and Infectious Disease category,** Purdue University, College of Health and Human Sciences (2018)
- **Winner of INP Poster Session – Basic Science and Animal Model**, Purdue University, Interdisciplinary Nutrition Program (2018)
- **Compton Graduate Research Travel Award**, Purdue University, College of Health and Human Sciences (2018)
- **Cancer Prevention and Internship Program Fellowship**, Purdue University (2017)

- **Mary Fuqua Scholarship**, Purdue University, Interdisciplinary Nutrition Program (2015-2016)
- **Lynn Fellowship**, Purdue University Graduate School (2013)
- **Margin of Excellence – Travel Award,** University of Illinois at Urbana-Champaign, Division of Nutritional Sciences (2012)

PUBLICATIONS

- **Liu KY,** Im S, Nakatsu, C Jones-Hall Y, and Jiang Q. Anticancer activity of the combination of aspirin and gamma-tocopherol. (In preparation)

- **Liu KY,** Nakatsu C, Jones-Hall Y, Kozik A, and Jiang Q. The protective effect of vitamin E alpha- and gamma-tocopherol on barrier function, colitis symptoms, and gut microbiome modulation in mice. (To be submitted to Free Radical Biology and Medicine)

- **Liu KY,** Yang C, Hernandez ML, Peden DB, and Jiang Q. Pharmacokinetics and excretion of metabolites of Vitamin E Forms Tocopherols and Tocotrienols. (Under review)

- Monaco MH, Comstock SS, **Liu KY**, Kvistgaard AS, Donovan SM. Dietary Osteopontin Modifies T-Cell Phenotype, Vaccine Response and Stimulates Cytokine Secretion in Neonatal Piglets (under review).

- **Liu KY**, Comstock SS, Shunk JM, Monaco MH, Donovan SM (2013). Natural killer cell populations and cytotoxic activity in pigs fed mother's milk, formula, or formula supplemented with bovine Lactoferrin. *Pediatric Research* 74(4):402-407.

- **Liu KY**, Chow JM, Sherry C (2013). Early Life Obesity and Diabetes: Origins in Pregnancy. *OJEMD* 3:1; 1-12.

ABSTRACTS

- **Liu KY**, Nakatsu C, Jones-Hall Y, and Jiang Q. Vitamin E alpha- and gamma-tocopherol protect intestinal barrier function in Caco-2 cells, attenuate colitis-associated damages and modulate gut microbiota in mice. *ASN 2018*

- **Liu KY** and Jiang Q. Pharmacokinetics of Vitamin E Forms, Tocopherols and Tocotrienols, and Time-Dependent Formation of Their Metabolites in Rats. *FASEB Journal* 2017; 31:801.3

- Monaco MH, Comstock SS, **Liu KY**, Staudt Kvistgaard A**,** Wejse PL, Donovan SM. Dietary bovine osteopontin increases vaccine response, T-cell phenotype and cytokine secretion in piglets. *FASEB Journal* 2014; 28: 623.7

- **Liu K**, Comstock SS, Burdette JM, Monaco MH, Donovan SM. NK cell populations and cytotoxic activity are greater in pigs fed mother's milk than formula. *FASEB Journal* 2012; 26: lb 325.

- Burdette JM, Comstock SS, **Liu K**, Monaco MH, Donovan SM. T-cell responses to ex vivo stimulations in neonatal piglets is influenced by diet and vaccination. *ASEB Journal* 2012; 26: lb 374.

RESEARCH EXPERIENCE

PURDUE UNIVERSITY, West Lafayette, IN

Research Assistant
Spring 2017 – Present
- Research Project: Anti-cancer effect of the combination of aspirin and vitamin E gamma-tocopherol in cells and mice

Research Assistant
Spring 2015 – Present
- Research Project: The protective effect of vitamin E alpha- and gamma-tocopherol against colitis in cell model and mouse model

Research Assistant
Spring 2014 – Present
- Research Project: Pharmacokinetic formation of vitamin E metabolites from tocopherols and tocotrienols in rats and human

UNIVERSITY OF ILLINOIS AT URBANA-CHAMPAIGN, Urbana, IL

Research Assistant
Fall 2010 – Spring 2012
- The effect of lactoferrin in human breast milk on natural killer cell activity and immune development in neonatal piglets

TEACHING EXPERIENCE

PURDUE UNIVERSITY, West Lafayette, IN

Teaching Assistant, Food Science (NUTR 205)
Summer 2015 – Spring 2017
- Taught lab classes and graded lab reports, quizzes, and projects

Teaching Assistant, Food Chemistry (NUTR 453)
Fall 2014 – Spring 2015
- Taught lab classes, facilitated with laboratory experiments and graded lab reports, quizzes, and projects

Teaching Assistant, Micronutrient Metabolism (NUTR 438)
Fall 2014
- Graded homework, quizzes, and exams

UNIVERSITY OF ILLINOIS AT URBANA-CHAMPAIGN, Urbana, IL

Teaching Assistant, Nutrition Educator
Fall 2008 – Spring 2009
- Facilitated and managed group activities to enhance understanding of the current nutrition recommendation

LEADERSHIP EXPERIENCE

PURDUE UNIVERSITY, West Lafayette, IN

Graduate Student Counsel for Cancer Prevention Internship Program
Fall 2017 – Current
- Collaborated with graduate and undergraduate students from different disciplines to promote cervical cancer prevention to college students at Purdue University
- Organized a movie screening about cervical cancer prevention for >150 audience and invited health professionals to a Q&A session to discuss about the potential issues (facts and fakes) in cervical cancer prevention with the audience after the movie

- Planned and managed several information booths in Purdue campus about cervical cancer or general cancer prevention

UNIVERSITY OF ILLINOIS AT URBANA-CHAMPAIGN, Urbana, IL

I-Program Leadership Conference
2007 – 2008
- Participated in team activities as leader who planned and managed group project, and as supporter that helped other team members on tasks

WORK EXPERIENCE

Abbott Nutrition R&D, Research Park University of Illinois
April 2012 – August 2012
- Conducted thorough literature review on topics related to pregnancy nutrition.
- Prepared internal papers, abstracts and manuscripts on these topics.